Chapter 7
Comparison Between Theory and Experiment and Future Perspectives

7.1 Experimental Results Confront Standard Theory

The anomalous magnetic moment of the muon provides one of the most precise tests of quantum field theory as a basic framework of elementary particle theory and of QED and the electroweak SM in particular. With what has been reached by the BNL muon $g-2$ experiment (see Table 7.1), namely the reduction of the experimental uncertainty by a factor 14 to $\sim 63 \times 10^{-11}$, a new quality in "diving into the sea of quantum corrections" has been achieved: the four/five loop order QED [$\sim 381/5 \times 10^{-11}$] known thanks to the heroic efforts of Aoyama, Hayakawa, Kinoshita and Nio [3, 4] and Laporta [5], the weak correction up to 2nd order [$\sim 154 \times 10^{-11}$] and the hadronic light–by–light scattering [$\sim 100 \times 10^{-11}$] are now in the focus. The uncertainty of the weak corrections has been substantially reduced with the discovery of the Higgs boson, which revealed its mass within a small error band. The hadronic vacuum polarization effects which played a significant role already for the last CERN experiment now is a huge effect of more than 11 SD's. As a non–perturbative effect it still has to be evaluated largely in terms of experimental data with unavoidable experimental uncertainties which yield the biggest contribution to the uncertainty of theoretical predictions. However, due to substantial progress in the measurement of total hadronic e^+e^-–annihilation cross sections, the uncertainty from this source has reduced to a remarkable $\sim 35 \times 10^{-11}$ only. This source of error now is only slightly larger than the uncertainty in the theoretical estimates of the hadronic light–by–light scattering contribution [$\sim 29 \times 10^{-11}$]. Nevertheless, we have a solid prediction with a total uncertainty of $\sim 45 \times 10^{-11}$, which is clearly below the experimental error of the muon $g-2$ measurement. A graphical representation for the sensitivity and the weight of the various contributions is presented in Fig. 3.8 (see also Table 7.2 and Fig. 7.3). For another recent summary see [6]. We now have at the same time, a new very sensitive test of our current theoretical understanding of the fundamental forces and the particle spectrum, and a stringent bound on physics beyond the SM entering at scales below about 1 TeV. But, may be more important is the actual deviation between theory and experiment at the $4\,\sigma$ level which is *a clear*

F. Jegerlehner, *The Anomalous Magnetic Moment of the Muon*,
Springer Tracts in Modern Physics 274, DOI 10.1007/978-3-319-63577-4_7

Table 7.1 Progress from CERN 1979 to BNL 2006 [* = CPT assumed]

	CERN 1979 [1]	BNL 2006 [2]
a_{μ^+}	$1165911(11) \times 10^{-9}$	$11659204(7)(5) \times 10^{-10}$
a_{μ^-}	$1165937(12) \times 10^{-9}$	$11659214(8)(3) \times 10^{-10}$
a_μ *	$1165924(8.5)10^{-9}$	$11659208(4)(3) \times 10^{-10}$
$(a_{\mu^+} - a_{\mu^-})/a_\mu$	$-(2.2\pm2.8) \times 10^{-5}$	$-(8.6\pm18.2) \times 10^{-7}$
d_μ (EDM) *	$(3.7\pm3.4) \times 10^{-19}\, e \cdot$ cm	$< 2.7 \times 10^{-19}\, e \cdot$ cm
a_μ^{the}	$1165921(8.3)10^{-9}$	$11659179.3(6.8)10^{-10}$
$a_\mu^{\text{the}} - a_\mu^{\text{exp}}$	$(-3.0\pm11.9) \times 10^{-9}$	$(-28.7\pm9.1) \times 10^{-10}$
$(a_\mu^{\text{the}} - a_\mu^{\text{exp}})/a_\mu^{\text{exp}}$	$-(2.6\pm10.2) \times 10^{-6}$	$-(2.5\pm0.8) \times 10^{-6}$

Table 7.2 Standard model theory and experiment comparison

Contribution	Value $\times 10^{10}$	Error $\times 10^{10}$	Reference
QED incl. 4-loops + 5-loops	11 658 471.886	0.003	[4, 5]
Hadronic LO vacuum polarization	689.46	3.25	(5.99)
Hadronic light–by–light	10.34	2.88	[9–13]
Hadronic HO vacuum polarization	−8.70	0.06	[7, 8]
Weak to 2-loops	15.36	0.11	[14–17]
Theory	11 659 178.3	3.5	–
Experiment	11 659 209.1	6.3	[2]
The. - Exp. 4.3 standard deviations	−30.6	7.2	–

indication of something missing. We have to remember that such high precision physics is extremely challenging for both experiment and for theory and it is not excluded that some small effect has been overlooked or underestimated at some place. To our present knowledge, it is hard to imagine that a 4 σ shift could be explained by known physics. Thus New Physics seems a likely interpretation, if it is not an experimental fluctuation (3 σ: 0.27% chance, 4 σ: 0.0063% chance).

It should be noted that among all the solid precision tests, to my knowledge, the muon $g-2$ shows the largest established deviation between theory and experiment. Actually, the latter has been persisting since the first precise measurement was released at BNL in February 2001 [18], and a press release announced "We are now 99 percent sure that the present Standard Model calculations cannot describe our data". A 2.6 σ deviation was found at that time for a selected choice of the hadronic vacuum polarization and with the wrong sign hadronic LbL scattering contribution.[1] In the meantime errors went further down experimentally as well as in theory,[2]

[1] With the correct sign of the hadronic LbL term the deviation would have been 1.5 σ based on the smallest available hadronic vacuum polarization. With larger values of the latter the difference would have been smaller.

[2] To mention the sign error and the issue of the high energy behavior in the LbL contribution or errors in the applied radiative corrections of e^+e^-–data or missing possible real photon radiation effects by the muons.

especially the improvement of the experimental e^+e^-–data, indispensable as an input for the "prediction" of the hadronic vacuum polarization, and the remedy of the wrong sign of the π^0 exchange LbL term has brought us forward a big step. The theoretical status, the main theme of this book, has been summarized in Sect. 3.2.3 (see Table 3.5 and Fig. 3.8) the experimental one in Sect. 6.5 (see Table 6.2 and Fig. 6.13). The jump in the precision is best reminded by a look at Table 7.1 which compares the results from the 1979 CERN final report [1] with the one's of the 2006 BNL final report [2].

The CPT test has improved by an order of magnitude. Relativistic QFT in any case guarantees CPT symmetry to hold and we assume CPT throughout in taking averages or estimating new physics effects etc. The world average experimental muon magnetic anomaly, dominated by the very precise BNL result, now is [2]

$$a_\mu^{\rm exp} = 1.16592091(54)(33) \times 10^{-3} \,, \tag{7.1}$$

with relative uncertainty 5.4×10^{-7}, which confronts the SM prediction

$$a_\mu^{\rm the} = 1.16591783(35) \times 10^{-3} \,, \tag{7.2}$$

and agrees up to the small but non–negligible deviation

$$\Delta a_\mu = a_\mu^{\rm exp} - a_\mu^{\rm the} = 306 \pm 72 \times 10^{-11} \,, \tag{7.3}$$

which is a 4.3σ effect. Errors have been added in quadrature. Note that the experimental uncertainty is still statistics dominated.[3] Thus just running the BNL experiment longer could have substantially improved the result. Originally the E821 goal was $\delta a_\mu^{\rm exp} \sim 40 \times 10^{-11}$. Figure 7.1 illustrates the improvement achieved by the BNL experiment, status by end 2009. The theoretical predictions mainly differ by the L.O. hadronic effects, which also dominates the theoretical error.

More recent progress in the determination of the HVP has been achieved mainly by the ISR hadronic cross section measurements. Some recent evaluations are collected in Fig. 7.2. The last entry [19] is based on the evaluation of all data and pQCD is used only where it can be applied safely according to [20, 21] and as discussed in Sect. 5.1.7. Differences in errors come about mainly by utilizing more "theory–driven" concepts[4]: use of selected data sets only, extended use of perturbative QCD in place of data [assuming local duality], sum rule methods, low energy effective

[3] The small spread in the central values does not reflect this fact, however.

[4] The terminology "theory–driven" means that we are not dealing with a solid theory prediction. As in some regions only old data sets are available, some authors prefer to use pQCD in place of the data also in regions where pQCD is not supposed to work reliably. The argument is that even under these circumstances pQCD may be better than the available data. This may be true, but one has to specified what "better" means. In this approach non–perturbative effects are accounted for by referring to local quark–hadron duality in relatively narrow energy intervals. What is problematic is a reliable error estimate. Usually, only the pQCD errors are accounted for, essentially only the uncertainty in α_s is taken into account. It is *assumed* that no other uncertainties from non–perturbative effects exist; this is why errors in this approach are systematically lower than in more conservative data

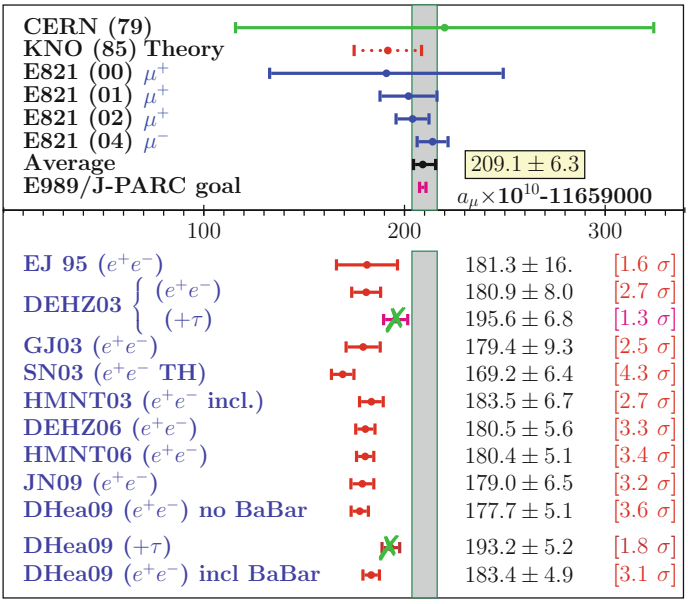

Fig. 7.1 Comparison between theory and experiment status 2009. Results differ by different L.O. hadronic vacuum polarizations and variants of the HLbL contribution (see Fig. 5.66). Some estimates include isospin rotated τ–data ($+\tau$)), which here are missing however $\gamma - \rho$ mixing corrections, why I marked them. EJ95 vs. JN09 illustrates the improvement of the e^+e^-–data between 1995 and 2009 (see also Table 5.4 and Fig. 6.13). E989 shows the expectation from the follow–up experiment of E821

methods [31–33]. The ** marked results include the most recent data from SND, CMD-2, KLOE, BaBar and BES-III [34–40].[5] In some analyses (as indicated) τ data from ALEPH, OPAL, CLEO and Belle [44–48] have been combined with the e^+e^-

(Footnote 4 continued)
oriented approaches. Note that applying pQCD in any case *assumes* quark–hadron duality to hold in large enough intervals, ideally from threshold to ∞ (global duality). My "conservative" evaluation of $a_\mu^{\rm had}$ estimates an error of 0.8%, which for the given quality of the data is as progressive as it can be, according to my standards concerning reliability. In spite of big progress in hadronic cross section measurements the agreement between different measurements is not as satisfactory as one would wish. Also more recent measurements often do not agree within the errors quoted by the experiments. Thus, one may seriously ask the question how such small uncertainties come about. The main point is that results in different energy ranges, as listed in Table 5.2 in Sect. 5.1.7, are treated as independent and all errors including the systematic ones are added in quadrature. By choosing a finer subdivision, like in the clustering procedure of [29], for example, one may easily end up with smaller errors (down to 0.6%). The subdivision I use was chosen originally in [30] and were more or less naturally associated with the ranges of the different experiments. The problem is that combining systematic errors is not possible on a commonly accepted basis if one goes beyond the plausible procedures advocated by the Particle Data Group.

[5]The analysis [41] does not include exclusive data in a range from 1.43 to 2 GeV; therefore also the new BaBar data are not included in that range. It also should be noted that CMD-2 and SND are not

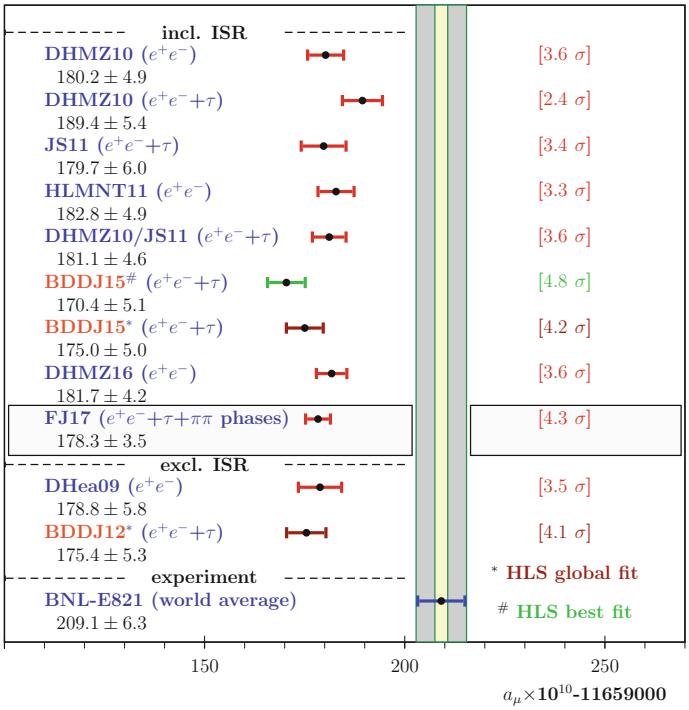

Fig. 7.2 Dependence of a_μ predictions on recent evaluations of $a_\mu^{\text{had,LO}}$. The HLS best fit BDDJ15# (NSK + KLOE10 + KLOE12) does not include BaBar $\pi\pi$ data [22], while BDDJ15* does. JS11/FJ16 [7, 8] is updated and include the new BES-III data. Further points are BDDJ12 [23], DHMZ10 [24], HLMNT11 [25] and DHea09 [26], The DHMZ10 ($e^+e^-+\tau$) result is not including the $\rho - \gamma$ mixing correction, i.e. it misses important isospin breaking effects. In contrast, DHMZ10/JS11 is obtained by including this correction, which brings the point into much better agreement with standard analyses based on e^+e^- data alone, as for example the DHMZ10 (e^+e^-) result. (see also [27, 28]). FJ17 represents our result (5.100). The narrow vertical band illustrates the E989 expectation

data. Some points are based on phenomenological low energy effective Lagrangian (specifically HLS) global fits [22, 23], constrained by data from additional channels, in particular the τ ones, and rewighting by the global fit qualities, which leads to somewhat lower central values with smaller errors.

Figure 7.3 illustrates how different physics contributions add up to the final answer. We note that the theory error is about 30% smaller now than the experimental one. It is fully dominated by the hadronic uncertainties of the hadronic low energy cross

(Footnote 5 continued)
fully independent measurements; data are taken at the same machine and with the same radiative correction program. The radiative corrections play a crucial role at the present level of accuracy, and common errors have to be added linearly. In [42, 43] pQCD is used in the extended ranges 1.8–3.7 GeV and above 5.0 GeV; furthermore [43] excludes the KLOE data.

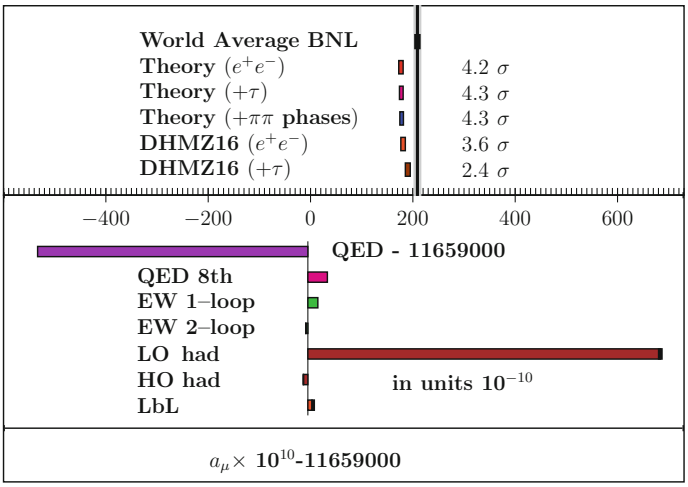

Fig. 7.3 All kinds of physics meet. Shown are the various contributions which add up to the theory prediction relative to the experimental result. The 8th order QED included in the QED part is shown separately. The 10th order QED is too small to be displayed here. For comparison also the extra contribution obtained by including the isospin rotated and isospin breaking corrected hadronic τ–decay data are shown. The "Theory" results are based on e^+e^- data (5.29), including τ after $\gamma - \rho$ mixing correction (5.99) and after including $\pi\pi$ phase shift data improvement [33] (5.100). The recent results DHMZ16 from [49] are also displayed. The second result DHMZ16 includes τ data without $\gamma - \rho$. The *black* heads on the bars represent the uncertainties. The *black vertical band* represents the future error band. Note that what seems to be a cancellation between "QED-11659000" and "LO had" is due to the QED off–set chosen. The complete QED and LO had are both positive and just add up. In any case the uncertainties and the deviation between theory and experiment look amazingly small in comparison to the various SM effect which are substantial for a precise prediction

section data on the one hand and not much less by the uncertainty of the hadronic light–by–light scattering contribution on the other hand. The history of muon $g-2$ measurements together with the theory values with which results were compared are listed once more in Table 7.3.

7.2 New Physics in $g-2$

The question about which unknown physics hides behind the SM was and is the main issue of theoretical particle physics since the emergence of the SM as *the* theory of "fundamental" particle interactions which we know today. Besides the SM's main shortcoming, which is that it lacks to include gravity, it rises many other questions about its structure, its many vastly different mass scales, and the answers always are attempts of embedding the SM into an extended theory. While the SM is very well established and is able to explain a plenitude of experimental data, and this so well

Table 7.3 Progress in a_μ measurements. Theory values as quoted in References (μSR = Muon Storage Ring)

Laboratory	Year	Ref.		Result (error) $\times 10^3$	Precision	Theory $\times 10^3$
Columbia	1960	[50]		1.22 (8)		1.16
CERN cyclotron	1961	[51]	μ^+	1.145 (22)		1.165
CERN cyclotron	1962	[52]	μ^+	1.162 (05)		1.165
CERN 1st μSR	1966	[53]	μ^-	1.165 (03)		1.165
CERN 1st μSR	1968	[54]	$\mu^\pm$	1.166 16 (31)		1.1656
CERN 2nd μSR	1977	[55]	$\mu^\pm$	1.165 924 0 (85)	7 ppm	1.165 921 0 (83)
BNL, 1997 data	1999	[56]	μ^+	1.165 925 (15)	13 ppm	1.165 916 3 (8)
BNL, 1998 data	2000	[57]	μ^+	1.165 919 1 (59)	5 ppm	1.165 916 3 (8)
BNL, 1999 data	2001	[18]	μ^+	1.165 920 2 (15)	1.3 ppm	1.165 916 0 (7)
BNL, 2000 data	2002	[58]	μ^+	1.165 920 4 (9)	0.73 ppm	1.165 917 7 (7)
BNL, 2001 data	2004	[59]	μ^-	1.165 921 4 (9)	0.72 ppm	1.165 918 1 (8)
World average	2004	[59]	$\mu^\pm$	1.165 920 80 (63)	0.54 ppm	1.165 917 93 (68)

that the more and more elaborate experimental efforts start to be a kind of frustrating, it is well known and as well established that the SM is *not* able to explain a number of facts, like the existence of non–baryonic Cold Dark Matter (CDM) (at most 5% of our universe's energy density is normal baryonic matter, about 21% are CDM), the matter–antimatter asymmetry in the universe, which requires baryon–number B and lepton–number L violation, the problem of the cosmological constant (see e.g. [60]) and so on. So, new physics must exist but how is it realized? What can the muon $g-2$ tell us about new physics?[6]

New physics contributions, which, if they exist, are an integral part of the measured numbers, typically are expected to be due to states or interactions which have not been seen by other experiments, either by a lack of sensitivity or, at the high energy frontier, because experimental facilities like accelerators are below the threshold of energy needed for producing the new heavy states or because the signal was still buried in the background. At the high energy frontier LEP, the Tevatron and the LHC have set limits on many species of possible new particles predicted in a plenitude of models beyond the SM. A partial list of existing bounds is collected in Table 7.4. The simplest possibility is to add a 4th fermion family called sequential fermions, where the neutrino has to have a large mass (>45 GeV) as additional light (nearly massless) neutrinos have been excluded by LEP.

Another possibility for extending the SM is the Higgs sector where one could add scalar singlets, an additional doublet, a Higgs triplet and so on. Two Higgs doublet models (THDM or 2HDM) are interesting as they predict 4 additional physical spin 0 bosons one neutral scalar H^0, a neutral pseudoscalar A, as well as the two charged

[6]The variety of speculations about new physics is mind–blowing and the number of articles on "physics beyond the SM" (BSM) almost uncountable. This short essay tries to reproduce a few of the main ideas for illustration, since a shift in one number can have many reasons and only in conjunction with other experiments it is possible to find out what is the true cause for an observed deviation from the SM prediction. My citations may be not very concise and I apologize for the certainly numerous omissions.

bosons $H^{\pm}$. Many new real and virtual processes, like $W^{\pm}H^{\mp}\gamma$ transitions, are the consequence. Any SUSY extension of the SM requires two Higgs doublets. Similarly, there could exist additional gauge bosons, like from an extra $U(1)'$. This would imply an additional Z boson, a sequential Z' which would mix with the SM Z and the photon. More attractive are extensions which solve some real or thought shortcomings of the SM. This includes Grand Unified Theories (GUT) [61] which attempt to unify the strong, electromagnetic and weak forces, which correspond to three different factors of the local gauge group of the SM, in one big simple local gauge group

$$G_{\rm GUT} \supset SU(3)_c \otimes SU(2)_L \otimes U(1)_Y \equiv G_{\rm SM}\,,$$

which is assumed to be spontaneously broken in at least two steps

$$G_{\rm GUT} \to SU(3)_c \otimes SU(2)_L \otimes U(1)_Y \to SU(3)_c \otimes U(1)_{\rm em}.$$

Coupling unification is governed by the renormalization group evolution of $\alpha_1(\mu)$, $\alpha_2(\mu)$ and $\alpha_3(\mu)$, corresponding to the SM group factors $U(1)_Y$, $SU(2)_L$ and $SU(3)_c$, with the experimentally given low energy values, typically at the Z mass scale, as starting values evolved to very high energies, the GUT scale $M_{\rm GUT}$ where couplings should meet. Within the SM the three couplings do not unify, thus unification requires new physics as predicted by a GUT extension. Also extensions like the left–right (LR) symmetric model are of interest. The simplest possible unifying group is $SU(5)$ which, however, is ruled out by the fact that it predicts protons to decay faster than allowed by observation. GUT models like $SO(10)$ or the exceptional group E_6 not only unify the gauge group, thereby predicting many additional gauge bosons, they also unify quarks and leptons in a GUT matter multiplet. Now quarks and leptons directly interact via the *leptoquark* gauge bosons X and Y which carry color, fractional charge ($Q_X = -4/3$, $Q_Y = -1/3$) as well as baryon and lepton number. Thus GUTs are violating B as well as L, yet with $B - L$ still conserved. The proton may now decay via $p \to e^+\pi^0$ or many other possible channels. The experimental proton lifetime $\tau_{\rm proton} > 2 \times 10^{29}$ years at 90% C.L. requires the extra gauge bosons to exhibit masses of about $M_{\rm GUT} > 10^{16}$ and excludes $SU(5)$ as it predicts unification at too low scales. $M_{\rm GUT}$ is the *GUT scale* which is only a factor 1000 below the Planck scale.[7] In general GUTs also have additional normal gauge bosons, extra W's and Z's which mix with the SM gauge bosons.

[7] GUT extensions of the SM are not very attractive for the following reasons: the extra symmetry breaking requires an additional heavier Higgs sector which makes the models rather clumsy in general. Also, unlike in the SM, the known matter–fields are *not* in the fundamental representations, while an explanation is missing why the existing lower dimensional representations remain unoccupied. In addition, the three SM couplings (as determined from experiments) allow for unification only with at least one additional symmetry breaking step $G_{\rm GUT} \to G' \to G_{\rm SM}$. In non-SUSY GUTs the only possible groups are $G_{\rm GUT} = E_6$ or $SO(10)$ and $G' = G_{LR} = SU(3)_c \otimes SU(2)_R \otimes SU(2)_L \otimes U(1)$ or $G_{PS} = SU(2)_R \otimes SU(2)_L \otimes SU(4)$ [62]. G_{LR} is the left–right symmetric extension of the SM and G_{PS} is the Pati–Salam model, where $SU(3)_c \otimes U(1)_Y$

Table 7.4 Present lower bounds on new physics states. Bounds are 95% C.L. limits from LEP (ALEPH, DELPHI, L3, OPAL), the Tevatron (CDF, D0) and the LHC (ATLAS, CMS)

Object	mass bound	comment
Heavy neutrino	$m^M_{\nu'} > 39$ GeV	Majorana-ν [$\nu \equiv \bar{\nu}$]
Heavy neutrino	$m^D_{\nu'} > 45$ GeV	Dirac-ν [$\nu \neq \bar{\nu}$]
Heavy lepton	$m_L > 100$ GeV	
4th family quark b'	$m_{b'} > 199$ GeV	$p\bar{p}$ NC decays
$W'_{\rm SM}$	$M_{W'} > 800$ GeV	SM couplings
W_R	$M_{W_R} > 715$ GeV	right–handed weak current
$Z'_{\rm SM}$	$M_{Z'} > 81.5$ TeV	SM couplings
Z_{LR} ($g_R = g_L$)	$M_{Z_{LR}} > 630$ GeV	of $G_{LR} = SU(2)_R \otimes SU(2)_L \otimes U(1)$
Z_χ ($g_\chi = e/\cos\Theta_W$)	$M_{Z_\chi} > 595$ GeV	of $SO(10) \to SU(5) \otimes U(1)_\chi$
Z_ψ ($g_\psi = e/\cos\Theta_W$)	$M_{Z_\psi} > 590$ GeV	of $E_6 \to SO(10) \otimes U(1)_\psi$
Z_η ($g_\eta = e/\cos\Theta_W$)	$M_{Z_\eta} > 620$ GeV	of $E_6 \to G_{LR} \otimes U(1)_\eta$
$h^0 \equiv H^0_1$ Higgs	$m_{H^0_1} > 92.8$ GeV	SUSY ($m_{H^0_1} < m_{H^0_2}$)
A^0 pseudoscalar Higgs	$m_A > 93.4$ GeV	THDM, MSSM
$H^\pm$ charged Higgs	$m_{H^\pm} > 80.0$ GeV	THDM, MSSM
LHC results pp direct searches		
4th family quark b'	$m_{b'} > 755$ GeV	NC decays
4th family quark t'	$m_{t'} > 782$ GeV	NC decays
$W'_{\rm SM}$	$M_{W'} > 3.71$ TeV	SM couplings
$Z'_{\rm SM}$	$M_{Z'} > 2.9$ TeV	SM couplings
Z_{LR} ($g_R = g_L$)	$M_{Z_{LR}} > 1.16$ TeV	of $G_{LR} = SU(2)_R \otimes SU(2)_L \otimes U(1)$
Z_χ ($g_\chi = e/\cos\Theta_W$)	$M_{Z_\chi} > 2.62$ TeV	of $SO(10) \to SU(5) \otimes U(1)_\chi$
Z_ψ ($g_\psi = e/\cos\Theta_W$)	$M_{Z_\psi} > 2.57$ TeV	of $E_6 \to SO(10) \otimes U(1)_\psi$
Z_η ($g_\eta = e/\cos\Theta_W$)	$M_{Z_\eta} > 1.87$ TeV	of $E_6 \to G_{LR} \otimes U(1)_\eta$

In deriving bounds on New Physics it is important to respect constraints not only from a_μ and the direct bounds of Table 7.4, but also from other precision observables which are sensitive to new physics via radiative corrections. Important examples are the electroweak precision observables [64, 65]:

$$M_W = 80.385(15)\ \text{GeV}\,, \tag{7.4}$$

(Footnote 7 continued)
of the SM is contained in the $SU(4)$ factor. Coupling unification requires the extra intermediate breaking scale to lie very high $M' \sim 10^{10}$ GeV for G_{LR} and $M' \sim 10^{14}$ GeV for G_{PS}. These are the scales of new physics in these extensions, completely beyond of being phenomenologically accessible. The advantage of SUSY GUTs is that they allow for unification of the couplings with the new physics scale being as low as M_Z to 1 TeV [63], and the supersymmetrized $G_{\rm GUT} = SU(5)$ extension of the SM escapes to be excluded.

$$\sin^2\Theta^{\ell}_{\rm eff} = 0.23152(5)\,, \quad \rho_0 = 1.00037(23)\,, \tag{7.5}$$

which are both precisely measured and precisely predicted by the SM or in extensions of it. The SM predictions use the very precisely known independent input parameters α, G_μ and M_Z, but also the less precisely known top quark mass

$$m_t = 173.21\pm0.87\ \text{GeV}\,, \tag{7.6}$$

and the Higgs boson mass [66]

$$m_H = 125.09(24)\ \text{GeV}\,, \tag{7.7}$$

are important.

The parameter ρ_0 is the tree level (SM radiative corrections subtracted) ratio of the low energy effective weak neutral to charged current couplings: $\rho = G_{\rm NC}/G_{\rm CC}$ where $G_{\rm CC} \equiv G_\mu$. This parameter is rather sensitive to new physics. In the SM at tree level $\rho_0 \equiv 1$ independent of any free parameter. This is due to the custodial symmetry of the minimal SM Higgs sector and consequently ρ is a SM prediction very similar to the anomalous lepton moments. In general, extensions of the SM, like GUTs or models including Higgs triplets etc., violate the custodial symmetry and if ρ_0 depends on parameters of the extension then ρ becomes a tunable quantity and one has a fine tuning problem [67]. The fact that $\rho_0 = 1$ in the SM allowed one to predict the top quark mass from a precision measurement of $\Delta\rho$ (4.40) at LEP prior to the discovery of the top quark at the Tevatron. The leading top quark mass effect in $\Delta\rho \propto m_t^2$ is lost if $\rho_0 \neq 1$ and such extensions are disfavored (see e.g. [68]).

Equally important are constraints by the B–physics branching fractions [69]

$$\text{BR}(b\to s\gamma) = (3.43\pm0.22)\times10^{-4}\,; \quad \text{BR}(B_s\to\mu^+\mu^-) = 2.8^{+0.7}_{-0.6}\times10^{-9}. \tag{7.8}$$

Concerning flavor physics, in particular the B factories Belle at KEK and BaBar at SLAC have set new milestones in confirming the flavor structure as inferred by the SM. In the latter Flavor–Changing Neutral Currents (FCNC) are absent at tree level due to the GIM mechanism and CP-violation and flavor mixing patterns seem to be realized in nature precisely as implemented by the three fermion–family CKM mixing scheme. Many new physics models have serious problems to accommodate this phenomenologically largely confirmed structure in a natural way. Therefore, the criterion of *Minimal Flavor Violation* (MFV) [70] has been conjectured as a framework for constructing low energy effective theories which include the SM Lagrangian without spoiling its flavor structure. The SM fermions are grouped into three families with two $SU(2)_L$ doublets (Q_L and L_L) and three $SU(2)_L$ singlets (U_R, D_R and E_R) and the largest group of unitary transformations which commutes

with the gauge group is $G_F = U(3)^5$ [71]. The latter may be written more specifically as

$$G_F = SU(3)_q^3 \otimes SU(3)_\ell^2 \otimes U(1)_B \otimes U(1)_L \otimes U(1)_Y \otimes U(1)_{PQ} \otimes U(1)_{E_R}$$

with $SU(3)_q^3 = SU(3)_{Q_L} \otimes SU(3)_{U_R} \otimes SU(3)_{D_R}$ and $SU(3)_\ell^2 = SU(3)_{L_L} \otimes SU(3)_{E_R}$. The SM Yukawa interactions break the subgroup $SU(3)_q^3 \otimes SU(3)_\ell^2 \otimes U(1)_{PQ} \otimes U(1)_{E_R}$. However, one may introduce three dimensionless auxiliary fields

$$Y_U \sim (3, \bar{3}, 1)_{SU(3)_q^3}, \; Y_D \sim (3, 1, \bar{3})_{SU(3)_q^3}, \; Y_E \sim (3, \bar{3})_{SU(3)_\ell^2}$$

which provide a convenient bookkeeping for constructing MFV effective theories. Formally the auxiliary fields allow to write down MFV compatible interactions as G_F invariant effective interactions. The MFV criterion requires that a viable dynamics of flavor violation is completely determined by the structure of the ordinary SM Yukawa couplings. Most of the promising and seriously considered new physics models, which we will consider below, belong to the class of MFV extensions of the SM. Examples are the R-parity conserving two doublet Higgs models, the R-parity conserving minimal supersymmetric extension of the SM [72] and the Littlest Higgs model without T-parity.

Another important object is the electric dipole moment which is a measure of CP–violation and was briefly discussed at the end of Sect. 3.3. Since extensions of the SM in general exhibit additional sources of CP violation, EDMs are very promising probes of new physics. An anomalously large EDM of the muon d_μ would influence on the a_μ extraction from the muon precession data as discussed at the end of Sect. 6.3.1. We may ask whether d_μ could be responsible for the observed deviation in a_μ. In fact (6.55) tells us that a non–negligible d_μ would increase the observed a_μ, and we may estimate

$$|d_\mu| = \frac{1}{2}\frac{e}{m_\mu}\sqrt{(a_\mu^{\rm exp})^2 - (a_\mu^{\rm SM})^2} = (2.53 \pm 0.31) \times 10^{-19}\, e \cdot {\rm cm}. \tag{7.9}$$

This also may be interpreted as an upper limit as given in Table 7.1. Recent advances in experimental techniques will allow to perform much more sensitive experiments for electrons, neutrons and neutral atoms [73]. For new efforts to determine d_μ at much higher precision see [74, 75]. In the following we will assume that d_μ is in fact negligible, and that the observed deviation has other reasons.

As mentioned many times, the general form of contributions from states of mass $M_{\rm NP} \gg m_\mu$ takes the form

$$a_\mu^{\rm NP} = \mathcal{C}\,\frac{m_\mu^2}{M_{\rm NP}^2} \tag{7.10}$$

where naturally $\mathcal{C} = O(\alpha/\pi)$, like for the weak contributions (4.47), but now from interactions and states not included in the SM. New fermion loops may contribute in the same way as a τ–lepton

Table 7.5 Typical New Physics scales required to satisfy $\Delta a_\mu^{\rm NP} = \Delta a_\mu$ (7.3)

$\mathcal{C}$	1	α/π	$(\alpha/\pi)^2$
$M_{\rm NP}$	$2.0^{+0.4}_{-0.3}$ TeV	100^{+21}_{-13} GeV	5^{+1}_{-1} GeV

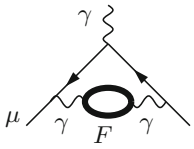

$$a_\mu^{(4)}(\text{vap}, F) = \sum_F Q_F^2 N_{cF} \left[\frac{1}{45}\left(\frac{m_\mu}{m_F}\right)^2 + \cdots\right]\left(\frac{\alpha}{\pi}\right)^2 ,$$

which means $\mathcal{C} = O((\alpha/\pi)^2)$. Note that the τ contribution to a_μ is 4.2×10^{-10} only, while the $3\,\sigma$ effect we are looking for is 28.7×10^{-10}. As the direct lower limit for a sequential fermion is about 100 GeV (see Table 7.4) such effects cannot account for the observed deviation. A 100 GeV heavy lepton only yields the tiny contribution[8] 1.34×10^{-13}.

A rough estimate of the scale $M_{\rm NP}$ required to account for the observed deviation is given in Table 7.5. An effective tree level contribution would extend the sensibility to the very interesting 2 TeV range, however, no compelling scenario I know of exists for this case (see below).

[8] It should be noted that heavy sequential fermions are constrained severely by the ρ–parameter (NC/CC effective coupling ratio), if doublet members are not nearly mass degenerate. A doublet (ν_L, L) with $m_{\nu_L} = 45$ GeV and $m_L = 100$ GeV only contributes $\Delta\rho \simeq 0.0008$, which however is violating already the limit from LEP electroweak fits (7.5). Not yet included is a similar type contribution from the 4th family (t', b') doublet mass–splitting, which also would add a large positive term

$$\Delta\rho = \frac{\sqrt{2}G_\mu}{16\pi^2}\, 3\, m_{t'}^2 \left(1 + \frac{m_{b'}^2}{m_{t'}^2}\, \ln \frac{m_{b'}^2}{m_{t'}^2}\right) + \cdots$$

in case of a large mass splitting $m_{t'}^2 \gg m_{b'}^2$, or a small correction $\Delta\rho = \frac{\sqrt{2}G_\mu}{16\pi^2}\, \frac{2\Delta^2}{\Sigma}$, which vanishes for small mass splitting $\Delta = |m_{t'}^2 - m_{b'}^2| \ll \Sigma = m_{t'}^2 + m_{b'}^2$. In this context it should be mentioned that the so called *custodial symmetry* of the SM which predicts $\rho_0 = 1$ at the tree level (independent of any parameter of the theory, which implies that it is not subject to subtractions due to parameter renormalization) is one of the severe constraints on extensions of the SM. Virtual top effect contributing to the radiative corrections of ρ allowed a determination of the top mass prior to the discovery of the top by direct production at Fermilab in 1995. The LEP precision determination of $\Delta\rho = \frac{\sqrt{2}G_\mu}{16\pi^2}\, 3\, m_t^2$ (up to subleading terms) from precision measurements of Z resonance parameters yields $m_t = 172.3^{+10.2}_{-7.6}$ GeV in excellent agreement with the direct determination $m_t = 171.4(2.1)$ GeV at the Tevatron and with the recent determinations $m_t = 172.84(0.70)$ GeV [76] from ATLAS and $m_t = 172.44(0.13)(0.47)$ GeV [77] from CMS (for CDF and D0 see [78]). In extensions of the SM in which ρ depends on physical parameters on the classical level, like in GUT models or models with Higgs triplets etc. one largely looses this prediction and thus one has a fine tuning problem [67]. But, also "extensions" which respect custodial symmetry like simply adding a 4th family of fermions should not give a substantial contribution to $\Delta\rho$, otherwise also this would spoil the indirect top mass prediction.

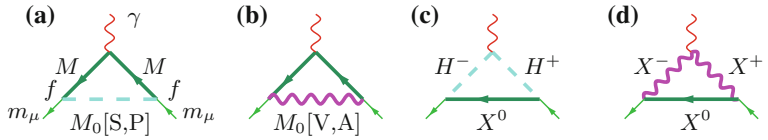

Fig. 7.4 Possible New Physics contributions. Neutral boson exchange: **a** scalar or pseudoscalar and **b** vector or axialvector, flavor changing or not. New charged bosons: **c** scalars or pseudoscalars, **d** vector or axialvector

7.2.1 Generic Contributions from Physics Beyond the SM

It is important to remember that the fermion anomalous magnetic moments are predictions only within the framework of a renormalizable theory. Therefore, extensions based on dimension 5 or higher operators in general loose most of the predictive power we have in the SM and they will not be considered in the following, except for a short account on anomalous gauge couplings.

Common to many of the extensions of the SM are predictions of new states: scalars S, pseudoscalars P, vectors V or axialvectors A, neutral or charged. They contribute via one–loop lowest order type diagrams shown in Fig. 7.4. Here, we explicitly assume all fermions to be Dirac fermions. Besides the SM fermions, μ in particular, new heavy fermions F of mass M may be involved, but fermion number is assumed to be conserved, like in $\Delta\mathcal{L}_S = f\bar{\psi}_\mu\psi_F S + \text{h.c.}$, which will be different in supersymmetric (SUSY) extensions discussed below, where fermion number violating Majorana fermions necessarily must be there.

Note that massive spin 1 boson exchange contributions in general have to be considered within the context of a gauge theory, in order to control gauge invariance and unitarity. We will present corresponding contributions in the unitary gauge calculated with dimensional regularization. We first discuss neutral boson exchange contributions from diagrams (a) and (b). Exotic neutral bosons of mass M_0 coupling to muons with coupling strength f would contribute [79, 80]

$$\Delta a_\mu^{\text{NP}} = \frac{f^2}{4\pi^2}\,\frac{m_\mu^2}{M_0^2}\,L,\;\; L = \frac{1}{2}\int_0^1 \mathrm{d}x\,\frac{Q(x)}{(1-x)\,(1-\lambda^2\,x)+(\epsilon\lambda)^2\,x}\,, \tag{7.11}$$

where $Q(x)$ is a polynomial in x which depends on the type of coupling:

$$\begin{aligned}
&\text{Scalar} && : Q_{\text{S}} = x^2\,(1+\epsilon-x)\\
&\text{Pseudoscalar} && : Q_{\text{P}} = x^2\,(1-\epsilon-x)\\
&\text{Vector} && : Q_{\text{V}} = 2x\,(1-x)\,(x-2\,(1-\epsilon)) + \lambda^2\,(1-\epsilon)^2\,Q_{\text{S}}\\
&\text{Axialvector} && : Q_{\text{A}} = 2x\,(1-x)\,(x-2\,(1+\epsilon)) + \lambda^2\,(1+\epsilon)^2\,Q_{\text{P}}
\end{aligned}$$

with $\epsilon = M/m_\mu$ and $\lambda = m_\mu/M_0$. As an illustration we first consider the regime of a heavy boson of mass M_0 and m_μ, $M \ll M_0$ for which one gets

$$\begin{aligned} L_{\rm S} &= \frac{M}{m_\mu}\left(\ln\frac{M_0}{M} - \frac{3}{4}\right) + \frac{1}{6} \overset{M=m_\mu}{=} \ln\frac{M_0}{m_\mu} - \frac{7}{12}, \\ L_{\rm P} &= -\frac{M}{m_\mu}\left(\ln\frac{M_0}{M} - \frac{3}{4}\right) + \frac{1}{6} \overset{M=m_\mu}{=} -\ln\frac{M_0}{m_\mu} + \frac{11}{12}, \\ L_{\rm V} &= \frac{M}{m_\mu} - \frac{2}{3} \overset{M=m_\mu}{=} \frac{1}{3}, \\ L_{\rm A} &= -\frac{M}{m_\mu} - \frac{2}{3} \overset{M=m_\mu}{=} -\frac{5}{3}. \end{aligned} \tag{7.12}$$

In accordance with the MFV requirement it is more realistic to assume a flavor conserving neutral current $M = m_\mu$ as given by the second form. Typical contributions are shown in Fig. 7.5. Taking the coupling small enough such that a perturbative expansion in f makes sense, we take $f/(2\pi) = 0.1$, only the scalar exchange could account for the observed deviation with a scalar mass 480 GeV $< M_0 <$ 690 GeV. Pseudoscalar and axialvector yield the wrong sign. The vector exchange is too small. We learn that substantial pseudoscalar, vector or axialvector contribution are stringently limited, in principle, unless enhanced scalar contributions cancel them.

As we will see later, in SUSY and littlest Higgs extensions the leading contributions actually come from the regime $m_\mu \ll M, M_0$ with $M \sim M_0$, which is of enhanced FCNC type, and thus differs from the case just presented in (7.12). For the combinations of fixed chirality up to terms of order $O(m_\mu/M)$ one gets

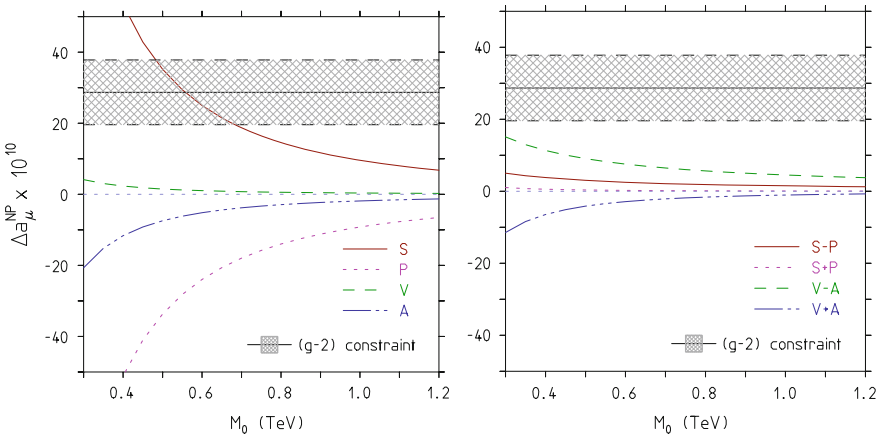

(a) Case: $m_\mu = M \ll M_0$ (b) Case: $m_\mu \ll M_0 = M$

Fig. 7.5 Single particle one–loop induced NP effects for $f^2/(4\pi^2) = 0.01$ (Note, a typical EW SM coupling would be $e^2/(4\pi^2\,\cos^2\Theta_W) = 0.003$). S, P, V, A denote scalar, pseudoscalar, vector and axialvector exchange. Panel **a** shows (7.12) for $M = m = m_\mu$, panel **b** the chiral combinations (7.13) for $m = m_\mu$ and $M = M_0$, with the large combinations $L_S - L_P$ and $L_V - L_A$ rescaled by the muon Yukawa coupling m_μ/v in order to compensate for the huge prefactor M/m_μ (see text)

$$
\begin{aligned}
L_S + L_P &= \frac{1}{6\,(1-z)^4}\left[2+3z-6z^2+z^3+6z\ln z\right] = \frac{1}{12}\,F_1^C(z),\\
L_S - L_P &= \frac{-M}{2m_\mu\,(1-z)^3}\left[3-4z+z^2+2\ln z\right] = \frac{M}{3m_\mu}\,F_2^C(z),\\
L_V + L_A &= \frac{-1}{6\,(1-z)^4}\left[8-38z+39z^2-14z^3+5z^4-18z^2\ln z\right] = -\frac{13}{12}\,F_3^C(z),\\
L_V - L_A &= \frac{M}{2m_\mu\,(1-z)^3}\left[4-3z-z^3+6z\ln z\right] = \frac{M}{m_\mu}\,F_4^C(z),
\end{aligned}
\tag{7.13}
$$

where $z = (M/M_0)^2 = O(1)$ and the functions F_i^C are normalized to $F_i^C(1) = 1$. The possible huge enhancement factors M/m_μ, in some combination of the amplitudes, typical for flavor changing transitions, may be compensated due to radiative contributions to the muon mass (as discussed below) or by a corresponding Yukawa coupling $f \propto y_\mu = \sqrt{2}\,m_\mu/v$, as it happens in SUSY or little Higgs extensions of the SM.

The second class of possible new physics transitions due to charged S, P, V and A modes are represented by the diagrams (c) and (d) in Fig. 7.4. It amounts to replace L in (7.11) according to

$$
\Delta a_\mu^{\rm NP} = \frac{f^2}{4\pi^2}\,\frac{m_\mu^2}{M_0^2}\,L,\;\; L = \frac{1}{2}\int_0^1 {\rm d}x\;\frac{Q(x)}{(\epsilon\lambda)^2\,(1-x)\,(1-\epsilon^{-2}\,x)+x}\;, \tag{7.14}
$$

where again $Q(x)$ is a polynomial in x which depends on the type of coupling:

$$
\begin{array}{ll}
\text{Scalar} & : Q_{\rm S} = -\,x\,(1-x)\,(x+\epsilon)\\
\text{Pseudoscalar} & : Q_{\rm P} = -\,x\,(1-x)\,(x-\epsilon)\\
\text{Vector} & : Q_{\rm V} = 2\,x^2\,(1+x-2\epsilon) - \lambda^2\,(1-\epsilon)^2\;Q_{\rm S}\\
\text{Axialvector} & : Q_{\rm A} = 2\,x^2\,(1+x+2\epsilon) - \lambda^2\,(1+\epsilon)^2\;Q_{\rm P}
\end{array}
$$

Again, results for V and A are in the unitary gauge calculated with dimensional regularization. For a heavy boson of mass M_0 and m_μ, $M \ll M_0$ one finds

$$
\begin{aligned}
L_{\rm S} &= -\tfrac{1}{4}\tfrac{M}{m_\mu} - \tfrac{1}{12} \overset{M=m_\mu}{=} -\tfrac{1}{3}\;,\; L_{\rm P} = \tfrac{1}{4}\tfrac{M}{m_\mu} - \tfrac{1}{12} \overset{M=m_\mu}{=} \tfrac{1}{6}\;,\\
L_{\rm V} &= -\tfrac{M}{m_\mu} + \tfrac{5}{6} \overset{M=m_\mu}{=} -\tfrac{1}{6}\;,\; L_{\rm A} = \tfrac{M}{m_\mu} + \tfrac{5}{6} \overset{M=m_\mu}{=} \tfrac{11}{6}.
\end{aligned}
\tag{7.15}
$$

The second form given is for a flavor conserving charged current transition with $M = m_\mu$.

Also for the charged boson exchanges the regime $m_\mu \ll M, M_0$ with $M \sim M_0$ is of interest in SUSY and littlest Higgs extensions of the SM and we find

$$L_S + L_P = \frac{-1}{6\,(1-z)^4}\left[1 - 6z + 3z^2 + 2z^3 - 6z^2\ln z\right] = -\frac{1}{12}\,F_1^N(z),$$
$$L_S - L_P = \frac{-M}{2m_\mu\,(1-z)^3}\left[1 - z^2 + 2z\ln z\right] = -\frac{M}{6m_\mu}\,F_2^N(z),$$
$$L_V + L_A = \frac{1}{6\,(1-z)^4}\left[10 - 43\,z + 78\,z^2 - 49\,z^3 + 4\,z^4 + 18\,z^3\ln z\right] = \frac{5}{3}\,F_3^N(z),$$
$$L_V - L_A = \frac{-M}{m_\mu\,(1-z)^3}\left[4 - 15\,z + 12\,z^2 - z^3 - 6\,z^2\ln z\right] = -\frac{2M}{m_\mu}\,F_4^N(z), \quad (7.16)$$

where $z = (M/M_0)^2 = O(1)$ and the functions F_i^N are normalized to $F_i^N(1) = 1$. For a general study of this kind of effects in view if the LHC mass limits see [81].

Another simple illustration of the one–loop sensitivity to new physics are heavier gauge bosons with SM couplings. From direct searches we know that they must be at least as heavy as 800 GeV. Contributions then follow from the weak one–loop contributions by rescaling with $(M_W/M_{W'_{\rm SM}})^2 \sim 0.01$ and hence 1% of 19.5×10^{-10} only, an effect much too small to be of relevance.

At $O((\alpha/\pi)^2)$ new physics may enter via vacuum polarization and we may write corresponding contributions as a dispersion integral (3.150):

$$\Delta a_\mu^{\rm NP} = \frac{\alpha}{\pi}\int\limits_0^\infty \frac{{\rm d}s}{s}\,\frac{1}{\pi}\,{\rm Im}\Delta\Pi_\gamma^{\rm NP}(s)\;K(s).$$

Since, we are looking for contributions from heavy yet unknown states of mass $M \gg m_\mu$, and ${\rm Im}\Delta\Pi_\gamma^{\rm NP}(s) \neq 0$ for $s \geq 4M^2$ only, we may safely approximate $K(s) \simeq \frac{1}{3}\frac{m_\mu^2}{s}$ for $s \gg m_\mu^2$ such that, with $\frac{1}{\pi}\,{\rm Im}\Delta\Pi_\gamma^{\rm NP}(s) = \frac{\alpha(s)}{\pi}\,R^{\rm NP}(s)$

$$\Delta a_\mu^{\rm NP} = \frac{1}{3}\frac{\alpha}{\pi}\left(\frac{m_\mu}{M}\right)^2 L \;\;,\;\; \frac{L}{M^2} = \frac{\alpha}{3\pi}\int\limits_0^\infty \frac{{\rm d}s}{s^2}R^{\rm NP}(s).$$

An example is a heavy lepton mentioned before. A heavy narrow vector meson resonance of mass M_V and electronic width $\Gamma(V\to e^+e^-)$ (which is $O(\alpha^2)$) contributes $R_V(s) = \frac{9\pi}{\alpha^2}\,M_V\,\Gamma(V\to e^+e^-)\,\delta(s-M_V^2)$ such that $L = \frac{3\Gamma(V\to e^+e^-)}{\alpha M_V}$ and hence

$$\Delta a_\mu^{\rm NP} = \frac{m_\mu^2\,\Gamma(V\to e^+e^-)}{\pi\,M_V^3} = \frac{4\alpha^2\,\gamma_V^2\,m_\mu^2}{3M_V^2}. \quad (7.17)$$

Here we have applied the Van Royen-Weisskopf formula [82], which for a $J^{PC} = 1^{--}$ vector state predicts

$$\Gamma(V\to e^+e^-) = 16\pi\alpha^2 Q_q^2\frac{|\psi_V(0)|^2}{M_V^2} = \frac{4}{3}\pi\alpha^2\gamma_V^2 M_V\,,$$

where $\psi_V(0)$ is the meson wave function at the origin (dim 3) and γ_V is the dimensionless effective photon vector–meson coupling defined by $j^\mu_{\rm em}(x) = \gamma_V M_V^2\, V^\mu(x)$ with $V^\mu(x)$ the interpolating vector–meson field. γ_V characterizes the strong interaction properties of the $\gamma - V$ coupling and typically has values 0.2 for the ρ to 0.02 for the Υ. For $\gamma_V = 0.1$ and $M_V = 200$ GeV we get $\Delta a_\mu \sim 2 \times 10^{-13}$. The hadronic contribution of a 4th family quark doublet assuming $m_{b'} = m_{t'} = 200$GeV would yield $\Delta a_\mu \sim 5.6 \times 10^{-14}$ only. Unless there exists a new type of strong interactions like Technicolor[9] [83–85]. New strong interaction resonances are not expected, because new heavy sequential quarks would be too shortlived to be able to form resonances. As we know, due to the large mass and the large mass difference $m_t \gg m_b$, the top quark is the first quark which decays, via $t \to Wb$, as a bare quark before it has time to form hadronic resonances. This is not so surprising as the top Yukawa coupling responsible for the weak decay is stronger than the strong interaction constant.

New physics effects here may be easily buried in the uncertainties of the hadronic vacuum polarization. In any case, we expect $O((\alpha/\pi)^2)$ terms from heavy states not yet seen to be too small to play a role here. Possible light dark states are discussed later in Sect. 7.2.6.

In general the effects related to single diagrams, discussed in this paragraph, are larger than what one expects in a viable extension of the SM, usually required to be a renormalizable QFT[10] and to exhibit gauge interactions which typically cause large cancellations between different contributions. But even if one ignores possible cancellations, all the examples considered so far show how difficult it actually is to reconcile the observed deviation with NP effects not ruled out already by LEP, Tevatron and LHC new physics searches. Apparently a more sophisticated extension of the SM is needed which is able to produce substantial radiative corrections in

[9] Searches for Technicolor states like color–octet techni–ρ were negative up to 260–480 GeV depending on the decay mode.

[10] Of course, there are more non-renormalizable extensions of the SM than renormalizable ones. For the construction of the electroweak SM itself renormalizability was the key guiding principle which required the existence of neutral currents, of the weak gauge bosons, the quark-lepton family structure and last but not least the existence of the Higgs. However, considered as a low energy effective theory one expects all kinds of higher dimension transition operators coming into play at higher energies. Specific scenarios are anomalous gauge couplings, little Higgs models, models with extra space–dimensions à la Kaluza–Klein. In view of the fact that non-renormalizable interactions primarily change the high energy behavior of the theory, we expect corresponding effects to show up primarily at the high energy frontier. The example of anomalous $W^+W^-\gamma$ couplings, considered in the following subsection, confirms such an expectation. Also in non-renormalizable scenarios, effects are of the generic form (7.10) possibly with $M_{\rm NP}$ replaced by a cut-off $\Lambda_{\rm NP}$. On a fundamental level we expect the Planck scale to provide the cut–off, which would imply that effective interactions of non-renormalizable character show up at the 1 ppm level at about 10^{16} GeV. It is conceivable that at the Planck scale a sort of cut-off theory which is modeling an "ether" is more fundamental than its long distance tail showing up as a renormalizable QFT [86]. Physics-wise such an effective theory, which we usually interpret to tell us the fundamental laws of nature, is different in character from what we know from QCD where chiral perturbation theory or the resonance Lagrangian type models are non-renormalizable low energy tails of a known renormalizable theory, as is Fermi's non-renormalizable low energy effective current–current type tail within the SM.

the low energy observable a_μ while the new particles have escaped detection at accelerator facilities so far and only produce small higher order effects in other electroweak precision observables. In fact supersymmetric extensions of the SM precisely allow for such a scenario, as we will discuss below.

7.2.2 *Flavor Changing Processes*

We already have seen that flavor changing processes could give large contributions to a_μ. As pointed out in [87, 88] taking into account just the vertex diagrams could be very misleading. The argument is that the same interactions and heavy states which could contribute to $a_\mu^{\rm NP}$ according to Fig. 7.4 would contribute to the muon self energy, via the diagrams Fig. 7.6. By imposing chiral symmetry to the SM, i.e. setting the SM Yukawa couplings to zero, lepton masses could be radiatively induced by flavor changing $f\bar{\psi}_\mu\psi_F S + \text{h.c.}$ and $f\bar{\psi}_\mu \,\mathrm{i}\,\gamma_5\psi_F P + \text{h.c.}$ interactions (F a heavy fermion, S a scalar and P a pseudoscalar) in a hierarchy $m_\mu \ll M_F \ll M_S, M_P$. Then with $m_\mu \propto f^2 M_F$ and $a_\mu \propto f^2 m_\mu M_F/M^2_{S,P}$ one obtains $a_\mu = \mathcal{C}\, m_\mu^2/M^2_{S,P}$ with $\mathcal{C} = O(1)$, and the interaction strength f has dropped from the ratio. The problem is that a convincing approach of generating the lepton/fermion mass spectrum by radiative effects is not easy to accommodate. Of course it is a very attractive idea to replace the Yukawa term, put in by hand in the SM, by a mechanism which allows us to understand or even calculate the known fermion mass-spectrum, exhibiting a tremendous hierarchy of about 13 orders of magnitude of vastly different couplings/masses [from m_{ν_e} to m_t]. The radiatively induced values must reproduce this pattern and one has to explain why the same effects which make up the muon mass do not contribute to the electron mass. Again the needed hierarchy of fermion masses is only obtained by putting it in by hand in some way. In the scenario of radiatively induced lepton masses one has to require the family hierarchy like $f_e^2 M_{F_e}/f_\mu^2 M_{F_\mu} \simeq m_e/m_\mu$, $f_P \equiv f_S$ in order to get a finite cut–off independent answer, and $M_0 \to M_S \neq M_P$, such that $m_\mu = \frac{f_\mu^2 M_{F_\mu}}{16\pi^2} \ln \frac{M_S^2}{M_P^2}$ which is positive only provided $M_S > M_P$. It looks one tries to replace one puzzle with another. But of course new fields exhibiting new interactions affect radiative corrections also through mass effects.

Another aspect of flavor changing transition in the lepton sector is the following: after neutrino oscillations and herewith right–handed singlet neutrinos and neutrino

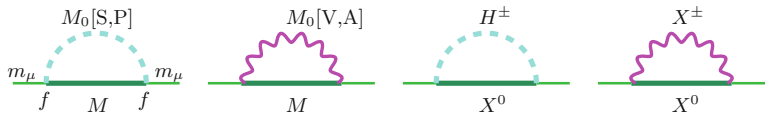

Fig. 7.6 Lepton self–energy contributions induced by the new interactions appearing in Fig. 7.4 may generate m_μ as a radiative correction effect

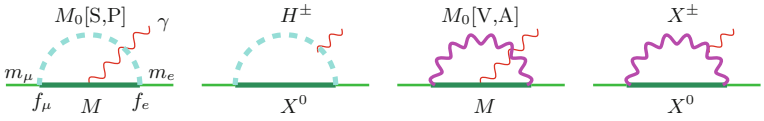

Fig. 7.7 $\mu \to e\gamma$ transitions by new interactions (overall flavor changing version of Fig. 7.4)

masses have been established, also lepton flavor violating (LFV) transitions like $\mu^\pm \to e^\pm\gamma$, see Fig. 7.7, are in the focus of further searches. The corresponding contributions here read

$$L_{\rm S}^{\mu} \simeq \frac{1}{6},\ L_{\rm P}^{\mu} \simeq \frac{1}{6},\ L_{\rm V}^{\mu} \simeq \frac{2}{3},\ L_{\rm A}^{\mu} \simeq -\frac{2}{3},$$
$$L_{\rm S}^{e} \simeq \frac{m_\mu}{m_e}\left(\ln\frac{M_0}{m_\mu} - \frac{3}{4}\right),\ L_{\rm P}^{e} \simeq -\frac{m_\mu}{m_e}\left(\ln\frac{M_0}{m_\mu} - \frac{3}{4}\right),\ L_{\rm V}^{e} \simeq \frac{m_\mu}{m_e},\ L_{\rm A}^{e} \simeq -\frac{m_\mu}{m_e}.$$

The latter flavor changing transitions are strongly constrained, first by direct rare decay search experiments which were performed at the Paul Scherrer Institute (PSI) and second, with the advent of the much more precise measurement of a_e. For example, for a scalar exchange mediating $e \to \mu \to e$ with $f^2/(4\pi^2) \simeq 0.01$ and $M_0 \simeq 100$ GeV we obtain $\Delta a_e^{NP} \simeq 33 \times 10^{-11}$ which is ruled out by (3.72) $|a_e^{\rm exp} - a_e^{\rm the}| \lesssim 1 \times 10^{-12}$. Either M_0 must be heavier or the coupling smaller: $f^2/(4\pi^2) < 0.0003$. The present limit for the branching fraction $Br(\mu \to e\gamma)$ from the MEG experiment at PSI is 4.2×10^{-13} (at 90% C.L.) [89] (see also [90]). Other LFV processes have been searched for are $\tau \to e\gamma, \tau \to \mu\gamma, \mu \to eee, \tau \to \mu\mu\mu$ and since no signal was observed stringent limits were derived. Note that

$$\Gamma(\mu \to e\gamma) = \frac{e^2 f_\mu^2 f_e^2}{16\pi^2}\, m_\mu^5\, (|F_{\rm M}^L|^2 + |F_{\rm M}^R|^2)\ , \tag{7.18}$$

where $F_{\rm M}^{L,R}$ are the left– and right–handed zero–momentum transfer magnetic $\mu e\gamma$ form factors. In the SM

$$Br(\mu \to e\gamma) \propto \frac{\alpha^3}{G_\mu^2}\,\frac{(\Delta m_\nu^2)_{\mu e}^2}{M_W^8}\ , \tag{7.19}$$

is extremely tiny. Only new physics can give rates in experimentally interesting ranges. In the quark sector CKM flavor mixing via the charged current is comparably huge and the $b \to s\gamma$ transitions is an established effect. This process also acquires enhanced SUSY contributions which makes it an excellent monitor for new physics [90], as we will see below. For a recent review see [92] and references therein. The detailed review [93] is focusing on the compatibility of the present and future constraints from Δa_μ and from the bound on $\mu \to e\gamma$ flavor violation for a variety of extensions of the SM as they contribute to the effective Lagrangian of the magnetic and electric dipole moment form (3.22).

7.2.3 Anomalous Couplings

Besides new states with new interactions also possible anomalous couplings of SM particles are very interesting. In particular the non–Abelian gauge boson self–interactions have to be checked for possible deviations. In the SM these couplings are dictated by the local gauge principle of Yang-Mills, once the interaction between the gauge bosons and the matter–fields (4.37) is given. For $g-2$ in particular the anomalous W–boson couplings are of interest, which occur in the 1st of the weak one–loop diagrams in Fig. 4.18. Possible is an anomalous magnetic dipole moment (see [94] and references therein)

$$\mu_W = \frac{e}{2m_W}(1+\kappa+\lambda)\,, \tag{7.20}$$

and an anomalous electric quadrupole moment

$$Q_W = -\frac{e}{2m_W}(\kappa-\lambda). \tag{7.21}$$

In the SM local gauge symmetry, which is mandatory for renormalizability of the SM, requires $\kappa=1$ and $\lambda=0$. The contribution to a_μ due to the deviation from the SM may be calculated and as a result one finds [95]

$$a_\mu(\kappa,\lambda) \simeq \frac{G_\mu m_\mu^2}{4\sqrt{2}\pi^2}\left[(\kappa-1)\ln\frac{\Lambda^2}{m_W^2}-\frac{1}{3}\lambda\right]. \tag{7.22}$$

Actually, the modification spoils renormalizability and one has to work with a cut–off Λ in order to get a finite answer and the result has to be understood as a low energy effective answer. For $\Lambda \simeq 1$ TeV the BNL constraint (7.3) would yield

$$\kappa-1 = 0.24\pm0.08\,,\quad \lambda = -3.58\pm1.17 \qquad \text{(BNL 04)}\,, \tag{7.23}$$

on the axes of the $(\Delta\kappa,\lambda)$–plane. Of course from one experimental number one cannot fix two or more parameters. In fact arbitrary large deviations from the SM are still possible described by the band Fig. 7.8: $\lambda = 3\ln\frac{\Lambda^2}{m_W^2}\,\Delta\kappa - \tilde{a_\mu}$ with $\tilde{a_\mu} = \frac{12\sqrt{2}\pi^2\,\delta a_\mu}{G_\mu m_\mu^2} \simeq 3.58\pm1.17$, as an interval on the λ–axis and a slope of about 15.

This possibility again is already ruled out by $e^+e^- \to W^+W^-$ data from LEP [96, 97] $\kappa-1 = -0.027\pm0.045, \lambda = -0.028\pm0.021$. Applying the LEP bounds we can get not more than $a_\mu(\kappa,0) \simeq (-3.3\pm5.3)\times10^{-10}$, $a_\mu(1,\lambda) \simeq (0.2\pm1.6)\times10^{-10}$, and thus the observed deviation cannot be due to anomalous $WW\gamma$ couplings. The constraint on those couplings from $g-2$ is at least an order of magnitude weaker than the one from LEP. Much more promising are the next examples, adding another Higgs doublet to the SM and the supersymmetrized SM.

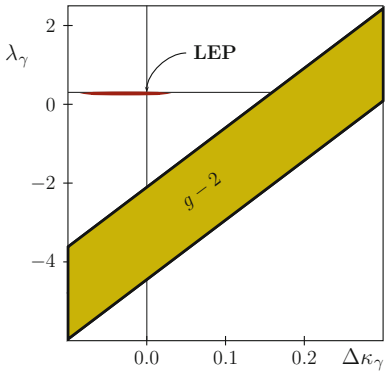

Fig. 7.8 Bounds on triple gauge couplings in $WW\gamma$

7.2.4 Two-Higgs Doublet Models

The minimal SM Higgs structure is very special as it implies automatically a custodial symmetry which predicts $\rho_0 = F_{\rm NC}/G_F = 1$ at three level and FCNCs are automatically highly suppressed. After the discovery of the Higgs particle the search for additional scalars has moved increasingly into focus of present and future collider physics. One possibility of extending the SM is to modify the Higgs sector where one could add scalar singlets, an additional doublet, a Higgs triplet and so on. From a theoretical point of view the case with two Higgs doublets is very attractive. General Two Higgs Doublet Models (2HDM) are interesting as they predict 4 additional physical spin 0 bosons. Two Higgs doublets are needed in Minimal Supersymmetric extensions of the SM (MSSM). One reason is supersymmetry itself, the other is anomaly cancellation of the SUSY partners of the Higgs particles. Our interest here: models with two Higgs doublets give additional contributions to a_μ which could bridge the discrepancy Δa_μ (7.3) [98–102].

While in the SM the complex Higgs doublet field $\Phi_b(x)$ of hypercharge $Y = 1$ and its hypercharge conjugate field $\Phi_t(x) = \mathrm{i}\,\tau_2\,\Phi_b^*$ of hypercharge $Y = -1$ (τ_2 the second 2×2 Pauli matrix) are build with the same two complex fields φ^0 and φ^+, in 2HDMs $\Phi_1(x)$ and $\Phi_2(x)$ are chosen to be two independent fields with hypercharges $Y = (-1, +1)$. A consequence is that 2HDMs exhibit tree level FCNCs, which are in contradiction with experimental findings [96]. In fact, the generic Yukawa Lagrangian with the SM fermionic content gives rise to FCNCs because the fermionic couplings of the two scalar doublets cannot be simultaneously diagonalized in flavor space. Conditions for the absence of FCNCs are well known [103–107] and interestingly FCNCs can be forbidden by a discrete Z_2 symmetry which exchanges the two doublets: $\Phi_1 \leftrightarrow \Phi_2$, the so called R–parity. The latter is also added as an additional selection rule in SUSY extension of the SM. R–parity in SUSY models implies the existence of a lightest SUSY particle (LSP), which is a dark matter candidate.

Here, one should keep in mind that the electroweak SM turned out to be the minimal renormalizable extension of "QED+charged weak current Fermi-theory":

which required neutral currents, local Yang-Mills symmetry (gauge bosons), chiral symmetry, lepton-quark family structure, last but not least the existence of the Higgs boson. Most important in our context, in the SM tree level FCNCs are automatically absent. Not foreseeable was the third fermion family, which however as we know is required for CP violation the be possible the way it appears to be realized. Renormalizability is a natural property which is emergent as a low energy effective phenomenon if the underlying physical system exhibits a physical cut-off, which likely is to be identified with the Planck cut–off (see e.g. [108]). Symmetries like the R–parity, which do not affect renormalizability but are not required by minimality, in such a context are unnatural as they are not emergent as an unavoidable low energy feature, but introduced ad hoc (added by hand).

The scalar potential must share the symmetry $\Phi_2 \to -\Phi_2$. The most general renormalizable Higgs potential is then given by

$$V = m_{11}^2(\Phi_1^+\Phi_1) + m_{22}^2(\Phi_2^+\Phi_2) - m_{12}^2(\Phi_1^+\Phi_2 + \Phi_2^+\Phi_1) + \frac{\lambda_1}{2}(\Phi_1^+\Phi_1)^2 + \frac{\lambda_2}{2}(\Phi_2^+\Phi_2)^2$$
$$+\lambda_3(\Phi_1^+\Phi_1)(\Phi_2^+\Phi_2) + \lambda_4(\Phi_1^+\Phi_2)(\Phi_2^+\Phi_1) + \frac{\lambda_5}{2}\left[(\Phi_1^+\Phi_2)^2 + (\Phi_2^+\Phi_1)^2\right]. \quad (7.24)$$

A soft Z_2 symmetry breaking term $\propto m_{12}^2$ has been added. This implies finite Higgs–mediated FCNCs at one loop and one has a fine tuning problem. Vacuum stability requires

$$\lambda_{1,2} > 0\,, \quad \lambda_3 > -\sqrt{\lambda_1\lambda_2}\,, \quad |\lambda_5| < \lambda_3 + \lambda_4 + \sqrt{\lambda_1\lambda_2}\,.$$

Applicability of perturbation theory requires $|\lambda_i| < \lambda_{\max} \sim 4\pi$.

In terms of the components of the two doublet fields

$$\Phi_i = \begin{pmatrix} \phi_i^+ \\ (v_i + \eta_i + \mathrm{i}\,\chi_i)/\sqrt{2} \end{pmatrix}\;; \quad (i = 1, 2)$$

of fixed hypercharge $Y_i = (-1, +1)$, the new physical scalars are the two scalars h and H, the pseudoscalar A and the charged Higgs bosons $H^\pm$. As an extension of the SM the 2HDM has to be in the broken phase in which both neutral components of the Φ_1 and the Φ_2 fields acquire a vacuum expectation value v_1 and v_2 and the physical states are the result of a mixing mechanism of the physical components of the Φ_i fields which requires diagonalizing the mass matrices. As a consequence mass squares m_{11}^2 and m_{22}^2 are functions of the λ_i's, the v_i's and the Z_2 symmetry breaking parameter m_{12}^2 [106]. The condition for the existence of a global minimum then reads

$$m_{12}^2\left(m_{11}^2 - m_{22}^2\sqrt{\lambda_2/\lambda_2}\right)\left(\tan\beta - (\lambda_1/\lambda_2)^{1/4}\right) > 0\,.$$

The parameter $\tan\beta$ is determined by

$$\tan\beta = \frac{v_2}{v_1} \equiv \frac{v_{\text{top}}}{v_{\text{bottom}}}\ ,\ 0 \le \beta \le \frac{\pi}{2}\ ,$$

where β is the rotation angle which rotates the original doublets into

$$\Phi_1' = \begin{pmatrix} G^+ \\ (v + S_1 + \mathrm{i}\, G^0)/\sqrt{2} \end{pmatrix};\ \Phi_2' = \begin{pmatrix} H^+ \\ (S_2 + \mathrm{i}\, A)/\sqrt{2} \end{pmatrix}\ ,$$

where Φ_2' has a vanishing VEV. Φ_1' may be identified with the SM Higgs field with vacuum expectation value $v = (v_1^2 + v_2^2)^{1/2}$. The fields $G^\pm$ and G^0 can be gauged away and hence represent the unphysical SM Higgs ghosts, absent in the unitary gauge.

The physical scalars are the charged Higgses $H^\pm$, a pseudoscalar A and two physical scalars H and h which are given by mixing of η_1 and η_2 with mixing angle α:

$$\begin{aligned} H^\pm &= -\sin\beta\ \phi_1^\pm + \cos\beta\ \phi_2^\pm\,, & H &= \quad \cos\alpha\ \eta_1 + \sin\alpha\ \eta_2\,, \\ A &= -\sin\beta\ \chi_1 + \cos\beta\ \chi_2\,, & h &= -\sin\alpha\ \eta_1 + \cos\alpha\ \eta_2\ . \end{aligned}$$

Accordingly, the neutral fields S_i

$$\begin{aligned} S_1 &= \cos(\alpha-\beta)\ H - \sin(\alpha-\beta)\ h\,, & H &= \cos(\beta-\alpha)\, S_1 - \sin(\beta-\alpha)\, S_2\,, \\ S_2 &= \sin(\alpha-\beta)\ H + \cos(\alpha-\beta)\ h\,, & h &= \sin(\beta-\alpha)\, S_1 + \cos(\beta-\alpha)\, S_2\,, \\ S_3 &= A\,, & A &= S_3 \end{aligned}$$

couple to the gauge bosons identical as the Higgs in the SM, and we easily find the couplings for H and h, which simply pick factors $\cos(\alpha-\beta)$ and $\pm\sin(\alpha-\beta)$ e.g. $VVH \to VVH\ \cos(\alpha-\beta) - VVh\ \sin(\alpha-\beta)$ $(V = W, Z)$. The inverse transformation we write

$$\phi_i(x) = \mathcal{R}_{ij} S_j(x)\ ;\quad \phi_i(x) = h(x), H(x), A(x). \tag{7.25}$$

In the CP violating case h and H would also mix with A [109]. Whereas β only depends on the ratio of the vacuum expectation values, α depends on all the parameters of the Higgs potential, $\tan 2\alpha = \frac{v_1 v_2(\lambda_3+\lambda_4+\lambda_5)}{2\lambda_2 v_2^2 - 2\lambda_1 v_1^2}$ $(-\frac{\pi}{2} \le \alpha \le 0)$.

In the phenomenologically interesting region of enhanced $\tan\beta$ together with a light Higgs for the CP-even part of the Higgs sector we have $\beta - \alpha - \pi/2 \equiv \eta$ small. Actually, for $\beta - \alpha = \pi/2$ the two scalars h and H are completely separated in the two doublets Φ_i', such that h has identical couplings as the SM Higgs boson and $\eta = 0$ is called the SM limit of a 2HDM. In this case the couplings of the light CP-even neutral Higgs h with the gauge bosons and fermions have the SM values. In fact, the measured signal strengths and production cross section of such a particle are in very good agreement with the corresponding SM predictions [110–122]. While h corresponds to the SM Higgs boson the second scalar is often denoted by H_1 in order to distinguish it from the SM Higgs boson H. Thus, $M_{H_1} > M_h$ and $M_h = m_H^{\text{SM}}$.

The 2HDM potential shares eight free parameters $\lambda_{i=1,\cdots,5}$, m_{11}^2, m_{22}^2 and m_{12}^2, seven more than the SM Higgs potential, which has two free parameters λ and the VEV v. The Higgs mass is then given by $m_H^2 = \lambda\, v^2/3$. Now, the mass–coupling relations include the four scalar masses the two mixing parameters α and β and v and read [104–106, 123, 124]

$$\begin{aligned}
\lambda_1 &= \frac{M_H^2\, c_\alpha^2 + M_h^2\, s_\alpha^2 - m_{12}^2\, t_\beta}{v^2 c_\beta^2}\,, \\
\lambda_2 &= \frac{M_H^2\, s_\alpha^2 + M_h^2\, c_\alpha^2 - m_{12}^2\, t_\beta^{-1}}{v^2 s_\beta^2}\,, \\
\lambda_3 &= \frac{(M_H^2 - M_h^2)\, c_\alpha s_\alpha + 2M_{H^\pm}\, s_\beta c_\beta - m_{12}^2}{v^2 s_\beta c_\beta}\,, \\
\lambda_4 &= \frac{(M_A^2 - 2M_{H^\pm}^2)\, s_\beta c_\beta + m_{12}^2}{v^2 s_\beta c_\beta}\,, \\
\lambda_5 &= \frac{m_{12}^2 - M_A^2\, s_\beta c_\beta}{v^2 s_\beta c_\beta}\,,
\end{aligned} \tag{7.26}$$

where $s_\alpha = \sin\alpha$, $c_\alpha = \cos\alpha$, $s_\beta = \sin\beta$, $c_\beta = \cos\beta$ and $t_\beta = \tan\beta$. The potential minimum conditions fix the potential masses to values [106]

$$\begin{aligned}
m_{11}^2 &= m_{12}^2\, t_\beta - \frac{1}{2}\, v^2 \left[\lambda_1\, c_\beta^2 + (\lambda_3 + \lambda_4 + \lambda_5)\, s_\beta^2\right], \\
m_{22}^2 &= m_{12}^2\, t_\beta^{-1} - \frac{1}{2}\, v^2 \left[\lambda_2\, s_\beta^2 + (\lambda_3 + \lambda_4 + \lambda_5)\, c_\beta^2\right].
\end{aligned}$$

The vacuum stability and perturbativity $|\lambda_i| < \lambda_{\max}$ conditions put sever constraints on the admitted mass ranges, in particular the mass difference $M_H - M_{H^\pm}$ is severely constraint as a function of M_A (see e.g. Fig. 1 in [125]).

In 2HDMs many new real and virtual processes, like $W^\pm H^\mp \gamma$ transitions, are the consequence. The non–observation of processes like $\Upsilon \to H + \gamma$ sets stringent lower bounds on the scalar masses. Together with the LEP bounds this prevents large 2HDM contribution to a_μ. Present bounds on scalars are $M_{H^\pm} > 80$ GeV, $M_A > 93$ GeV and $M_{H_1} > 93$ GeV. In general, in type I models, fermions get contributions to their masses from the VEVs of both Higgs scalars. Phenomenologically preferred and most interesting are the type II models where a discrete symmetry guarantees that the upper and the lower entries of the fermion doublets get their masses from different VEVs ($m_t \propto v_2$, $m_b \propto v_1$) in order to prevent FCNCs [103]. Only the type II models satisfy the MFV criterion. Such models are also interesting because one easily may get $m_t \gg m_b$ without having vastly different Yukawa couplings. Anyway, the possibility of two Higgs doublets is an interesting option and therefore has been studied extensively [98, 99, 101, 102, 124–128] in the past. We assume couplings of the 2HDMs to be real (CP conserving case), for a discussion of the complex case see [129, 130].

The naming of 2HDMs has been changed recently [125, 131]: as already mentioned a major constraint on 2HDMs is the absence/suppression of FCNCs. Requiring "Natural Flavor Conservation" (NFC)[11] restricts the models to four different classes (so called aligned models A2HDMs) which differ by the manner in which the Higgs doublets couple to fermions [106, 129, 132]. They are organized via discrete symmetries like Z_2 under which different matter sectors, such as right-handed leptons or left-handed quarks, have different charge assignments.

For flavor conserving A2HDMs, the non-diagonal neutral couplings can be eliminated by requiring the alignment in flavor space of the Yukawa matrices [131]: the two Yukawa matrices which couple to a given type of right-handed fermions are assumed to be proportional to each other and can, therefore, be diagonalized simultaneously. The three proportionality parameters ζ_f ($f = u, d, l$) are arbitrary complex numbers and introduce new sources of CP violation. We consider the CP conserving case with real ζ's only.

One considers type I, II, X and Y models depending on the possible implementations of the Yukawa couplings which we denote as $\mathrm{y}_f^\phi \frac{m_f}{v} \bar{f} f \phi$ for the scalars $\phi = h, H$ and as $\mathrm{i}\,\mathrm{y}_f^A \frac{m_f}{v} \bar{f} \gamma_5 f A$ for the pseudoscalar A. In terms of the fermion mass-eigenstates fields, the Yukawa interactions of the A2HDM read

$$\begin{aligned}\mathcal{L}_Y = \sqrt{2}\, H^+ \left(\bar{u}\left[V_{\mathrm{CKM}}\, y_d^A\, P_R + y_u^A\, V_{\mathrm{CKM}}\, P_L\right] d \,+ \bar{\nu} y_l^A P_R l\right) \\ - \sum_{i=h,H,A,\ f=u,d,l} \phi_i\ \bar{f}\ y_f^i\ P_R f \,+\ \text{h.c.}\,,\end{aligned} \tag{7.27}$$

where $P_{R,L} \equiv \frac{1\pm\gamma_5}{2}$ are the right-handed and left-handed chirality projectors. The normalized Yukawa couplings are then given by $\mathrm{y}_{d,l}^i = \mathcal{R}_{i1} + (\mathcal{R}_{i2} + \mathrm{i}\ \mathcal{R}_{i3})\ \zeta_{d,l}$ and $\mathrm{y}_u^i = \mathcal{R}_{i1} + (\mathcal{R}_{i2} - \mathrm{i}\ \mathcal{R}_{i3})\ \zeta_u^*$ and the standard ones by

$$y_f^i = \mathrm{y}_f^i\, m_f/v\ ; \quad \begin{array}{l} \mathrm{y}_f^h = \sin(\beta-\alpha) + \cos(\beta-\alpha)\,\zeta_f \\ \mathrm{y}_f^H = \cos(\beta-\alpha) - \sin(\beta-\alpha)\,\zeta_f\,. \\ \mathrm{y}_{d,l}^A = -\zeta_{d,l}\ ,\ \ \mathrm{y}_u^A = \zeta_u \end{array} \tag{7.28}$$

The Z_2 breaking parameter η affects only the couplings $\mathrm{y}_f^h = 1 + \eta\,\zeta_f$ and $\mathrm{y}_f^H = -\zeta_f + \eta$. The possibilities are listed in Table 7.6 For the type II model the relevant couplings read

$$\begin{array}{lll} H\bar{f}f, & f = b, t & -\frac{g}{2}\left(\frac{m_b}{M_W}\frac{\cos\alpha}{\cos\beta},\ \frac{m_t}{M_W}\frac{\sin\alpha}{\sin\beta}\right) \\ h\bar{f}f, & f = b, t & -\frac{g}{2}\left(-\frac{m_b}{M_W}\frac{\sin\alpha}{\cos\beta},\ \frac{m_t}{M_W}\frac{\cos\alpha}{\sin\beta}\right) \\ A\bar{f}\,\mathrm{i}\,\gamma_5 f, & f = b, t & -\frac{g}{2}\left(\ \frac{m_b}{M_W}\tan\beta,\ \ \frac{m_t}{M_W}\cot\beta\right) \\ H^+\bar{t}\,b & & \frac{g}{\sqrt{2}}\left(\ \frac{m_b}{M_W}\tan\beta\,\frac{1+\gamma_5}{2} + \frac{m_t}{M_W}\cot\beta\,\frac{1-\gamma_5}{2}\right) V_{tb}\ . \end{array} \tag{7.29}$$

[11] In my opinion "natural" here is misleading. Imposing ad hoc Z_2 selection rules have no natural explanation.

Table 7.6 The normalized Yukawa couplings of the neutral bosons to up- and down-type quarks and charged leptons. The usual Yukawa couplings are $y_f^i = \mathrm{Y}_f^i \, m_f/v$

	$\mathrm{Y}_u^A = \zeta_u$	$\mathrm{Y}_d^A = -\zeta_d$	$\mathrm{Y}_l^A = -\zeta_l$	Y_u^H	Y_d^H	Y_l^H	Y_u^h	Y_d^h	Y_l^h
Type I	$\cot\beta$	$-\cot\beta$	$-\cot\beta$	$\frac{\sin\alpha}{\sin\beta}$	$\frac{\sin\alpha}{\sin\beta}$	$\frac{\sin\alpha}{\sin\beta}$	$\frac{\cos\alpha}{\sin\beta}$	$\frac{\cos\alpha}{\sin\beta}$	$\frac{\cos\alpha}{\sin\beta}$
Type II	$\cot\beta$	$\tan\beta$	$\tan\beta$	$\frac{\sin\alpha}{\sin\beta}$	$\frac{\cos\alpha}{\cos\beta}$	$\frac{\cos\alpha}{\cos\beta}$	$\frac{\cos\alpha}{\sin\beta}$	$-\frac{\sin\alpha}{\cos\beta}$	$-\frac{\sin\alpha}{\cos\beta}$
Type X	$\cot\beta$	$-\cot\beta$	$\tan\beta$	$\frac{\sin\alpha}{\sin\beta}$	$\frac{\sin\alpha}{\sin\beta}$	$\frac{\cos\alpha}{\cos\beta}$	$\frac{\cos\alpha}{\sin\beta}$	$\frac{\cos\alpha}{\sin\beta}$	$-\frac{\sin\alpha}{\cos\beta}$
Type Y	$\cot\beta$	$\tan\beta$	$-\cot\beta$	$\frac{\sin\alpha}{\sin\beta}$	$\frac{\cos\alpha}{\cos\beta}$	$\frac{\sin\alpha}{\sin\beta}$	$\frac{\cos\alpha}{\sin\beta}$	$-\frac{\sin\alpha}{\cos\beta}$	$\frac{\cos\alpha}{\sin\beta}$

The masses in units of v: $m_f/v = \frac{g}{2}\frac{m_f}{M_W}$ with g the $SU(2)$ SM gauge coupling.

The SM Higgs contribution (4.48) is tiny, due to the fact that the $H\bar{\mu}\mu$ Yukawa coupling $y_\mu = \sqrt{2}\, m_\mu/v$ is very small because the SM Higgs VEV is large: $v = 246.221(1)$ GeV. In 2HDMs of type II and type X the Yukawa couplings may be enhanced by large factors $\tan\beta = v_2/v_1$. This is particularly important for the heavier fermions. It is evident that if 2HDMs are expected to explain Δa_μ, then only models of type II and X have a chance to do so.

The couplings for the other fermions are given by analogous expressions. For example, the coupling for the τ may be obtained by substituting $m_t \to 0, \quad m_b \to m_\tau$.

A class of 2HDMs also exists where one of the Higgs doublets does not participate in the dynamics and remains *inert* [133, 134]. Finally, in the so-called type III models (previously type I) both up and down fermions couple to both Higgs doublets. A detailed analysis of flavor and CP violation in type III models can be found in [135] and references therein.

The parameter space compatible with collider and flavor physics data has been updated in [125]: the direct LEP bound is $M_{H^\pm} > 80$ GeV, however, given (7.8) the 2HDM calculation of the decay rates of the radiative quark–level transitions $b \to s\gamma$ $b \to d\gamma$ and their CP-conjugates for type II models yields a $\tan\beta$–independent bound of $M_{H^\pm} > 580$ GeV [136]. Constraints from LHC data on the alignment parameters ζ_f are [121]:

$$0 < |\zeta_u| < 1.2\,, \qquad 0 < |\zeta_d| < 50\,, \qquad 0 < |\zeta_l| < 100\,. \tag{7.30}$$

The complete 1–loop result (see Fig. 7.9a) reads [79, 80, 137]

$$a_\mu^{(2)\,\mathrm{2HDM}} = \frac{G_\mu\, m_\mu^2}{4\pi^2\sqrt{2}} \sum_j \left(\mathrm{Y}_\mu^j\right)^2 r_\mu^j \, f_j(r_\mu^j), \tag{7.31}$$

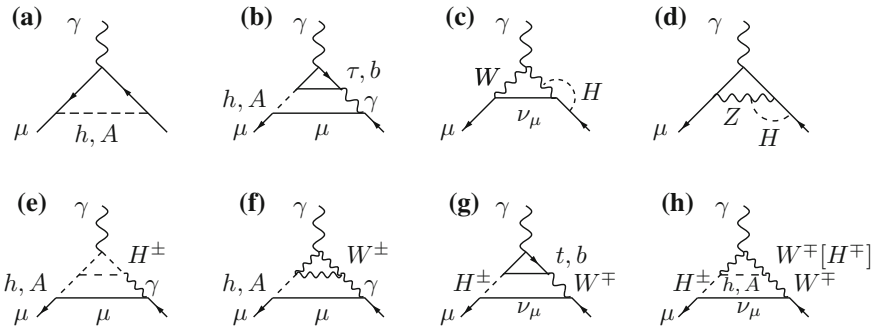

Fig. 7.9 Leading 2HDM graphs **a** and **b** contributing to a_μ. Diagrams **c** and **d**, with $H \to h, H, A$, are examples of subleading bosonic contributions which are modified with respect to the SM weak bosonic contributions due to the extended Higgs structure. Graphs **e**–**h** have been shown to give substantial contributions as well [109, 124]

where $j = \{h, H, A, H^\pm\}$, $r_\mu^j = m_\mu^2/M_j^2$, and

$$\begin{aligned} f_{h,H}(r) &= \int_0^1 \mathrm{d}x\, \frac{x^2(2-x)}{1-x+rx^2} = -\ln r - 7/6 + O(r), \\ f_A(r) &= \int_0^1 \mathrm{d}x\, \frac{-x^3}{1-x+rx^2} = +\ln r + 11/6 + O(r), \\ f_{H^\pm}(r) &= \int_0^1 \mathrm{d}x\, \frac{-x(1-x)}{1-(1-x)r} = -1/6 + O(r). \end{aligned} \tag{7.32}$$

The normalized Yukawa couplings $y_\mu^{h,H,A}$ are listed in Table 7.6, and $y_\mu^{H^\pm} = y_\mu^A$. In any case we have $r \ll 1$ such that $f_{H^\pm}(r)$ is small relative to $f_{h,H,A}(r)$.

In case $\alpha \approx \beta$ the enhanced terms are (see (7.25))

$$\begin{aligned} a_\mu^{(2)\,\mathrm{2HDM}}(h) &\simeq \frac{G_\mu m_\mu^2}{4\pi^2\sqrt{2}} \tan^2\beta\, \frac{m_\mu^2}{M_h^2} \left(\ln\frac{M_h^2}{m_\mu^2} - \frac{7}{6}\right) > 0\,, \\ a_\mu^{(2)\,\mathrm{2HDM}}(A) &\simeq \frac{G_\mu m_\mu^2}{4\pi^2\sqrt{2}} \tan^2\beta\, \frac{m_\mu^2}{M_A^2} \left(-\ln\frac{M_A^2}{m_\mu^2} + \frac{11}{6}\right) < 0, \\ a_\mu^{(2)\,\mathrm{2HDM}}(H^\pm) &\simeq \frac{G_\mu m_\mu^2}{4\pi^2\sqrt{2}} \tan^2\beta\, \frac{m_\mu^2}{M_{H^\pm}^2} \left(-\frac{1}{6}\right) < 0. \end{aligned} \tag{7.33}$$

Since we need a positive contribution M_A and $M_{H^\pm}$ must be large (above 100 GeV) in order to make the negative contribution small and the contribution is entirely due to the light scalar h, the mass of which we identify with the 125 GeV resonance found at CERN. This then is the SM Higgs contribution (4.48) enhanced by $\tan^2\beta$. If this should match Δa_μ it would require the unreasonably large value $\tan\beta \approx 380$.

When considering the case $\beta - \alpha \approx \pi/2$, in which h has the same couplings as the SM Higgs boson, h appears replaced by H relative to the $\sin(\beta - \alpha) \approx 0$ case of (7.33). In the decoupling limit, $M_H \simeq M_A \simeq M_{H^\pm}$ [the mass differences are of $O(M_Z^2/M_A)$] we then get

$$a^{(2)\,\mathrm{2HDM}} \simeq \frac{G_\mu m_\mu^2}{4\pi^2\sqrt{2}} \tan^2\beta \, \frac{m_\mu^2}{M_A^2} \left(\frac{1}{2} - \frac{2m_\mu^2}{M_A^2} \ln \frac{M_A^2}{m_\mu^2} \right). \tag{7.34}$$

The contribution of h is not $\tan\beta$-enhanced and is thus negligible and part of a_μ^{EW} already. For 100 GeV $< M_A <$ 1000 GeV, and $30 < \tan\beta < 100$, the 2HDM contribution to a_μ ranges from about 1.3×10^{-11} to 2.1×10^{-14}, which in the best case is two orders of magnitude below what is needed to explain the BNL measurement of a_μ.

At 2–loops the Barr-Zee diagrams Fig. 7.9 can yield an enhanced contribution, which can exceed the 1–loop result substantially. The enhancement factor m_b^2/m_μ^2 actually compensates the suppression by α/π as $(\alpha/\pi) \times (m_b^2/m_\mu^2) \sim 4 > 1$. For the type II case diagram Fig. 7.9b dominates and yields

$$a_\mu^{(4)\,\mathrm{2HDM-BZ}}(h, A) = \frac{G_\mu\, m_\mu^2}{4\pi^2\,\sqrt{2}} \frac{\alpha}{\pi} \sum_{i=h,H,A;\, f} N_{cf}\, Q_f^2\, Y_\mu^i Y_f^i\, r_f^i\, g_i(r_{if}), \tag{7.35}$$

with $r_{if} = m_f^2/M_i^2$ $(i = h, H, A)$ and

$$\begin{aligned} g_{h,H}(r) &= \int_0^1 \mathrm{d}x\, \frac{2x\,(1-x)-1}{x\,(1-x)-r} \ln \frac{x\,(1-x)}{r} = -2\,(\ln r + 2) + (2r-1)\, g_A(r), \\ g_A(r) &= \int_0^1 \mathrm{d}x\, \frac{1}{x\,(1-x)-r} \ln \frac{x\,(1-x)}{r} = \frac{2}{y} \left\{ \mathrm{Li}_2\left(1 - \frac{1-y}{2r}\right) - \mathrm{Li}_2\left(1 - \frac{1+y}{2r}\right) \right\}, \end{aligned} \tag{7.36}$$

with $y = \sqrt{1-4r}$.

In [109] the complete set of Barr-Zee type diagrams Fig. 7.9 have been calculated for the first time. Using the effective vertices from the previous section for calculating the second loop, ignoring suppressed terms proportional to higher powers of m_μ^2/M^2 (with M a *heavy* mass) in the numerator and the muon mass in the denominator, we obtain the various contributions to the anomalous magnetic moment of the muon:

$$\Delta a_\mu^{(b)} = \sum_{i,f} \frac{\alpha\,\sqrt{2}\,G_\mu\, m_\mu^2}{4\,\pi^3}\, N_c^f\; Q_f^2\; Y_f^i\, Y_l^i\; F^{(1)}\left(\frac{m_f^2}{M_i^2}\right), \tag{7.37}$$

$$\Delta a_\mu^{(e)} = \sum_i \frac{\alpha\, m_\mu^2}{8\,\pi^3\, M_i^2}\, Y_l^i\, \lambda_{\phi_i H^+ H^-}\; F^{(2)}\left(\frac{M_{H^\pm}^2}{M_i^2}\right). \tag{7.38}$$

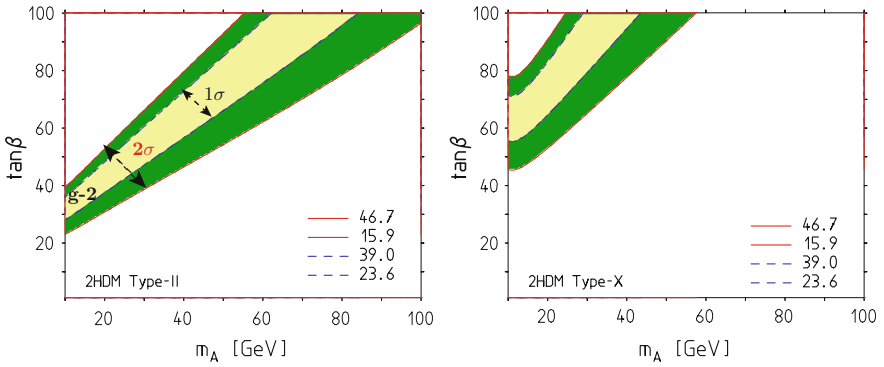

Fig. 7.10 Parameter ranges where the A2HDMs of type II or type X could explain Δa_μ. Predictions including relevant effects from leading Barr-Zee diagrams of Fig. 7.9 for $M_H = M_{H^\pm} = 500$ GeV. For small m_{12}^2 the perturbativity constraints $\lambda_1, \lambda_2 < 4\pi$ can barely be satisfied for large M_H, $M_{H^\pm}$. See [125] for details

$$\Delta a_\mu^{(f)} = \sum_i \frac{\alpha\,\sqrt{2}\,G_\mu m_\mu^2}{8\,\pi^3}\,\mathrm{y}_l^i\;\mathcal{R}_{i1}\;F^{(3)}\!\left(\frac{M_W^2}{M_i^2}\right). \tag{7.39}$$

$$\Delta a_\mu^{(g)} = \frac{\alpha\,\sqrt{2}\,G_\mu\,m_\mu^2\,N_c\,|V_{tb}|^2}{32\,\pi^3\,s_W^2\,(M_{H^\pm}^2 - M_W^2)} \int_0^1 \mathrm{d}x\,\Big[\,Q_t x + Q_b(1-x)\,\Big]$$
$$\times\,\Big[\zeta_d\zeta_l\,m_b^2 x(1-x) + \zeta_u\zeta_l\,m_t^2 x(1+x)\Big]\Big[\mathcal{G}\Big(\frac{m_t^2}{M_{H^\pm}^2},\frac{m_b^2}{M_{H^\pm}^2}\Big) - \mathcal{G}\Big(\frac{m_t^2}{M_W^2},\frac{m_b^2}{M_W^2}\Big)\Big], \tag{7.40}$$

$$\Delta a_\mu^{(h_1)} = \frac{\alpha\,\sqrt{2}\,G_\mu\,m_\mu^2}{64\,\pi^3\,s_W^2\,(M_{H^\pm}^2 - M_W^2)} \sum_i \Big[\zeta_l\,\mathcal{R}_{i1}(\mathcal{R}_{i2} - \mathrm{i}\,\mathcal{R}_{i3})\Big] \int_0^1 \mathrm{d}x\,x^2$$
$$\times\,\Big[\,(M_{H^\pm}^2 + M_W^2 - M_i^2)(1-x) - 4M_W^2\,\Big]\Big[\mathcal{G}\Big(\frac{M_W^2}{M_{H^\pm}^2},\frac{M_i^2}{M_{H^\pm}^2}\Big) - \mathcal{G}\Big(1,\frac{M_i^2}{M_W^2}\Big)\Big], \tag{7.41}$$

$$\Delta a_\mu^{(h_2)} = \frac{\alpha\,m_\mu^2}{64\,\pi^3\,s_W^2\,(M_{H^\pm}^2 - M_W^2)} \sum_i \Big[\zeta_l\,(\mathcal{R}_{i2} - \mathrm{i}\,\mathcal{R}_{i3})\Big]\lambda_{\phi_i H^+ H^-} \int_0^1 \mathrm{d}x\,x^2(x-1)$$
$$\times\,\Big[\mathcal{G}\Big(1,\frac{M_i^2}{M_{H^\pm}^2}\Big) - \mathcal{G}\Big(\frac{M_{H^\pm}^2}{M_W^2},\frac{M_i^2}{M_W^2}\Big)\Big]. \tag{7.42}$$

We denoted $s_W^2 = 1 - M_W^2/M_Z^2$. The needed loop functions are given by:

$$F^{(1)}(r) = \frac{r}{2}\int_0^1 \mathrm{d}x\, \frac{2x(1-x)-1}{x(1-x)-r}\, \ln(x(1-x)/r)\,, \tag{7.43}$$

$$F^{(2)}(r) = \frac{1}{2}\int_0^1 \mathrm{d}x\, \frac{x(x-1)}{x(1-x)-r}\, \ln(x(1-x)/r)\,, \tag{7.44}$$

$$F^{(3)}(r) = \frac{1}{2}\int_0^1 \mathrm{d}x\, \frac{x\,[3x(4x-1)+10]r - x(1-x)}{x(1-x)-r}\, \ln(x(1-x)/r)\,, \tag{7.45}$$

and

$$\mathcal{G}(r_a, r_b) = \frac{\ln\left(\dfrac{r_a\, x + r_b\,(1-x)}{x(1-x)}\right)}{x(1-x) - r_a\, x - r_b\,(1-x)}\,. \tag{7.46}$$

The triple Higgs couplings $\lambda_{\phi_i H^+ H^-}$ deriving from the Higgs potential is given by [138]

$$\lambda_{hH^+H^-} = -\frac{1}{v}\left[\left(M_h^2 - \frac{m_{12}^2}{s_\beta c_\beta}\right)\frac{c_{\beta+\alpha}}{s_\beta c_\beta} + \left(2\,M_{H^\pm}^2 - M_h^2\right)\, s_{\beta-\alpha}\right].$$

The first two contributions are the well known classical results [98–102, 123, 125, 137–141]. The analysis [125] has shown (see Fig. 7.10) that the parameter space of the A2HDMs allows for substantial contributions to the muon $g-2$, when one of the neutral scalars is essentially degenerate with the charged scalar. The constraints from collider and flavor physics only admit the type X model to possibly explain Δa_μ.

A first complete 2–loop A2HDM calculation has been presented recently in [124]. The analysis confirms the results [109, 125] concerning the leading effects, just discussed. However, the bosonic correction calculated for the first time can contribute effects of the size of the future experimental accuracy:

$$a_\mu^{\mathrm{B}} = (2 \cdots 4) \times 10^{-10}$$

for $\eta = 0, 0.1$ constrained by 2×10^{-10} and $\eta = -0.1$ where the larger values are obtained.

As an illustration we present some values for 1–loop and 2–loop contributions separately and for the sum for selected parameters with $M_h = 125$ GeV and choosing $M_{H^\pm} = M_H$ in units of 10^{-11}:

$(M_A, M_H, \tan\beta)$	$a_\mu^{(2)}(H)$	$a_\mu^{(2)}(A)$	$a_\mu^{(4)}(H)$	$a_\mu^{(4)}(A)$	sum
(50, 125, 10)	0.32	−1.09	−2.14	7.19	4.26
(50, 250, 10)	0.17	−1.09	−1.29	7.19	4.96
(50, 500, 10)	0.09	−1.09	−0.77	7.19	5.40
(50, 250, 100)	16.84	− 109.20	− 129.40	718.79	496.94
(50, 500, 100)	8.86	−109.20	−77.16	718.79	541.25
(100, 500, 10)	0.09	−0.31	−0.77	2.70	1.69
(100, 125, 40)	5.11	−4.95	−34.23	43.19	9.06
(100, 250, 40)	2.69	−4.95	−20.70	43.19	20.20

Typically, 1–loop and 2–loop terms as well as CP–even and CP–odd ones enter with alternating signs and there are substantial cancellations. Substantial positive contributions require not only large $\tan\beta$ but also small M_A. The LEP bound is at 90 GeV, and $\tan\beta$ much larger than 40 look not very natural. It is rather unlikely the 2HDMs are the origin of the yet unexplained deviation. If $M_A \sim M_h$ the contributions largely cancel. Given M_h, to get a large $M_A - M_h$ mass splitting requires a large M_A, which however yields a large contribution of the disfavored negative sign. This means that the muon $g-2$ constraint gives a bound on M_A which, however, strongly depends on $\tan\beta$ (see e.g. [101, 102, 128, 138, 142] for a more detailed discussion). Besides the dominant 2-loop contributions from Fig. 7.9b a 2–loop calculation of the 2HDM contributions, including diagrams like Figs. 7.9c, d, within the context of the MSSM has been presented in [15]. The contributions from diagrams Fig. 7.9e–h, depending on the parameters, can change the leading result by about 10%.

If one identifies M_h with m_H of the SM the correction is found to be small: $a_\mu^{\text{bos,2L}}(\text{MSSM} - \text{SM}) < 3 \times 10^{-11}$ in the parameter range $M_A \gtrsim 50$ GeV and $\tan\beta \lesssim 50$. In fact, in the LL approximation, the 2HDM sector in the MSSM at 2–loops does not change the SM result. The reason is that at the 1–loop level the electroweak SM result numerically remains practically unchanged, because the additional 2HDM diagrams all are suppressed by the small Yukawa coupling of the μ (like the SM Higgs contribution).

For an effective field theory approach to 2HDMs I refer to [143].

In summary: A2HDMs exhibit a special narrow corner in parameter space which would allow to explain Δa_μ, namely the type X alignment with a light A of mass about 50 GeV and essentially degenerate $M_H \sim M_{H^\pm}$ of about 200 GeV and a large $\tan\beta \gtrsim 50$. This is a boarder line case and may be excluded by corroborating the LEP limit $M_A > 93$ GeV.

7.2.5 *Supersymmetry*

Supersymmetry (SUSY) is a theoretically very attractive idea, however, should it be realized in nature as a property of the spectrum of elementary particles, the non–observation of any SUSY partner up the present collider energies, tells us that SUSY would be highly broken. Searches at the LHC have pushed up possible SUSY partner

mass limits to the TeV range. While in pre–LHC times SUSY looked to be the perfect candidate for explaining the Δa_μ deviation (7.3), this has changed after the first years of LHC running. Besides the fact that no new physics has been found, the discovery of the Higgs particle with mass 125 GeV has a great impact on SUSY extensions and essentially has excluded the most attractive constrained SUSY scenarios (see e.g. [144–146] and references therein). This does not exclude SUSY as a possible solution of the muon $g-2$ deviation and we will discuss the possibilities in the following.

Supersymmetric extensions of the SM, in particular the Minimal Supersymmetric Standard Model (MSSM), are still a promising possibility for physics beyond the SM. Supersymmetry implements a symmetry mapping

$$\text{boson} \overset{\text{Q}}{\leftrightarrow} \text{fermion}$$

between bosons and fermions, by changing the spin by $\pm 1/2$ units [147]. The SUSY algebra [graded Lie algebra] reads

$$\left\{Q_\alpha, \overline{Q}_\beta\right\} = -2\ (\gamma^\mu)_{\alpha\beta}\ P_\mu\ ;\ P_\mu = (H, \mathbf{P})\,,$$

with P_μ the generators of space–time translations, Q_α four component Majorana (neutral) spinors and $\overline{Q}_\alpha = \left(Q^+\gamma^0\right)_\alpha$ the Pauli adjoint. It represents the only possible non–trivial unification of internal and space–time symmetry in a quantum field theory. The Dirac matrices in the Majorana representation play the role of the structure constants. The SUSY extension of the SM associates with each SM state X a supersymmetric "sstate" $\tilde{X}$ where sfermions are bosons and sbosons are fermions as shown in Table 7.7.

SUSY is a global symmetry imposed on the SM particle spectrum, the SM gauge group remains untouched and there are no new gauge bosons. Also the matter fields remain the same. SUSY and gauge invariance are compatible only if a second Higgs

Table 7.7 The particle spectrum of a MSSM

SM particles ($R_p = +1$)	SUSY partners ($R_p = -1$)	
$\begin{pmatrix}\nu_e\\ e^-\end{pmatrix}_L, \begin{pmatrix}\nu_\mu\\ \mu^-\end{pmatrix}_L, \begin{pmatrix}\nu_\tau\\ \tau^-\end{pmatrix}_L$ $\nu_{eR}, e_R^-, \nu_{\mu R}, \mu_R^-, \nu_{\tau R}, \tau_R^-$	$\begin{pmatrix}\tilde{\nu}_e\\ \tilde{e}^-\end{pmatrix}_L, \begin{pmatrix}\tilde{\nu}_\mu\\ \tilde{\mu}^-\end{pmatrix}_L, \begin{pmatrix}\tilde{\nu}_\tau\\ \tilde{\tau}^-\end{pmatrix}_L$ $\tilde{\nu}_{eR}, \tilde{e}_R^-, \tilde{\nu}_{\mu R}, \tilde{\mu}_R^-, \tilde{\nu}_{\tau R}, \tilde{\tau}_R^-$	Sneutrinos, sleptons
$\begin{pmatrix}u\\ d\end{pmatrix}_L, \begin{pmatrix}c\\ s\end{pmatrix}_L, \begin{pmatrix}t\\ b\end{pmatrix}_L$ $u_R, d_R, c_R, s_R, t_R, b_R$	$\begin{pmatrix}\tilde{u}\\ \tilde{d}\end{pmatrix}_L, \begin{pmatrix}\tilde{c}\\ \tilde{s}\end{pmatrix}_L, \begin{pmatrix}\tilde{t}\\ \tilde{b}\end{pmatrix}_L$ $\tilde{u}_R, \tilde{d}_R, \tilde{c}_R, \tilde{s}_R, \tilde{t}_R, \tilde{b}_R$	Squarks (stop, ...)
$W^\pm, H^\pm$	$\tilde{W}^\pm, \tilde{H}^\pm \to \tilde{\chi}^\pm_{1,2}$	Charginos
γ, Z, h^0, H^0, A^0	$\tilde{\gamma}, \tilde{Z}, \tilde{h}^0, \tilde{H}^0, \tilde{A}^0 \to \tilde{\chi}^0_{1,2,3,4}$	Neutralinos
g, G	$\tilde{g}, \tilde{G}$	Gluino, gravitino

doublet field is introduced where H_1 induces the masses of all down–type fermions and H_2 the masses of all up–type fermions. A second complex Higgs doublet is also required for the anomaly cancellation of the fermionic sboson sector. This means 4 additional scalars (H^0, A^0, $H^\pm$) and their SUSY partners. The lighter neutral scalar denoted by h^0 corresponds to the SM Higgs boson H. Both Higgs fields exhibit a neutral scalar and acquire vacuum expectation values v_1 and v_2. The parameter $\tan\beta = v_2/v_1$ is one of the very important basic parameters as we will see. As $m_t \propto v_2$ and $m_b \propto v_1$ in such a scenario the large mass splitting $m_t/m_b \sim 40$ could be "explained" by a large ratio v_2/v_1, which means a large $\tan\beta$. So values $\tan\beta \sim 40$ look natural.

Digression on Supergravity and SUSY Breaking

A very interesting question is what happens if one attempts to promote global SUSY to local SUSY. Since SUSY entangles internal with space–time symmetries of special relativity, local SUSY implies supergravity (SUGRA) as one has to go from global Poincaré transformation to local ones. This means general coordinate invariance which in turn relates to geometry and gravity according to Einstein's general relativity. SUGRA must include the spin 2 graviton and its superpartner, the spin 3/2 gravitino. Such a QFT is necessarily non–renormalizable [148]. Nevertheless it is attractive to consider the MSSM as a low energy effective theory of a non–renormalizable SUGRA scenario with $M_{\text{Planck}} \to \infty$ [149]. SUSY is spontaneously broken in the hidden sector by fields with no $SU(3)_c \otimes SU(2)_L \otimes U(1)_Y$ quantum numbers and which couple to the observable sector only gravitationally. Denoting by M_{SUSY} the SUSY breaking scale, the gravitino acquires a mass

$$m_{3/2} \sim M^2_{\text{SUSY}}/M_{\text{Planck}}\,,$$

with M_{Planck} the inherent scale of gravity.[12] SUSY is not realized as a perfect symmetry in nature. SUSY partners of the known SM particles have not yet been observed because sparticles in general are heavier than the known particles. Like the SM local G_{SM} symmetry is broken by the electroweak symmetry breaking (EWSB), SUGRA is broken at some higher scale M_{SUSY} by a super–Higgs mechanism. The Lagrangian takes the form

$$\mathcal{L}^{\text{MSSM}} = \mathcal{L}^{\text{SUSY}}_{\text{global}} + \mathcal{L}^{\text{SUSY}}_{\text{breaking}}$$

with

$$\mathcal{L}^{\text{SUSY}}_{\text{global}} = \mathcal{L}^{\text{SUSY}}(SU(3)_c \otimes SU(2)_L \otimes U(1)_Y; W)$$

[12] $M_{\text{Pl}} = (G_N/c\hbar)^{-1/2} \simeq 1.22 \times 10^{19}$ GeV, G_N Newton's gravitational constant, c speed of light, $\hbar$ Planck constant.

with W the following gauge invariant and B and L conserving superpotential[13]

$$W = W_{\rm Y} - \mu H_1 H_2\,;\; W_{\rm Y} = \sum_F (h_U \tilde{Q}_L \tilde{U}^c_L H_2 + h_D \tilde{Q}_L \tilde{D}^c_L H_1 + h_L \tilde{L} \tilde{E}^c_L H_1)$$

(Y = Yukawa; F = families) where[14] $\tilde{Q}_L$ and $\tilde{L}$ denote the $SU(2)_L$ doublets $(\tilde{U}_L, \tilde{D}_L)$, $(\tilde{N}_L, \tilde{E}_L)$ and $\tilde{U}^c_L$, $\tilde{D}^c_L$, $\tilde{E}^c_L$ are the scalar partners of the right–handed quarks and leptons, written as left–handed fields of the antiparticle (^{c} = charge conjugation). $SU(2)_L$ and $SU(3)_c$ indices are summed over. h_U, h_D and h_L are the Yukawa couplings, the complex 3×3 matrices in family space of the SM. In the Minimal Super Gravity (mSUGRA) scheme, also related to the less constrained "Constrained MSSM" (CMSSM) [150], one assumes universality of all soft parameters.[15] The mSUGRA ansatz exhibits super gravity induced SUSY breaking with $m_{3/2} = m_0$ at the bare level. In addition the Kähler flat supergravity relation $B_0 = A_0 - m_0$ implies that $\tan\beta$ in mSUGRA is not a free parameter. So mSUGRA exhibits only 3 free parameters $m_{1/2}$, m_0 and A_0. The LSP in this scenario barely can accommodate the observed dark matter relict density (see [150] and references therein). The CMSSM drops the relation between B_0 and A_0 and assumes B_0 and μ to be quantities related to the EW symmetry breaking scale. In addition there is no relation between m_0 and the gravitino mass.

In this case the SUSY breaking term has the form

$$\mathcal{L}^{\rm SUSY}_{\rm breaking} = -m^2 \sum_i |\varphi_i|^2 - M \sum_a \lambda_a \lambda_a + (A\, m\, W_{\rm Y} - B\, m\, \mu H_1 H_2 + \text{h.c.})\,.$$

[13] One could add other gauge invariant couplings like

$$(\tilde{U}^c_L \tilde{D}^c_L \tilde{D}^c_L)\,,\; (\tilde{Q}_L \tilde{L} \tilde{D}^c_L)\,,\; m(\tilde{L} H_2)\,,\; (\tilde{L} \tilde{L} \tilde{E}^c_L)$$

which violate either B or L, however. In the minimal model they are absent.

[14] We label $U = (u, c, t)$, $D = (d, s, b)$, $N = (\nu_e, \nu_\mu, \nu_\tau)$ and $E = (e, \mu, \tau)$.

[15] Even with the constraints mentioned, SUSY extensions of the SM allow for about 100 free symmetry breaking parameters. Free parameters typically are masses and mixings of the neutralinos, the higgsino mass μ (the $+\mu H_1 H_2$ term of the 2HDM Higgs potential) and $\tan\beta$. This changes if one merges GUT concepts with SUSY, in fact SUSY-GUTs (e.g. as based on $SU(5)$) are the only theories which allow for grand unification broken at a low scale (∼1 TeV). This provides strong constraints on the SUSY breaking mechanism, specifically we distinguish the constrained CMSSM a SUSY-GUT with soft breaking masses universal at the GUT scale. The NUHM is as CMSSM with non-universal Higgs masses: • the CMSSM defined to have universal couplings at the GUT scale has the free parameters: m_0, $m_{1/2}$, A_0, $\tan\beta$ and $\text{sign}(\mu)$. • NUHM1 considers M_A as an additional free parameter at the EW scale. • NUHM2 in addition assumes μ to be independent at the EW scale. These models assume many degeneracies of masses and couplings in order to restrict the number of parameters. Typically, SM parameters are supplemented by $m_{1/2}$ (scalar-matter mass, like $m_{\tilde{q}}$, $m_{\tilde{\ell}}$), m_0 (the $U(1)_Y \otimes SU(2)_L$ gaugino masses, $m_{\tilde{\gamma}}$, $m_{\tilde{Z}}$, $m_{\tilde{W}}$ and gluino mass $m_{\tilde{g}}$), $\text{sign}(\mu)$, $\tan\beta$, A (trilinear soft breaking term), and more for less constrained models.

The essential new parameters are

- μ the supersymmetric higgsino mass
- m is the universal mass term for all scalars φ_i
- M is the universal mass term to all gauginos λ_a
- A, B are the breaking terms in the superpotential W.

Thus in addition to the SM parameters we have 5 new parameters

$$\mu, m, M, A \text{ and } B.$$

The SUSY breaking lifts the degeneracy between particles and sparticle and essentially makes all sparticles to be heavier than all particles.

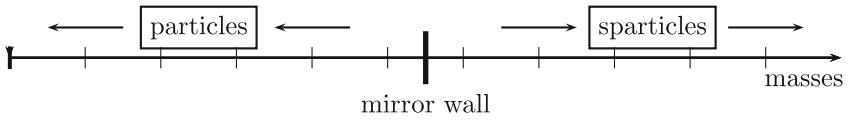

This scenario leads to universal masses for all SUSY partners:

- s–matter: $m_{\tilde{q}} = m_{\tilde{\ell}} = m_{\tilde{H}} = m_{1/2}$
- gauginos: $M_3 = M_2 = M_1 = m_0$

where M_3, M_2 and M_1 are the mass scales of the spartners of the gauge bosons in $SU(3)_c$, $SU(2)_L$ and $U(1)_Y$, respectively. The non–observation of any sparticles so far requires a mass bound of about $m_{3/2}, m_{1/2}, m_0 \sim 100 \div 1000$ GeV , which is of the order of the weak scale 246 GeV or higher.

In general one expects different masses for the different types of gauginos:

- M' the $U(1)_Y$ gaugino mass
- M the $SU(2)_L$ gaugino mass
- $m_{\tilde{g}}$ the $SU(3)_c$ gluino mass.

However, the grand unification assumption

$$M' = \frac{5}{3}\tan^2\Theta_W\, M \;= \frac{5}{3}\frac{\alpha}{\cos^2\Theta_W\,\alpha_s}\, m_{\tilde{g}}\,,$$

with $\sin^2\Theta_W = 1 - M_W^2/M_Z^2$, leads back to the CMSSM scenario. A very attractive feature of this scenario is the fact that the known SM Yukawa couplings now may be understood by evolving couplings from the GUT scale down to low energy by the corresponding RG equations. One interesting outcome is that the Higgs mechanism gets triggered naturally as one of the running mass squares, the one of the Higgs boson, gets negative for appropriate regions in SUSY parameter space (there exist no–EWSB ranges as well). This also implies the form of the muon Yukawa coupling $y_\mu \propto \tan\beta$, as

$$y_\mu = \frac{m_\mu}{v_1} = \frac{m_\mu\, g_2}{\sqrt{2} M_W\, \cos\beta} \tag{7.47}$$

where $g_2 = e/\sin\Theta_W$ and $1/\cos\beta \approx \tan\beta$. This enhanced coupling is central for the discussion of the SUSY contributions to a_μ. In spite of the fact that SUSY and GUT extensions of the SM have completely different motivations and in a way are complementary, supersymmetrizing a GUT is very popular as it allows coupling constant unification together with a low GUT breaking scale which promises nearby new physics. Actually, supersymmetric $SU(5)$ circumvents the problems of the normal $SU(5)$ GUT and provides a viable phenomenological framework. The extra GUT symmetry requirement is attractive also because it reduces the number of independent parameters. The discovery of the Higgs boson of mass 125 GeV, which requires large squark masses in a SUSY extension of the SM, and the fact that no non-SM particle has been found at the LHC, largely rules out scenarios like the CMSSM. Nevertheless, such minimal scenarios may provide a viable starting point for proceeding with less constrained non-minimal SUSY models.

End of the Digression

While supersymmetrizing the SM fixes all gauge and Yukawa couplings of the sparticles (see Fig. 7.11), there are a lot of free parameters to fix the SUSY breaking and masses, such that mixings of the sparticles remain quite arbitrary: the mass eigenstates of the gaugino–Higgsino sector are obtained by unitary transformations which mix states with the same conserved quantum numbers (in particular the charge)

$$\chi_i^+ = V_{ij}\psi_j^+\,,\ \chi_i^- = U_{ij}\psi_j^-\,,\ \chi_i^0 = N_{ij}\psi_j^0 \tag{7.48}$$

where ψ_j^a denote the spin 1/2 sparticles of the SM gauge bosons and the two Higgs doublets. In fact, a SUSY extension of the SM in general exhibits more than 100 parameters, while the SM has 28 including masses and mixings parameters of the neutrinos. Also, in general SUSY extensions of the SM lead to tree level FCNCs and unsuppressed non-CKM type CP–violation, which both are absent in the SM, in agreement with observation. Actually, just a SUSY extension of the SM, while solving the pretended naturalness problem of the SM Higgs sector [151], creates its own naturalness problem as it leads to proton decay and the evaporation of baryonic matter in general. An elegant way to get rid of the latter problem is to impose the so called R–parity, which assigns $R_p = +1$ to all normal particles and $R_p = -1$ to all sparticles. If R–parity is conserved sparticles can only be produced in pairs and there must exist a stable Lightest Supersymmetric Particle (LSP), the lightest neutralino. Thus all sparticles at the end decay into the LSP plus normal matter. The LSP is

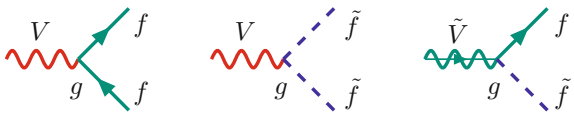

Fig. 7.11 Yukawa coupling = gauge coupling in the MSSM

a Cold Dark Matter (CDM) candidate [152] if it is neutral and colorless. From the precision mapping of the temperature and polarization anisotropies in the Cosmic Microwave Background (CMB), the Planck Collaboration has determined the relict density of cold dark matter to [96, 153, 154]

$$\Omega_{\rm CDM} = \rho_{\rm CDM}/\rho_{\rm crit} = 0.1186(20)\mathrm{h}^{-2} = 0.258(11). \tag{7.49}$$

This sets severe constraints on the SUSY parameter space [155–157]. Note that SUSY is providing a new source for CP–violation, which could help in understanding the matter–antimatter asymmetry $n_B = (n_b - n_{\bar{b}})/n_\gamma \simeq 6 \times 10^{-10}$ observed in our world.

However, what should cause R–parity to be conserved is another question. It just means that certain couplings one usually would assume to be there naturally are excluded. If R is not conserved sparticles may be produced singly and the LSP is not stable and would not provide a possible explanation of CDM. Then also (7.49) would not provide information on SUSY parameters.

The main theoretical motivation for a supersymmetric extension of the SM is the **hierarchy** or **naturalness** problem[16] of the latter: chiral symmetry requires fermions to be massless, local gauge symmetries require the gauge bosons to be massless, so the only SM particle which is not required to be massless, before the spontaneous symmetry breaking by the Higgs mechanism, is the scalar Higgs boson, together with the mass–degenerate later Higgs–ghosts (all fields in the Higgs doublet). This argument, however, only is true in the symmetric phase. In the broken phase, triggered by a negative bare Higgs potential mass square term, all masses including the Higgs particle itself, exhibit a mass proportional to the Higgs VEV v according to (4.46). Therefore, the Higgs mass in the broken phase cannot be expected to be much larger than the heavier of the SM particles, unless the dimensionless Higgs self-coupling λ for unknown reasons would be much larger than the gauge couplings or the top quark Yukawa coupling. What is actually tuned when renormalizing the Higgs mass is λ because v is given as the universal electroweak scale, which is determined by the Fermi constant, an object independent of any SM interaction parameters at leading order or to all orders by definition. The Higgs VEV v is to be viewed as an orderparameter, which breaks the symmetry of the vacuum (by a collective long range order) and has no direct correlation to the short distance cutoff, which is the Planck mass if one equips the bare SM with a Planck cutoff (see [108, 151]).

[16] Stating that a small parameter (like a small mass) is unnatural unless the symmetry is increased by setting it to zero. The equivalent hierarchy problem addresses the fine–tuning problem encountered in Higgs mass renormalization: the renormalized (observed) low energy effective mass square

$$m^2_{\rm ren} = m^2_{\rm bare} - \delta m^2$$

is $O(v^2)$ of the order of the electroweak scale square, while in the bare theory exhibiting the Planck mass as a UV cutoff, $m^2_{\rm bare}$ and the counterterm δm^2 are of order $\Lambda^2_{\rm Planck}$. So the observed Higgs mass appears as a highly fine–tuned difference of two very large numbers. Exact supersymmetry eliminates the fine–tuning by canceling positive bosonic contributions to δm^2 exactly by negative fermionic ones, such that quadratic UV singularities are absent.

Table 7.8 Lower bounds (95% C.L.) on SUSY states. Bounds from LEP (ALEPH, DELPHI, L3, OPAL), Tevatron (CDF, D0) and LHC (ATLAS,CMS) [158, 159]

Object	Mass bound (GeV)			Comment
Sleptons	$m_{\tilde{e},\tilde{\mu},\tilde{\tau}}$	$>$	98, 94, 82	$m_{\tilde{\mu}\tilde{\tau}} - m_{\tilde{\chi}_1^0} > 10, 15$ GeV
Sbottom, stop	$m_{\tilde{b},\tilde{t}}$	$>$	600, 730	for $m_{\tilde{b},\tilde{t}} - m_{\tilde{\chi}_1^0} = 8, 10$ GeV
Squarks$\neq \tilde{t}, \tilde{b}$	$m_{\tilde{q}}$	$>$	1450	
chargino	$m_{\tilde{\chi}_1^\pm}$	$>$	345	for $m_{\tilde{\nu}} > 300$ GeV
Stable neutralino (LSP)	$m_{\chi_1^0}$	$>$	46	all $\tan\beta$, all Δm, all m_0
Unstable neutralino	$m_{\chi_1^0}$	$>$	380	$\tilde{\chi}_1^0 \to Z\tilde{G}$, GMSB[a]
Neutralinos $\tilde{\chi}_2^0, \tilde{\chi}_3^0, \tilde{\chi}_4^0$	$m_{\tilde{\chi}^0}$	$>$	345	
Charginos $\tilde{\chi}_1^\pm, \tilde{\chi}_2^\pm$	$m_{\tilde{\chi}^\pm}$	$>$	345	
Sneutrino $\tilde{\nu}$	$m_{\tilde{\nu}}$	$>$	94	
Gluino	$m_{\tilde{g}}$	$>$	1150	any $m_{\tilde{q}}[m_{\tilde{g}} = m_{\tilde{q}}]$

[a]Gauge mediated supersymmetry breaking (GMSB) is an elegant mechanism to transmit supersymmetry breaking from the hidden to the MSSM observable sector, which solves the supersymmetric flavor problem

In the symmetric phase the Higgs particles have a mass which is a truly free parameter, independent of it couplings. The only known symmetry which requires scalar particles to be massless in the symmetry limit is supersymmetry.[17] Simply because a scalar is now always a supersymmetric partner of a fermion which is required to be massless be chiral symmetry. Thus only in a supersymmetric theory it is natural to have a "light" Higgs, so the commonly accepted jargon. In any case in a SUSY extension of the SM the lightest scalar h^0, which corresponds to the SM Higgs, is bounded to have mass $m_{h^0} \leq M_Z$ at tree level.

It is one of the most striking consequences of supersymmetrizing the SM that the Higgs boson mass is a predicted quantity now, although depending on other new free parameters showing up in the SUSY extension. The basic reason is that supersymmetrizing the Higgs self–coupling $HHHH \leftrightarrow HH\tilde{H}\tilde{H}$ relates λ to the gauge and Yukawa couplings:

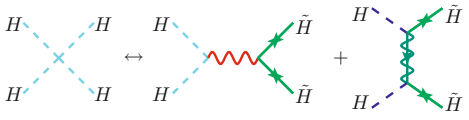

[17]Conformal symmetry would require severe fine tuning of parameters, just what we want to avoid in this context.

In the MSSM it implies constraints on the 2HDM potential (7.24):

$$\lambda_1 = \lambda_2 = -(\lambda_3 + \lambda_4 + \lambda_5) = \frac{1}{4}\left(g^2 + g'^2\right) \; ; \quad \lambda_4 = -\frac{1}{2}g^2 \; ; \quad \lambda_5 = 0\,,$$

and as a consequence, in the minimal SUSY models the masses of the extra Higgses at tree level are severely constrained by the following mass- and coupling-relationships:

$$M^2_{H^\pm} = M^2_W + M^2_A \; , \quad M^2_{H,h} = \frac{1}{2}\left(M^2_Z + M^2_A \pm \sqrt{(M^2_Z - M^2_A)^2 + 4M^2_Z M^2_A \sin^2 2\beta}\right),$$
$$\tan(2\alpha) = \tan(2\beta)\,\frac{M^2_A + M^2_Z}{M^2_A - M^2_Z} \; , \quad \sin^2(\alpha-\beta) = \frac{M^2_H}{M^2_A}\,\frac{M^2_Z - M^2_H}{M^2_Z + M^2_A - 2M^2_H} \; . \tag{7.50}$$

Only two independent parameters are left, which we may choose to be $\tan\beta$ and M_A.[18] This tree level Higgs mass prediction receives large radiative corrections from the $t/\tilde{t}$ sector (see Fig. 7.12), which changes the upper bound to [160]

$$m^2_{h^0} \leq M^2_Z + \frac{\sqrt{2}G_\mu}{2\pi^2 \sin^2\beta}\, 3m^4_t \, \ln\left(\frac{m_{\tilde{t}_1}\, m_{\tilde{t}_2}}{m^2_t}\right) + \cdots \tag{7.51}$$

which in any case is well below 200 GeV. For improved bounds obtained by including higher order corrections[19] I refer to [161, 162] (see also [163]). In the MSSM one

[18] In [138] the CP conserving 2HDM case is considered without imposing the $\Phi_2 \to -\Phi_2$ symmetry, which allows for two more terms in the potential $V \to V + \left[\lambda_6\,(\Phi_1^+\Phi_1) + \lambda_7\,(\Phi_2^+\Phi_2)\right](\Phi_1^+\Phi_2) +$ h.c.. The CP-even mass matrix is of the form

$$\mathcal{M}^2 = \begin{pmatrix} \lambda_1 v^2 & \lambda_6 v^2 \\ \lambda_6 v^2 & M^2_A + \lambda_5 v^2 \end{pmatrix}$$

and one has to distinguish the following special limits:

- Decoupling limit: $M^2_A \gg \lambda_i v^2$ implying $M^2_h \sim \lambda_1 v^2$ and $|c_{\beta-\alpha} \ll 1|$ and the lighter scalar h is the SM like one.
- Alignment limits: $\lambda_6 = 0$ with two possibilities:

(1) $\lambda_1 < \lambda_5 + M^2_A/v^2$ and again h is identical with the SM Higgs and $c_{\beta-\alpha} = 0$
(2) $\lambda_1 > \lambda_5 + M^2_A/v^2$ in which case H is identical with SM Higgs and $c_{\beta-\alpha} = 1$. This is an unexpected possibility, namely the discovered Higgs is to be identified the heavier scalar. The lighter would have masses in the range 20–90 GeV and would have escaped detection so far, because of suppressed couplings to SM states.

[19] Denoting by M^2_h the corrected light Higgs on–shell mass, and by m^2_h the tree level mass given in (7.50), then including leading logarithms in α_s and y_t up to 3 loops on finds

$$M^2_h = m^2_h + \hat{v}^2\,\hat{y}^4_t \left[12\,L\,\kappa_L - 12\,L^2\,\kappa^2_L\left(16\,\hat{g}^2_3 - 3\,\hat{y}^2_t\right)\right.$$
$$\left. +4\,L^3\,\kappa^3_L\left(736\hat{g}^4_3 - 240\,\hat{g}^2_3\,\hat{y}^2_t - 99\,\hat{y}^4_t\right) + \cdots\right],$$

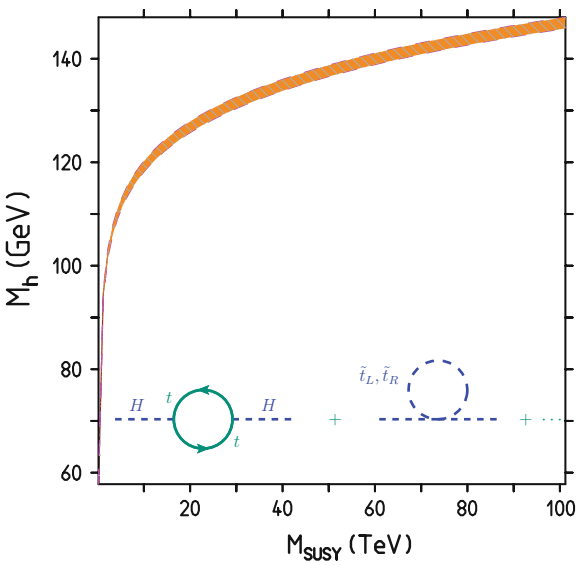

Fig. 7.12 The MSSM lightest Higgs mass as a function of $M_{\rm SUSY}$ for $\tan\beta = 5$ and $m_A = 60$ GeV at 3 loops leading log order. Note that the $M_{\rm SUSY}$ independent "offset" LO value (7.50) depends substantially on m_A and $\tan\beta$, and thus also affects M_h. The stop mixing parameter X_t is chosen zero here. Inlaid diagrams: leading one–loop corrections to the Higgs pole mass

can reach $m_H \lesssim 135$ GeV, in non-minimal SUSY this limit can go up by 5 GeV or more [164]. In any case one has to relax from too much constraints on the SUSY parameter space to avoid conflict with phenomenological bounds. In Table 7.8 some important direct search bounds on sparticle masses are listed.

It is worthwhile to mention that in an exactly supersymmetric theory the anomalous magnetic moment must vanish, as observed by Ferrara and Remiddi in 1974 [165]:

$$a_\mu^{\rm tot} = a_\mu^{\rm SM} + \Delta a_\mu^{\rm SUSY} = 0.$$

Thus, since $a_\mu^{\rm SM} > 0$, in the SUSY limit, in the unbroken theory, we would have

$$\Delta a_\mu^{\rm SUSY} = -a_\mu^{\rm SM} < 0.$$

However, we know that SUSY must be drastically broken, not a single supersymmetric partner has been observed so far. All super–partners of existing particles seem to be too heavy to be produced up to now. If SUSY is broken a_μ may have either sign. In fact, the 3–4 standard deviation $(g_\mu - 2)$–discrepancy requires $\Delta a_\mu^{\rm SUSY} > 0$, of the same sign as the SM contribution and of at least the size of the weak contribution [$\sim 200 \times 10^{-11}$] (see Fig. 3.8).

The leading SUSY contributions, like the weak SM contributions, are due to one–loop diagrams. Most interesting are the ones which get enhanced for large $\tan\beta$. Such supersymmetric contributions to a_μ stem from sneutrino–chargino and

(Footnote 19 continued)
with $L = \ln M_{\rm SUSY}/M_t$, $\hat{v} = v^{\rm SM}(M_t)$, $\hat{g}_3 = g_3^{\rm SM}(M_t)$, $\hat{y}_t = y_t^{\rm SM}(M_t)$ and $\kappa_L = 1/(16\pi^2)$. The 3–loop term is scheme dependent and depends on specific approximations made [161].

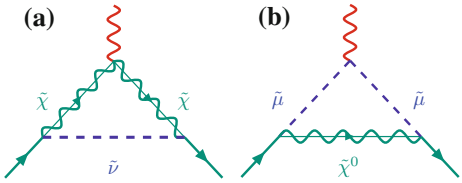

Fig. 7.13 Physics beyond the SM: leading SUSY contributions to $g-2$ in a supersymmetric extension of the SM. Diagrams **a** and **b** correspond to diagrams **a** and **b** of Fig. 7.4, respectively

smuon–neutralino loops Fig. 7.13 and yield [166–169]:

$$\Delta a_\mu^{\text{SUSY (1)}} = a_\mu^{\chi^\pm} + a_\mu^{\chi^0} \tag{7.52}$$

with

$$a_\mu^{\chi^\pm} = \frac{m_\mu}{16\pi^2}\sum_k \left\{ \frac{m_\mu}{12 m^2_{\tilde{\nu}_\mu}} (|c_k^L|^2 + |c_k^R|^2)\, F_1^C(x_k) + \frac{m_{\chi_k^\pm}}{3 m^2_{\tilde{\nu}_\mu}} \text{Re}[c_k^L c_k^R]\, F_2^C(x_k) \right\}$$

$$a_\mu^{\chi^0} = \frac{m_\mu}{16\pi^2}\sum_{i,m} \left\{ -\frac{m_\mu}{12 m^2_{\tilde{\mu}_m}} (|n_{im}^L|^2 + |n_{im}^R|^2)\, F_1^N(x_{im}) + \frac{m_{\chi_i^0}}{3 m^2_{\tilde{\mu}_m}} \text{Re}[n_{im}^L n_{im}^R]\, F_2^N(x_{im}) \right\}$$

and $k = 1, 3$ and $i = 1, \ldots, 4$ denote the chargino and neutralino indices, $m = 1, 2$ is the smuon index, and the couplings are given by

$$\begin{aligned}
c_k^L &= -g_2\, V_{k1}, \\
c_k^R &= y_\mu\, U_{k2}, \\
n_{im}^L &= \frac{1}{\sqrt{2}} (g_1 N_{i1} + g_2 N_{i2})\, U_{m1}^{\tilde{\mu}\,*} - y_\mu N_{i3}\, U_{m2}^{\tilde{\mu}\,*}, \\
n_{im}^R &= \sqrt{2}\, g_1 N_{i1}\, U_{m2}^{\tilde{\mu}} + y_\mu N_{i3}\, U_{m1}^{\tilde{\mu}},
\end{aligned}$$

with mixing matrices V_{ij}, U_{ij} and N_{ij} defined in (7.48). The kinematical variables are the mass ratios $x_k = m^2_{\chi_k^\pm}/m^2_{\tilde{\nu}_\mu}$, $x_{im} = m^2_{\chi_i^0}/m^2_{\tilde{\mu}_m}$, and the one–loop vertex functions read

$$\begin{aligned}
F_1^C(x) &= \frac{2}{(1-x)^4}\,[2 + 3x - 6x^2 + x^3 + 6x\, \ln x]\,, \\
F_2^C(x) &= \frac{3}{2\,(1-x)^3}\,[-3 + 4x - x^2 - 2\, \ln x]\,, \\
F_1^N(x) &= \frac{2}{(1-x)^4}\,[1 - 6x + 3x^2 + 2x^3 - 6x^2\, \ln x]\,, \\
F_2^N(x) &= \frac{3}{(1-x)^3}\,[1 - x^2 + 2x\, \ln x]\,,
\end{aligned}$$

and are normalized to $F_i^J(1) = 1$. The functions $F_i^C(x)$ are the ones calculated in (7.13) and $F_i^N(x)$ in (7.16), respectively. The couplings g_i denote the $U(1)$ and $SU(2)$ gauge couplings $g_1 = e/\cos\Theta_W$ and $g_2 = e/\sin\Theta_W$, respectively, and y_μ is the muon's Yukawa coupling (7.47). The interesting aspect of the SUSY contribution to a_μ is that they are enhanced for large $\tan\beta$ in contrast to SUSY contributions to electroweak precision observables, which mainly affect $\Delta\rho$ which determines the ρ–parameter and contributes to M_W. The anomalous magnetic moment thus may be used to constrain the SUSY parameter space.

Simplifying (7.52) to include the most relevant terms only, we note that the leading SUSY contributions [167, 168] to the muon $g-2$ are given by the chargino–sneutrino loop

$$a_\mu^{\chi^\pm} = \frac{\alpha m_\mu^2\, M_2\, \mu \tan\beta}{4\pi \sin^2\theta_W m_{\tilde{\nu}_\mu}^2} \left(\frac{f_\chi(M_2^2/m_{\tilde{\nu}_\mu}^2) - f_\chi(\mu^2/m_{\tilde{\nu}_\mu})}{M_2^2 - \mu^2} \right) \tag{7.53}$$

and the bino–smuon loop

$$a_\mu^{\chi^0} = \frac{\alpha m_\mu^2\, M_1\, \left(\mu\tan\beta - A_\mu\right)}{4\pi \cos^2\theta_W \left(m_{\tilde{\mu}_R}^2 - m_{\tilde{\mu}_L}^2\right)} \left(\frac{f_N(M_1^2/m_{\tilde{\mu}_R}^2)}{m_{\tilde{\mu}_R}^2} - \frac{f_N(M_1^2/m_{\tilde{\mu}_L}^2)}{m_{\tilde{\mu}_L}^2} \right) \tag{7.54}$$

where $m_{\tilde{\mu_L}}$ and $m_{\tilde{\mu_L}}$ are the smuon masses and

$$f_\chi(x) = \frac{x^2 - 4x + 3 + 2\ln x}{(1-x)^3}\,, \quad f_\chi(1) = -2/3\,,$$
$$f_N(x) = \frac{x^2 - 1 - 2x\ln x}{(1-x)^3}\,, \quad f_N(1) = -1/3.$$

For most of the MSSM parameter space $\Delta a_\mu^{\rm SUSY}$ is dominated by the chargino–smuon contribution, which decouples for large $m_{\tilde{\nu}_\mu}^2$. However, this contribution can still be of the order of the SM weak contribution $a_\mu^{\rm EW}$ even when the masses are much larger than M_W because of the $\tan\beta$ enhancement of the muon Yukawa coupling.

An expansion in $1/\tan\beta$ and because SUSY partners of SM particles are heavier than the latter one usually also expands in $M_W/M_{\rm SUSY}$ which is leading to the handy approximations

$$a_\mu^{\chi^\pm} = \frac{g_2^2}{32\pi^2}\,\frac{m_\mu^2}{M_{\rm SUSY}^2}\,\mathrm{sign}(\mu M_2)\tan\beta\left[1 + O(\tan\beta^{-1},\, M_W/M_{\rm SUSY})\right]\,,$$
$$a_\mu^{\chi^0} = \frac{g_1^2 - g_2^2}{192\pi^2}\,\frac{m_\mu^2}{M_{\rm SUSY}^2}\,\mathrm{sign}(\mu M_2)\tan\beta\left[1 + O(\tan\beta^{-1},\, M_W/M_{\rm SUSY})\right]\,,$$

where parameters have been taken to be real and M_1 and M_2 of the same sign. Provided all SUSY masses are about equal to $M_{\rm SUSY}$ and $\tan\beta$ has moderate values one then obtains

$$\Delta a_\mu^{\rm SUSY} \simeq \text{sign}(\mu)\frac{\alpha(M_Z)}{8\pi\,\sin^2\Theta_W}\frac{(5+\tan^2\Theta_W)}{6}\frac{m_\mu^2}{\widetilde{m}^2}\tan\beta\left(1-\frac{4\alpha}{\pi}\ln\frac{\widetilde{m}}{m_\mu}\right) \quad (7.55)$$

$\widetilde{m}$ a typical SUSY loop mass and μ is the Higgsino mass. Here we also included the leading 2–loop QED logarithm as an RG improvement factor [170]. In Fig. 7.14 contributions are shown for various values of $\tan\beta$. Above $\tan\beta \sim 5$ and $\mu > 0$ the SUSY contributions from the diagrams Fig. 7.13 easily could explain the observed deviation (7.3) with SUSY states of masses in the interesting range 100 to 500 GeV. However, after the LHC experiments ATLAS and CMS have pushed up the limits on possible sparticles masses, we observe a possible conflict and previously favored SUSY scenarios like CMSSM are ruled out. Therefore one should look at the SUSY setup more closely. What matters are the sleptons, neutralinos and charginos which are to be light to explain the muon $g-2$ discrepancy. In contrast squarks are favored to be rather heavy in order to explain the Higgs boson mass and to satisfy the LHC bounds. Indeed a hierarchy

$$m_{\tilde{q}} \gg m_{\tilde{\ell}}, m_{\tilde{\chi}^\pm}, m_{\tilde{\chi}^0}$$

still is perfectly in accord with the limits collected in Table 7.8. Perspectives for direct searches of neutralinos and sleptons at the LHC are discussed in [171].

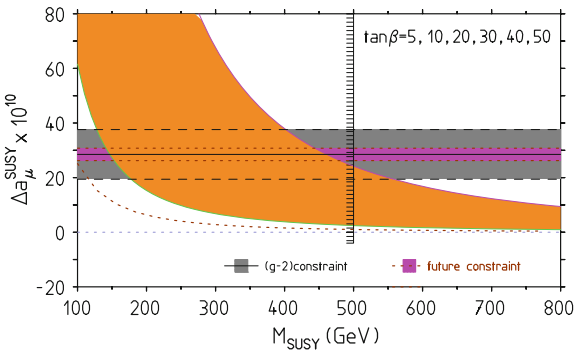

Fig. 7.14 Constraint on large $\tan\beta$ SUSY contributions as a function of $M_{\rm SUSY}$. The horizontal band shows $\Delta a_\mu^{\rm NP} = \Delta a_\mu$. The region left of $M_{\rm SUSY} \sim 500$ GeV is excluded by LHC searches for CMSSM scenarios with $M_{\rm SUSY}$ a universal SUSY mass. For $m_h \sim 125$ GeV actually $M_{\rm SUSY} >$ 800 GeV depending on details of the stop sector ($\{\tilde{t}_1, \tilde{t}_2\}$ mixing and mass splitting) and weakly on $\tan\beta$. *Orange* shaded range $\tan\beta = 5 \div 50$

More recently, also the $\tan^2\beta$ enhanced contributions have been calculated [172].[20] They arise from the $\tan\beta$ enhanced shift $\Delta_\mu \propto \alpha\ \tan\beta$ in the on mass–shell muon mass renormalization:

$$m_\mu \to m_\mu + \delta m_\mu = \frac{m_\mu}{1+\Delta_\mu} + \text{non}-\tan\beta-\text{enhanced terms.} \tag{7.56}$$

In the case that all SUSY masses are equal and much larger than M_W the correction reads

$$\Delta_\mu \simeq -0.0018\ \tan\beta\ \text{sign}(\mu). \tag{7.57}$$

Extracting $\tan\beta$ from a_μ^{exp}, the resulting value would be smaller by about 10% when $\tan\beta \sim 50$. Corrections can be even larger in certain regions of SUSY parameter space. Typically, for large $\tan\beta$ they are larger than other 2–loop contributions. The contributions of the 2HDM sector of the MSSM have been discussed earlier in Sect. 7.2.4.

The very large $\tan\beta$ regime (motivated by the possibility that v_1 could be vanishing and the muon mass induced radiatively as advocated e.g. in [87]) has been studied in [173]. In the simplified case that all SUSY masses are equal to M_{SUSY} and $\tan\beta$ is moderate the one loop SUSY result takes the form

$$\Delta a_\mu^{\text{SUSY,1L}} \approx 13\times 10^{-10}\ \text{sign}(\mu)\ \tan\beta\ \left(\frac{100\ \text{GeV}}{M_{\text{SUSY}}}\right)^2.$$

For large $\tan\beta$ higher order terms change the linear behavior in $\tan\beta$. The higher order terms can be resummed [172] to

$$\Delta a_\mu^{\text{SUSY}} = \frac{\Delta a_\mu^{\text{SUSY,1L}}}{1+\Delta_\mu},$$

which has finite limit

$$\Delta a_{\mu\,\text{lim}}^{\text{SUSY}} = \lim_{\tan\beta\to\infty} \frac{\Delta a_\mu^{\text{SUSY,1L}}}{\Delta_\mu} \approx -72\times 10^{-10}\left(\frac{1\ \text{TeV}}{M_{\text{SUSY}}}\right)^2$$

still assuming degenerate SUSY masses. If we want to make SUSY effects responsible for positive deviation Δa_μ the case that all SUSY masses are of similar size is ruled out. In order to get a positive result one has to assume large mass splittings. Two possible regimes, which are not in conflict with bounds from other observables, have been considered in [173]:

- the $\tilde{B}\tilde{\mu}_L\tilde{\mu}_R$ contributions dominate for $M_1, m_L, m_R \ll \mu$: "large μ–limit",
- the $\tilde{B}\tilde{H}\tilde{\mu}_L$ contributions dominate for $M_1, \mu, m_R \ll m_L$: "$\tilde{\mu}_R$–dominance".

[20] The highest power in $\tan\beta$ at a given order L in the loop expansion is $\alpha^L\ \tan^L\beta$. As a correction only the leading one of order $\alpha^2\ \tan^2\beta$ is numerically significant.

We remind that gauginos are denoted by $\tilde{W}$ for the $SU(2)$ and by $\tilde{B}$ for the $U(1)_Y$ gauge groups. In both regimes the result changes to

$$\Delta a_{\mu\,\mathrm{lim}}^{\mathrm{SUSY}} \approx 37 \times 10^{-10} \left(\frac{1\ \mathrm{TeV}}{M_{\mathrm{SUSY}}}\right)^2 ,$$

assuming $M_A = 50$ GeV. Typically, of order 1 σ effects are obtained only for sufficiently small M_A and sufficiently large $\tan\beta$. This behavior is reflecting what happens in general two Higgs doublet models of type II and X, as discussed before.

A remarkable 2–loop calculation within the MSSM has been performed by Heinemeyer, Stöckinger and Weiglein [140]. They evaluated the exact 2–loop correction of the SM 1–loop contributions Figs. 4.1, and 4.18. These are all diagrams where the μ–lepton number is carried only by μ and/or ν_μ. In other words, SM diagrams with an additional insertion of a closed sfermion– or charginos/neutralino–loop. Thus the full 2–loop result from the class of diagrams with closed sparticle loops is known. This class of SUSY contributions is interesting because it has a parameter dependence completely different from the one of the leading SUSY contribution and can be large in regions of parameter space where the 1–loop contribution is small. The second class of corrections are the 2–loop corrections to the SUSY 1–loop diagrams Fig. 7.13, where the μ–lepton number is carried also by $\tilde{\mu}$ and/or $\tilde{\nu}_\mu$. This class of corrections is expected to have the same parameter dependence as the leading SUSY 1–loop ones and only the leading 2–loop QED corrections are known [170] as already included in (7.55). More recently, an extended more complete calculation has been presented in [174].

The prediction of $\Delta a_\mu^{\mathrm{SUSY}}$ as a function of the mass of the Lightest Observable SUSY Particle $M_{\mathrm{LOSP}} = \min(m_{\tilde{\chi}_1^\pm}, m_{\tilde{\chi}_2^0}, m_{\tilde{f}_i})$, from a MSSM parameter scan with $\tan\beta = 50$, including the 2–loop effects is shown in Fig. 7.15. Plotted is the maximum value of a_μ obtained by a scan of that part of SUSY parameter space which is allowed by the other observables like m_h, M_W and the b–decays. The 2–loop corrections in general are moderate (few %). However, not so for lighter M_{LOSP} in case of heavy smuons and sneutrinos when corrections become large (see also [175]). The remaining uncertainty of the calculation has been estimated to be below 3×10^{-10}, which is satisfactory in the present situation. This may however depend on details of the SUSY scenario and of the parameter range considered. A comprehensive review on supersymmetry, the different symmetry breaking scenarios and the muon magnetic moment has been presented by Stöckinger [169]. Low energy precision test of supersymmetry and present experimental constraints also are reviewed and discussed in [176].

The results for the SUSY contributions to a_μ up to two-loops may be found in [169, 172, 174], and may be written as

$$\Delta a_\mu^{\mathrm{SUSY}} = \Delta a_\mu^{\mathrm{SUSY,1L}} \left(1 - \frac{4\alpha}{\pi} \log \frac{M_{\mathrm{SUSY}}}{m_\mu}\right) \left(\frac{1}{1+\Delta_\mu}\right) + a_\mu^{(\chi\gamma H)} + a_\mu^{(\tilde{f}\gamma H)} + a_\mu^{(\chi\{W,Z\}H)} + a_\mu^{(\tilde{f}\{W,Z\}H)} + a_\mu^{\mathrm{SUSY,ferm,2L}} + a_\mu^{\mathrm{SUSY,bos,2L}} + \ldots . \quad (7.58)$$

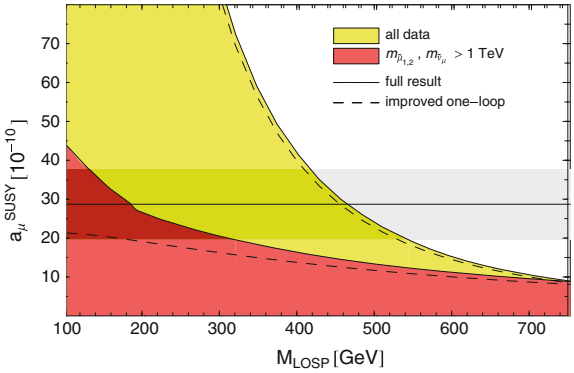

Fig. 7.15 Allowed values of MSSM contributions to a_μ as a function of the mass of the Lightest Observable SUSY Particle $M_{\rm LOSP}$, from an MSSM parameter scan with $\tan\beta = 50$. The 1σ region corresponding to the deviation (7.3) is indicated as a horizontal band. The *yellow* region corresponds to all input parameter points that satisfy the experimental constraints from b–decays, m_h (here prior to the Higgs discovery) and $\Delta\rho$. In the *red* region, smuons and sneutrinos are heavier than 1 TeV. The *dashed lines* correspond to the contours that arise from ignoring the 2–loop corrections from chargino/neutralino– and sfermion–loop diagrams. Courtesy of D. Stöckinger [169]

The labels $(\chi\gamma H)$ etc. identify contributions from Fig. 7.9b type diagrams which would be labeled by $(\tau h\gamma)$, with possible replacements $\gamma \to V = \gamma, Z, W^\pm$, $h \to H = h, H, A, H^\pm$ and $\tau^\mp \to X = \chi^\mp, \chi^0, \tilde{f}$. Contributions (XVV) correspond to Fig. 4.19a, d with corresponding substitutions. The remaining terms $a_\mu^{\rm SUSY,ferm,2L}$ and $a_\mu^{\rm SUSY,bos,2L}$ denote small terms like the fermionic contribution Fig. 7.9b and the bosonic contributions Fig. 7.9c, d, which differ from the SM result due to the modified Higgs structure. The ellipsis denote the known but negligible 2–loop contributions as well as the missing 2–loop and higher order contributions. As in the 2HDM case, all leading terms come from Barr-Zee type diagrams. In terms of the functions $F_{h,H}(z) = z\, g_{h,H}(z)$ and $F_A(z) = z\, g_A(z)$ with $g_i(z)$ given by (7.36), the results read [98, 99, 139, 141, 175, 177]

$$a_\mu^{(\chi\gamma H)} = \frac{\sqrt{2}G_\mu m_\mu^2}{8\pi^2}\,\frac{\alpha}{\pi}\sum_{k=1,2}\left[\,\mathrm{Re}[\lambda_\mu^A \lambda_{\chi_k^+}^A]\, F_A(m_{\chi_k^+}^2/m_A^2) + \sum_{S=h,H}\mathrm{Re}[\lambda_\mu^S \lambda_{\chi_k^+}^S]\, F_h(m_{\chi_k^+}^2/m_S^2)\right],$$

$$a_\mu^{(\tilde{f}\gamma H)} = \frac{\sqrt{2}G_\mu m_\mu^2}{8\pi^2}\,\frac{\alpha}{\pi}\sum_{\tilde{f}=\tilde{t},\tilde{b},\tilde{\tau}}\sum_{i=1,2}\left[\sum_{S=h,H}(N_c Q^2)_{\tilde{f}}\,\mathrm{Re}[\lambda_\mu^S \lambda_{\tilde{f}_i}^S]\, F_{\tilde{f}}(m_{\tilde{f}_i}^2/m_S^2)\right],$$

with $F_{\tilde{f}}(z) = z\,(2 + \ln z - F_A(z))/2$ and couplings (see Eqs. (7.29, 7.48))

$$\begin{aligned}
\lambda_{\mu}^{h,H,A} &= (-\sin\alpha/\cos\beta, \cos\alpha/\cos\beta, \tan\beta)\ , \\
\lambda_{\chi_k^+}^{h,H,A} &= \sqrt{2} M_W/m_{\chi_k^+}\,(U_{k1}V_{k2}\,(\cos\alpha, \sin\alpha, -\cos\beta) + U_{k2}V_{k1}(-\sin\alpha, \cos\alpha, -\sin\beta))\ , \\
\lambda_{\tilde{\tau}_i}^{h,H} &= 2m_\tau/(m_{\tilde{\tau}_i}^2 \cos\beta)\,(-\mu^*\,(\cos\alpha, \sin\alpha) + A_\tau\,(-\sin\alpha, \cos\alpha))\,(U^{\tilde{\tau}_{i1}})^* U^{\tilde{\tau}_{i2}}.
\end{aligned}$$

The last expression given for the $\tilde{\tau}$ applies to the $\tilde{b}$ with $\tau \to b$ everywhere, and for the $\tilde{t}$ with $\tau \to t$ together with $(\mu, \cos\beta, \cos\alpha, \sin\alpha) \to (-\mu, \sin\beta, \sin\alpha, -\cos\alpha)$.

For the potentially enhanced Barr-Zee type contributions the following simple approximations have been given [15, 169]:

$$\begin{aligned}
a_\mu^{(\chi VH)} &\approx \ \ 11 \times 10^{-10} \left(\frac{\tan\beta}{50}\right)\left(\frac{100\ \text{GeV}}{M_{\text{SUSY}}}\right)^2 \ \text{sign}(\mu M_2), \\
a_\mu^{(\tilde{t}\gamma H)} &\approx -13 \times 10^{-10} \left(\frac{\tan\beta}{50}\right)\left(\frac{m_t}{m_{\tilde{t}}}\right)\left(\frac{\mu}{20M_H}\right) \ \text{sign}(X_t), \\
a_\mu^{(\tilde{b}\gamma H)} &\approx -3.2 \times 10^{-10} \left(\frac{\tan\beta}{50}\right)\left(\frac{m_b \tan\beta}{m_{\tilde{b}}}\right)\left(\frac{A_b}{20M_H}\right) \ \text{sign}(\mu)\ .
\end{aligned}$$

The parameter X_t is determined by the SUSY breaking parameter A_f, μ and $\tan\beta$ by $X_t = A_t - \mu^* \cot\beta$. Like for the leading 1–loop case, the first approximation applies if all SUSY masses are approximately equal (e.g. $\mu \sim M_2 \sim m_A$) (but the relevant masses are different in the two cases), and the second and third are valid if the stop/sbottom mixing is large and the relevant stop/sbottom and Higgs masses are of similar size. We refer to the review by Stöckinger [169] for a more detailed presentation of the higher order SUSY effects. The latter have been reconsidered and updated recently in [174].

Constraints from M_W

Here we are looking at SM precision observables like G_F (muon lifetime), Z observables M_Z, Γ_Z, g_V, g_A, $\sin^2\Theta_{\text{eff}}$ (LEP1/SLD) W boson and t quark observables M_W, Γ_W, m_t and Γ_t (LEP2/Tevatron/LHC). An important observable is the W mass predicted to satisfy

$$M_W^2\left(1 - \frac{M_W^2}{M_Z^2}\right) = \frac{\pi\alpha}{\sqrt{2}G_F}\,(1 + \Delta r)\ , \tag{7.59}$$

where $\Delta r = f(\alpha, G_F, M_Z, m_t, \cdots)$ represents the radiative correction to the tree level mass-coupling relation, which depends on the independent parameters of the theory. They differ from the SM by additional contributions in extensions of the SM and thus allow to constrain the parameter space of the extended model. In SUSY models M_W is sensitive to the top/stop sector parameters and actually M_W is essentially the only observable which tends to slightly improve the fit when including MSSM

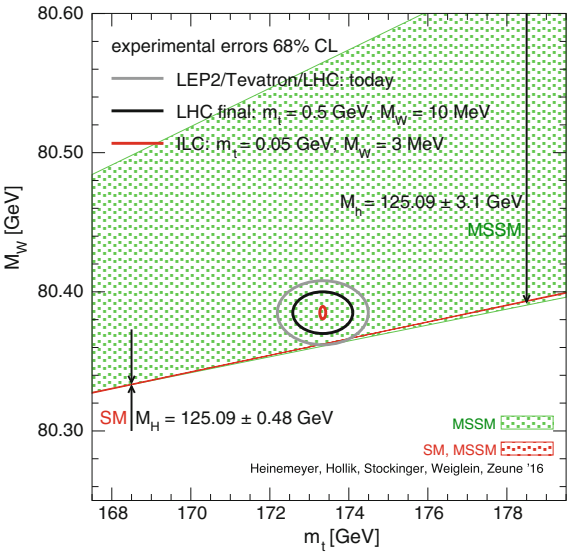

Fig. 7.16 Prediction for M_W as a function of m_t. The *green* region shows the allowed region for the MSSM M_W prediction. It has been obtained by scanning over the MSSM parameters as described in [178]. The cuts $m_{\tilde{t}_2}/m_{\tilde{t}_1} < 2.5$ and $m_{\tilde{b}_2}/m_{\tilde{b}_1} < 2.5$ are applied. The *red* strip indicates the overlap region of the SM and the MSSM, with $M_M^{\rm SM} = 125.6 \pm 0.7$ GeV. The *two arrows* indicate the possible size of the slepton and the chargino (and neutralino) contributions. Courtesy of S. Heinemeyer et al. Reproduced from [178]

contributions. This is shown in Fig. 7.16. In contrast, the other well controlled precision observable $\sin^2 \Theta_{\rm eff}$, as defined in terms of the Z boson NC couplings (4.36),

$$\sin^2 \Theta_{\rm eff} = \frac{1}{4}\left(1 - {\rm Re}\frac{v_{\rm eff}}{a_{\rm eff}}\right), \tag{7.60}$$

remains unaffected when including SUSY effects [181] (see Figs. 14 and 15 of [182] and Fig. 1 of [183] and Fig. 4 of [181]). The global fit of LEP data [184] does not improve when going from the SM to the MSSM, i.e. SUSY effects are strongly constrained here. MSSM results merge into SM results for larger SUSY masses, as decoupling is at work.

In comparison to $(g_\mu - 2)$, the SM prediction of M_W [185, 186], as well as of other electroweak observables, as a function of m_t for given α, G_μ and M_Z, is in much better agreement with the experimental result (at 1σ), although the MSSM prediction for suitably chosen MSSM parameters is slightly favored by the data, as shown in Fig. 7.16. The very recent M_W determination by ATLAS moves results closer towards the SM prediction as shown in Fig. 7.17. Thus large extra corrections to the ones of the SM are not tolerated. The radiative shift of M_W is represented by (4.42) and the leading SUSY contributions mainly come in via $\Delta\rho$. As we know, $\Delta\rho$ is most sensitive to weak isospin splitting and in the SM is dominated by the contribution from the (t, b)–doublet. In the SUSY extension of the SM these effects are enhanced by the contributions from the four SUSY partners $\tilde{t}_{\rm L,R}, \tilde{b}_{\rm L,R}$ of t, b, which can be as large as the SM contribution itself for $m_{1/2} \ll m_t$ [light SUSY], and tends to zero for $m_{1/2} \gg m_t$ [heavy SUSY]. It is important to note that these contributions are not enhanced by $\tan\beta$. Thus, provided $\tan\beta$ enhancement is at

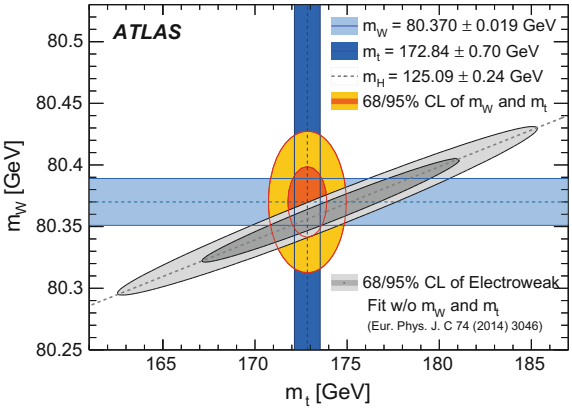

Fig. 7.17 The 68 and 95% confidence-level contours of the M_W and m_t indirect determination from the global electroweak fit [179] are compared to the 68 and 95% confidence-level contours of the ATLAS measurements of the top-quark and W-boson masses. The determination from the electroweak fit uses as input the LHC measurement of the Higgs-boson mass, $m_H = 125.09 \pm 0.24$ GeV [66]. Reprinted from [180], CERN-EP-2016-305: ©2016-2017 CERN (License: CC-BY-4.0)

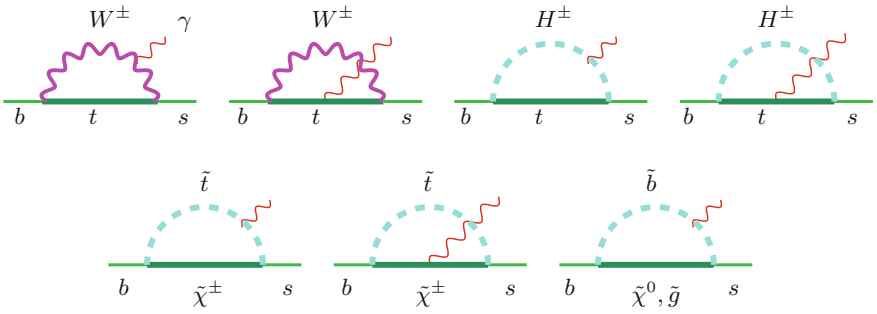

Fig. 7.18 Leading graphs in $b \to s\gamma$. SM, 2HDM and SUSY specific contributions

work, it is quite natural to get a larger SUSY contribution to $(g_\mu - 2)$ than to M_W, otherwise some tension between the two constraints would be there as M_W prefers the heavy SUSY domain.

Constraints from *B*–physics

Data on the penguin loop induced $B \to X_s\gamma$ transition (see Fig. 7.18) yields another strong constraint on deviations from the SM [187]. Indeed, the SM prediction [70, 188, 189] $\text{BR}(b \to s\gamma)_{\text{NNLL}} = (3.15 \pm 0.23) \times 10^{-4}$ is consistent within 1.2 σ with the experimental result [96, 190] $\text{BR}(b \to s\gamma) = (3.43 \pm 0.22) \times 10^{-4}$. It implies that SUSY requires heavier $m_{1/2}$ and/or m_0 in order not to spoil the good agreement.

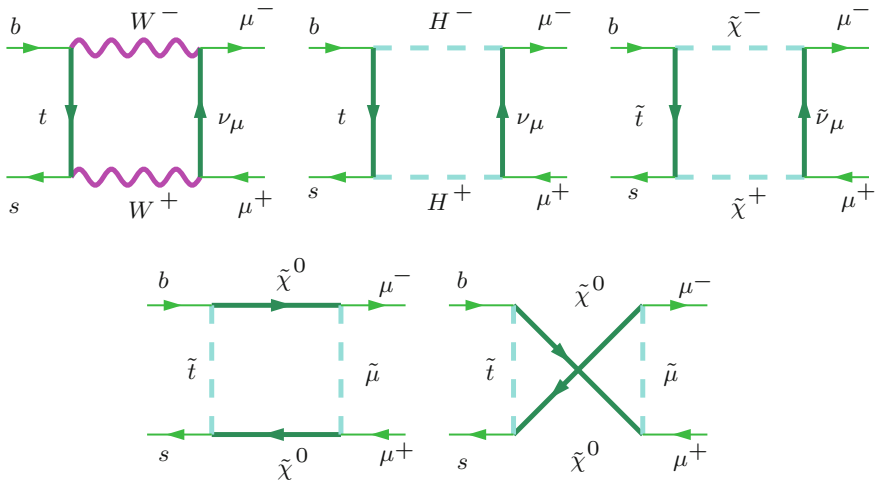

Fig. 7.19 Leading graphs in $B_s \to \mu^+\mu^-$. SM, 2HDM and SUSY specific contributions

The very rare box loop induced decay $B_s \to \mu^+\mu^-$ (see Fig. 7.19) is very interesting because SUSY contributions (box contributions with W's replaced by charged Higgses $H^\pm$) are able to enhance the SM value $\mathrm{BR}(\bar{B}_s \to \mu^+\mu^-) = (3.1 \pm 1.4) \times 10^{-9}$ by two orders of magnitude, especially in scenarios with non-universal Higgs masses (NUHM). A first measurement recently by LHCb [96, 191] found $\mathrm{BR}(B_s \to \mu^+\mu^-) = 2.8^{+0.7}_{-0.6} \times 10^{-9}$, in agreement with the SM value. Again this is limiting significant effects from physics beyond the SM.

Since the SM predictions are in good agreement with the experimental values (7.8), only small extra radiative corrections are allowed ($1.5\,\sigma$). Generally, in SUSY extensions of the SM [192], this excludes light $m_{1/2}$ and m_0, requiring larger values depending on $\tan\beta$. Reference [188] also illustrates the updated $b \to s\gamma$ bounds on M_{H^+} ($>$295 GeV for $2 \leq \tan\beta$) in the 2HDM (Type II) [193]. Important constraints also come from $B_u \to \tau\nu$ [194].

Constraints from CDM

In R–parity conserving SUSY extensions which provide a dark matter candidate the CDM constraint (7.49) can have a tough impact on the SUSY scenario, as can be observed in Fig. 7.20 where the different constraints are combined. The upper panel illustrates the pre–LHC situation when the Higgs mass has been assumed to lie at most little above the LEP limit $m_H \simeq 114$ GeV. It was truly remarkable that in spite of the different highly non–trivial dependencies on the MSSM parameters, with $g-2$ favoring definitely $\mu > 0$, $\tan\beta$ large and/or light SUSY states, there is a common allowed range, although a quite narrow one, depending strongly on $\tan\beta$.

Before the Higgs discovery and LHC mass bounds, assuming the CMSSM scenario, besides the direct limits from LEP and Tevatron, the most important constraints were coming from $(g_\mu - 2)$, $b \to s\gamma$ and from the dark matter relic density (cosmo-

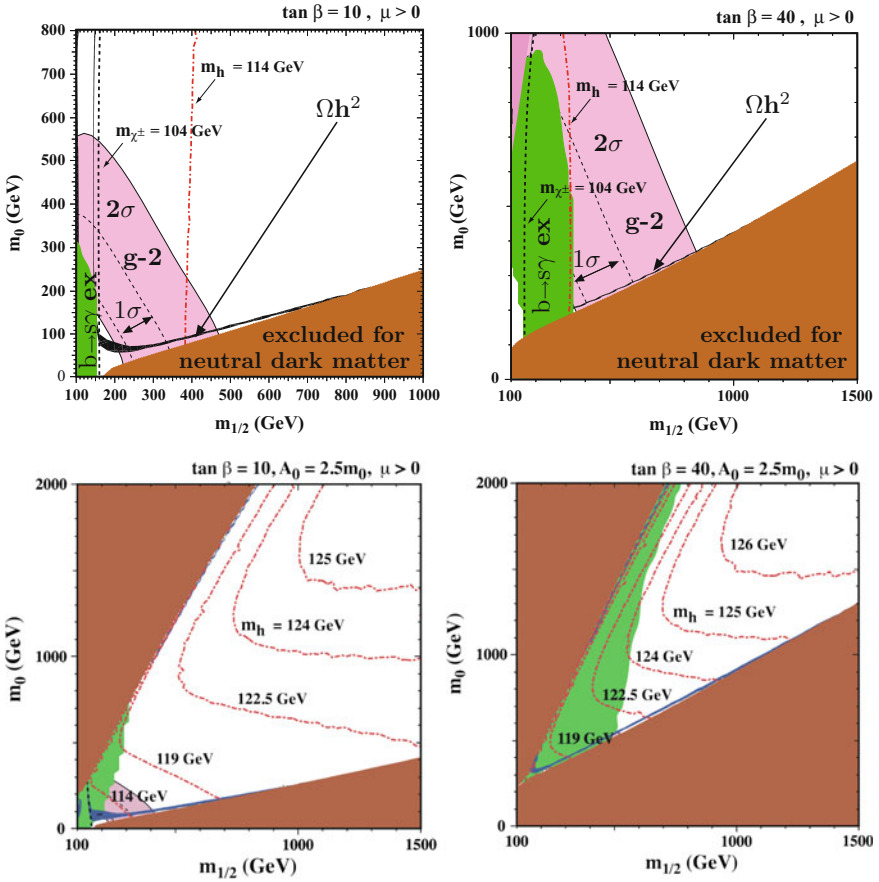

Fig. 7.20 *Top row* the pre–LHC case. The $(m_0, m_{1/2})$ plane for $\mu > 0$ for **a** $\tan\beta = 10$ and **b** $\tan\beta = 40$ in the CMSSM scenario. The allowed region by the cosmological neutral dark matter constraint (7.49) is shown by the *black/blue* parabolic shaped region. The disallowed region where $m_{\tilde{\tau}_1} < m_\chi$ has *brown* shading. The regions excluded by $b \to s\gamma$ have *green* shading (*left*). The $(g_\mu - 2)$ favored region at the 2 σ $[(287\pm182) \times 10^{-11}]$ (between dashed lines the 1 σ $[(287\pm91) \times 10^{-11}]$ band) level has *pink* shading. The LEP constraint on $m_{\chi^\pm} = 104$ GeV and $m_h = 114$ GeV are shown as near vertical lines excluding the region left of it. *Bottom row* after LHC run I. The Higgs discovery has changed it all. Plot courtesy of K. Olive updated from [155] upper part and from [157], with kind permission of The European Physical Journal (EPJ) [lower part]

logical bound on CDM) given in (7.49) [155, 156]. Due to the precise value of $\Omega_{\rm CDM}$ the lightest SUSY fermion (sboson) of mass m_0 is given as a function of the lightest SUSY boson (sfermion) with mass $m_{1/2}$ within a narrow band. This is illustrated in Fig. 7.20 together with the constraints from $(g_\mu - 2)$ (7.3) and $b \to s\gamma$ (7.8). Since m_h for given $\tan\beta$ is fixed by $m_{1/2}$ via (7.51) with $\min(m_{\tilde{t}_i}; i = 1, 2) \sim m_{1/2}$, the allowed region is to the right of the (almost vertical) line $m_h = 114$ GeV which is the direct LEP bound. Again there is an interesting tension between the SM like

lightest SUSY Higgs mass m_h which in case the Higgs mass goes up from the present limit to higher values requires heavier sfermion masses and/or lower $\tan\beta$, while a_μ prefers light sfermions and large $\tan\beta$. Another lower bound from LEP is the line characterizing $m_{\chi^\pm} > 104$ GeV. The CDM bound gives a narrow hyperbola like shaped band. The cosmology bound is harder to see in the $\tan\beta = 40$ plot, but it is the strip up the $\chi - \tilde{\tau}$ degeneracy line, the border of the excluded region (dark) which would correspond to a charged LSP which is not allowed. The small shaded region in the upper left is excluded due to no–EWSB there. The latter must be tuned to reproduce the correct value for M_Z. The $\tan\beta = 40$ case is much more favorable, since $(g_\mu - 2)$ selects the part of the (pre–Planck) WMAP strip which has a Higgs above the LEP bound. Within the CMSSM the discovery of the Higgs and the determination of its mass essentially is fixing m_0 and $m_{1/2}$. So far the very encouragingly looking pre–LHC setting.[21]

However, the Higgs boson discovery by ATLAS and CMS at the LHC revealing $m_H \simeq 125$ GeV dramatically changed this to situation as illustrated in the bottom panel of Fig. 7.20 [157]. The change of a single number m_H by about 9% was able to spoil the very attractive CMSSM scenario and the assumption of universal masses is ruled out as a candidate to accommodate the different phenomenological facts simultaneously.

As we have seen, the present LHC data have a quite dramatic impact on SUSY scenarios. The main lesson is that in constrained models like mSUGRA, CMSSM, NUHM1 or NUHM2 (see e.g. [196]) all allowed parameter points with $m_h \sim 125$ GeV are inconsistent with the observed $(g_\mu - 2)$ [197–199]. However, unconstrained SUSY extensions of the SM can be tuned to accommodate Δa_μ [145]. Only direct searches for sneutrino, chargino, smuon and neutralino states (or corresponding mass bounds) can lead to definite conclusions. The muon $g - 2$ can also be reconciled with the Higgs boson mass of 125 GeV by extending the MSSM so that extra contributions to the Higgs potential appear [200] (see also [201]). Also GMSB models remain in the game [202]. In SUSY scenarios there are plenty of possibilities to escape yesterdays constraints. Clearly, if the $(g_\mu - 2)$ discrepancy is taken serious, any scenario assuming universal squark–slepton masses is ruled out. Therefore acceptable global fits are possible only by detaching squarks and gluinos from the other electroweak superpartners. Such scenarios are the phenomenological pMSSM's [203] and a recent analysis adopting an 8 parameter pMSSM8 scenario: with one 3rd generation squark mass parameters $m_{\tilde{q}3}$, three slepton mass parameters $m_{\tilde{l}_{1,2,3}}$, a gaugino masses M_2, the trilinear coupling A_t, Higgs sector parameters M_A and $\tan\beta$ and the Higgs mixing parameter μ, allows one to fit reasonably well all relevant observables [196, 198] (see also [158, 159]).

While the searches for SUSY states at the LHC have produced heavy constraints on colored superpartners the squarks and gluinos with limits of 1.5 TeV at 95% C.L., for the muon $g-2$ a key problem remains. The searches for charginos $(\tilde{\chi}_1^\pm)$, neutralinos $(\tilde{\chi}_2^0)$, and sleptons $(\tilde{l}_L = \tilde{e}_L, \tilde{\mu}_l)$ through direct electroweak production. These channels face the difficulty that their production cross sections are much lower, resulting

[21] For scenarios beyond the CMSSM see [169, 195].

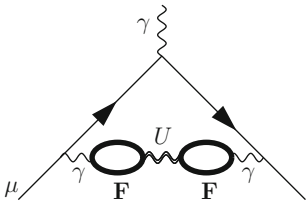

Fig. 7.21 Dark Photon U exchange providing a shift in a_μ. The dark photon is mixing with the photon trough loops of very heavy fermions F charged under both the SM $U(1)_Y$ and the dark $U(1)_\mathrm{D}$

in much weaker exclusion bounds. For the interesting mass ranges around the EW scale, the $\tilde{\chi}^\pm$ coannihilation (like $\chi\tilde{\tau}^\pm \to \tau^\pm\gamma/Z^0$, $\chi_1^0\tilde{l}_1 \to \tau/\mu\gamma$, $\chi^0\chi^0 \to f\bar{f}$ etc.) region exhibits a dense population of states (compressed spectrum) and thus is hard to be disentangled at the LHC (see e.g. [204, 205] and references therein). So possibly only a future e^+e^- collider will be able to resolve such possible opaque spots.

7.2.6 *Dark Photon/Z and Axion Like Particles*

With mass bounds on possible new particles going up, the $(g_\mu-2)$ deviation becomes harder to accommodate given the scaling law (7.10), which requires relatively light new states of the order of the electroweak scale $v = 246$ GeV. But what about light hidden states which could have escaped detection? Certainly, such states should be neutral and couple to SM fermions only by mixing with the photon, similar to the ρ's coupling to leptons. If the new state is light, with mass of order m_μ say, this "dark photon" can be very weakly coupling to muons and still accommodate Δa_μ. The dark photon or U boson was originally motivated by cosmology [206–208]. It mediates a force originating from an extra $U(1)_\mathrm{D}$ local gauge group factor, which thus is neutral (dark) relative to the SM gauge interactions, but coupes to SM fermions via mixing mediated by new very heavy charged fermions F (see Fig. 7.21). Such higher-order $\gamma - U$ effective interaction is modeled by the effective Lagrangian[22]

$$\mathcal{L}_\mathrm{mix} = -\epsilon\, F_Y^{\mu\nu} F_{\mu\nu\,\mathrm{D}}\,, \tag{7.61}$$

where $F_Y^{\mu\nu}$ is the $U(1)_Y$ field strength tensor and $F_\mathrm{D}^{\mu\nu}$ is $U(1)_\mathrm{D}$ counterpart. The parameter ϵ represents the mixing strength and is the ratio of the dark and electromagnetic coupling constants. U boson searches typically can be studied in processes like $e^+e^- \to U\gamma$ and subsequent decay like $U \to e^+e^-$. The phenomenology of

[22] It resembles the VMD type II Lagrangian (5.72), which describes the effective interaction of the neutral ρ meson with the photon. The role of the quarks is assumed to be played by new charged very heavy Fermions F.

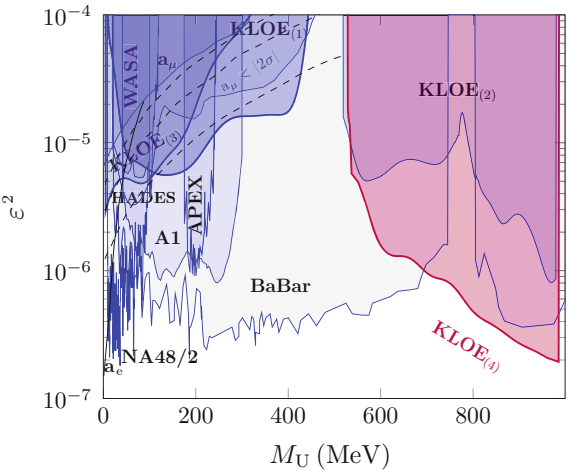

Fig. 7.22 Exclusion limits on the kinetic mixing parameter squared, ϵ^2, as a function of the U boson mass. The red curve labeled KLOE$_{(3)}$ shows the exclusion boundary from [221, 222], while the curves labeled KLOE$_{(1)}$ and KLOE$_{(2)}$ indicate the previous KLOE results. Also shown are the exclusion limits provided by E141, E774, Apex, WASA, HADES, A1, BaBar, and NA48/2. The *gray* band delimited by the *dashed white lines* indicates the mixing level and m_U parameter space that could explain the discrepancy observed between the measurement and SM calculation of the muon $(g-2)_\mu$. Courtesy of the KLOE-2 Collaboration. Reprinted from [222], http://dx.doi.org/10.1016/j.physletb.2016.04.019

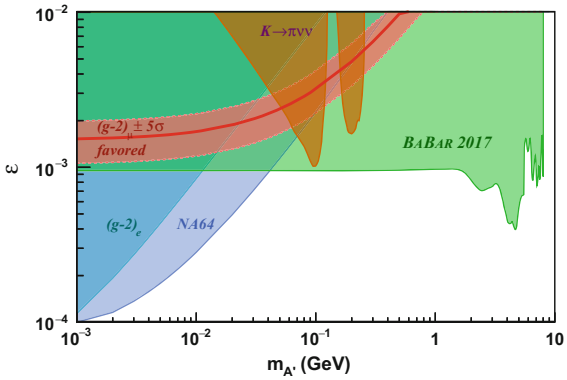

Fig. 7.23 Exclusion plot from BaBar [218] ϵ as a function of the "dark Z boson" mass $m_{A'}$ together with the NA64 [220] contour. BaBar essentially rules out dark photons as a source of the muon $g-2$ discrepancy. Courtesy of the BaBar Collaboration. Reprinted from [218]

such "dark Z" models has been analyzed in [209] (and references therein). Present limit are summarized in Figs. 7.22 and 7.23 along with the indirect limits from the measurements of (g_e-2) and $(g_\mu-2)$ at 5σ, shown with dashed curves. Limits from direct searches are shown as shaded regions and solid curves: E141 [210], E774 [210], KLOE($\phi \to \eta U$, $U \to e^+e^-$) [211], Apex [212], WASA [213], HADES [214], A1 [215], KLOE($e^+e^- \to U\gamma$, $U \to \mu^+\mu^-$) [216], BaBar [217, 218], NA48/2 [219], NA64 [220] and KLOE($e^+e^- \to U\gamma$, $U \to e^+e^-$) [221].

The $g-2$ contribution is given by

$$a_\mu^{\text{dark photon}} = \frac{\alpha}{2\pi}\,\epsilon^2\,F(M_U/m_\mu) \tag{7.62}$$

where $F(x) = \int_0^1 2z\,(1-z)^2/[(1-z)^2+x^2 z]\,\mathrm{d}z$. For values of $\epsilon \sim 1-2\times 10^{-3}$ and $M_U \sim 10-100\,\text{MeV}$, this could explain the muon $g-2$ discrepancy. Searches for the dark photon signals are going on. Another scenario is the "dark Higgs" or "axion–like" one.[23] Contributions of axion–like particles to lepton dipole moments have been discussed in [226]. For a pseudoscalar (a) and scalar (s) axion the interaction Lagrangian considered reads

$$\mathcal{L} = \frac{1}{4}\,g_{a\gamma\gamma}\,a\,F^{\mu\nu}\tilde{F}_{\mu\nu} + g_{a\psi}a\bar{\psi}\,\mathrm{i}\,\gamma_5\psi + \frac{1}{4}\,g_{s\gamma\gamma}\,s\,F^{\mu\nu}F_{\mu\nu} + g_{s\psi}s\bar{\psi}\psi. \tag{7.63}$$

For recent account of the phenomenology see [227–229] and references therein. Contributions of a spin 0 axion-like particle (ALP) to lepton dipole moments, $g-2$ and EDMs, have been examined. Barr-Zee (BZ),[24] light-by-light and vacuum polarization loop effects yield (see also [126, 230, 231])

$$\begin{aligned}
a_{\ell,a}^{\text{BZ}} &\simeq \left(\frac{m_\ell}{4\pi^2}\right) g_{a\gamma\gamma}\,y_{a\ell}\,\ln\frac{\Lambda}{m_a}\,,\\
a_{\ell,a}^{\text{LbL}} &\simeq 3\frac{\alpha}{\pi}\left(\frac{m_\ell g_{a\gamma\gamma}}{4\pi}\right)^2\ln^2\frac{\Lambda}{m_a}\,,\\
a_{\ell,a}^{\text{VP}} &\simeq \frac{\alpha}{\pi}\left(\frac{m_\ell g_{a\gamma\gamma}}{12\pi}\right)^2\ln\frac{\Lambda}{m_a}\,,
\end{aligned}$$

from a light pseudoscalar ALP. The BZ and the LbL contributions are found to be capable of resolving the long-standing muon $g-2$ discrepancy at the expense of relatively large ALP$-\gamma\gamma$ couplings. In fact, for a new pseudoscalar a the contribution to a_μ requires four parameters $g_{a\gamma\gamma}$, $y_{a\mu}$, m_a and Λ to be constrained, including two new mass scales not correlated to any known physics.

A pseudoscalar ALP would show up in $e^+e^- \to \gamma^* \to \gamma a$, analogous to $\pi^0\gamma$ production, which is characterized by the differential cross section

---

[23] One of the biggest unsolved problems of the SM is the non-observation of strong CP violation which would be provided by a non-vanishing $\frac{\Theta}{32\pi^2}\,G_{\mu\nu}\tilde{G}^{\mu\nu}$ term supplementing the QCD Lagrangian with $G_{\mu\nu}$ the gluon field strength tensor and $\tilde{G}^{\mu\nu}$ its dual. For non-zero quark masses this term predicts observable CP violation in strong interactions "the strong CP problem". A fairly convincing answer could be provided by the Peccei-Quinn [223–225] extension of the SM by a $U(1)$ approximate global symmetry, which is spontaneously broken at some low scale f_a. The axion a is the pseudo Nambu-Goldstone boson of this symmetry of mass $m_a \ll \Lambda_{\text{QCD}}$.

[24] The Barr-Zee diagram Fig. 7.9b, typically found in 2HDMs, here appears reduced to a one–loop diagram, where the lepton/quark (τ, b) triangle in the heavy mass limit is shrunk to a point, now the $g_{a\gamma\gamma}$ effective coupling. The h, A muon coupling here is $y_{a\ell}$.

$$\frac{\mathrm{d}\sigma}{\mathrm{d}\cos\theta} = \frac{\alpha}{64}\, g_{a\gamma\gamma}^2 \left(1 - \frac{m_a^2}{s}\right)^3 \left(1 + \cos^2\theta\right) ,$$

where θ is the angle between the ALP and the beam axis in the center-of-mass. As one believes to include all states $e^+e^- \to$ anything other than leptons, attributed to hadrons usually, within uncertainties it would just mean that the error estimates have been missing a substantial contribution. Bounds on such effects are provided by e^+e^- annihilation facilities like LEP, KLOE [222], CMD, SND, BaBar, Belle and BES. For details I refer to [226]. For a comprehensive review see [232].

These dark hidden states scenarios are particularly interesting because they can naturally bridge to the dark matter problem, one of the most mysterious missing parts of present day particle physics. However, some possibilities like the dark Z scenario are essentially ruled out by data already.

There a numerous other beyond the SM scenarios (see e.g. [233–235]), which exhibit new particles that could be contributing to the muon $g-2$, and where parameters are limited by phenomenology. From the examples we have discussed we leaned that it is by far not simple to obtain a 3 to 4 σ effects in a_μ. Most of the models yield contributions represented by diagrams either of the generic 1–loop type or by Barr-Zee type 2–loop diagrams only the masses and the couplings are specific as far as they are known. For little Higgs models the correction to a_μ have been computed in Ref. [236] and were found to be negligible $a_\mu^{LH} \approx 1 \times 10^{-10}$. An interesting new physics option are extra dimension scenarios, which however yield negative contributions of order $a_\mu^{(2)\mathrm{KK}} \approx -1 \times 10^{-10}$ from the Kaluza-Klein excitations [237, 238]. Short summaries of these topics and more references may be found in [13].

7.3 Outlook on the Upcoming Experiments

Next generation muon $(g-2)$ experiments are going to happen soon. The two experiments under construction E989 at Fermilab [239–242] and E34 at J-PARC [243–245], both measure the difference between the spin precession and the cyclotron motion for a muon in a magnetic field. In order to reach a high precision experiments have to be setup such that the equation of motion

$$\boldsymbol{\omega_a} = \frac{e}{m_\mu c}\left(a_\mu \mathbf{B} - \left[a_\mu - \frac{1}{\gamma^2 - 1}\right]\frac{\mathbf{v}\times\mathbf{E}}{c^2}\right) , \tag{7.64}$$

takes the form of a linear relation between the Larmor precession frequency and the homogeneous magnetic field:

$$\boldsymbol{\omega_a} = \frac{e}{m_\mu c}\, a_\mu \mathbf{B}. \tag{7.65}$$

The main point is to get rid of the effect from the electric field. This requires to work at magic γ by tuning the beam energy such that $a_\mu - 1/(\gamma^2 - 1) = 0$ or alternatively

to avoid any external electric field. The two experiments are complementary since they are using alternative possibilities. E989 is a traditional "magic γ" experiment working with highly relativistic muons of magic energy $E \approx 3.1$ GeV.The muon energy determines the size of the storage ring diameter to about 14 m for a field of 1.5 Tesla, which is what can be reached in practice. So the ring of the BNL experiment can and actually is being used by the Fermilab experiment. The novel E34 experiment working with slow muons ($E \sim 300$ MeV) is a much smaller experiment (diameter of muon orbit 70 cm) working with a magnetic muon trap, with the main challenge to rule out any external electric field. Needless to say that the two approaches have very different systematic uncertainties. The E989 experiment will reduce the experimental error by a factor four to

$$\delta a_\mu = 16 \times 10^{-11}. \tag{7.66}$$

The BNL experimental error was statistics dominated, the Fermilab experiment will provide a factor of 20 more in statistics, more muons at higher injection rate. There will be much less background from pion decays by having a longer beam line which also helps improving the polarization. Further improvements concern a more uniform magnetic field, a more precise magnetic field calibration probe and a better centered beam using an improved focusing system. In addition, the signal processing will be improved by segmented detectors, by pileup and muon loss reduction (using better kickers), and by applying refined methods of analysis.

While the Fermilab experiment uses an approach which has been used and further developed since the 1970s in the CERN experiment, the J-PARC experiment is a new "from scratch" design, where the most critical part seems to be the shielding of electric fields. In contrast to the Fermilab experiment the J-PARC experiment works without the need of beam focusing. As a big advantage one should note that it is much easier to provide a homogeneous magnetic field when the fiducial volume is very much smaller. A shortcoming of an experiment with slow muons is that the degree polarization appears reduced, which evidently reduces the signal. Still, one can expect that a precision at the level of the BNL experiment can be reached such that the E34 experiment can provide a very important cross check of the BNL result.

In any case, the next generation experiments will scrutinize the presently seen deviation in $(g_\mu - 2)$. If the deviation is confirmed at least a 5σ significance will be reached. If the deviation would get reduced one would have one more precision test of the SM and a severe constraint on possible SM extensions. The E989 experiment is scheduled to begin data taking in early 2017 and a new measurement can be expected in about one year later.

7.4 Perspectives for the Future

The electron's spin and magnetic moment were evidenced from the deflection of atoms in an inhomogeneous magnetic field and the observation of fine structure by optical spectroscopy [246, 247]. Ever since, magnetic moments and g–values of

particles in general and the $g-2$ experiments with the electron and the muon in particular, together with high precision atomic spectroscopy, have played a central role in establishing the modern theoretical framework for particle physics: relativistic quantum field theory in general and quantum electrodynamics in particular, the prototype theory which developed further into the SM of electromagnetic, weak and strong interactions based on a local gauge principle and spontaneous symmetry breaking, with local gauge group $SU(3)_c \otimes SU(2)_L \otimes U(1)_Y$ spontaneously broken to $SU(3)_c \otimes U(1)_{\rm em}$. Not only particle physics, also precision atomic physics and nuclear theory are based on relativistic QFT methods.[25]

New milestones have been achieved not too long ago with the BNL muon $g-2$ experiment together with the Harvard electron $g-2$ experiment. Both experiments exploited all ingenuity to reach the next level of precision, and together with theory efforts maybe the next level of understanding of how it works. On the theory side, what we learned from the BNL experiment and what we will learn from the upcoming experiments depends a lot on how well we can corroborate the theoretical prediction. There is certainly common agreement that the hadronic light–by–light scattering contribution is the most problematic one, since no theoretically established method so far allowed us to calculate this contribution in a model independent way and with a satisfactorily controlled precision.

A very promising novel access of the HLbL is the data–driven dispersive approach advocated in [248–250]. The detailed theoretical framework has been developed in [251]. The method could improve the reliability of HLbL estimates dramatically, provided the data basis can be ameliorated by dedicated experiments of hadron production in light-by-light processes. More experimental information is also important for better modeling by effective theories. A typical example where data is missing is the $\pi^0\gamma^*\gamma^*$ form factor for both photons off–shell or direct light–by–light scattering in $e^+e^- \to e^+e^-\gamma^*\gamma^* \to e^+e^-\gamma\gamma$ or $e^+e^-\gamma^*\gamma$ with the virtual final state photon converting to a pair.

Another big hope for the long term future are the non–perturbative calculations of electromagnetic current correlators by means of lattice QCD [252–255]. This has to go in steps from two–point amplitudes (vacuum polarization and/or Adler function) to three–point form factors (non-perturbative effects in VVA correlators) and the four–point function linked to light–by–light scattering.

The hadronic vacuum polarization in principle may be substantially improved by continuing $e^+e^- \to$ hadrons cross–section measurements with higher precision. Substantial differences in the dominating $e^+e^- \to \pi\pi$ channel (at the few % level) between the KLOE results on the one hand and the BaBar result[26] on the other hand

[25] Not to forget the role of QFT for other systems of infinite (large) numbers of degrees of freedom: condensed matter physics and critical phenomena in phase transitions (Ken Wilson 1971). The Higgs mechanism as a variant of the Ginzburg-Landau effective theory of superconductivity (1950) and the role QFT and the renormalization group play in the theory of phase transitions are good examples for synergies between elementary particle physics and condensed matter physics.

[26] The KLOE and BaBar measurements have been obtained via the radiative return method which is a next to leading order approach. On the theory side one expects that the handling of the photon radiation requires one order in α more than the scan method for obtaining the same accuracy.

are persisting. Still, data taken with BaBar and Belle before the facilities were shut down are being analyzed. Fortunately, ongoing measurements with BES-III [260] and at the VEPP-2000 [261] facility are improving the data collection, such that the error of the HVP estimates continues to get smaller. Here, the ab initio lattice QCD results are getting closer to the data–driven dispersion relations results. Soon competitive results will be available and provide important cross checks.

Another previously disturbing problem, the deviations at the 10% level between e^+e^-–data and the isospin violations corrected hadronic τ–decay spectral functions, fortunately could be resolved in the meantime [7, 23]. If one corrects τ data for missing $\rho^0 - \gamma$ mixing, the τ data based results are in good agreement with the e^+e^- data based ones.

An interesting possibility in this respect is a novel approach to determine $a_\mu^{\rm had}$ via a direct space-like measurement of $\alpha(-Q^2)$ in μe scattering as proposed in [262], recently (see also [263]). This approach completely avoids a number of problems one encounters with the standard time-like approach. In the latter case collecting hadron production data, applying radiative corrections to hadron production, vacuum polarization subtraction and problems related to thresholds and resonances are rather challenging. In contrast, a single space-like process like μe scattering is much simpler and the needed radiative corrections are under much better control of perturbation theory.

There is no doubt that performing doable improvements on both the theory and the experimental side allows to substantially sharpen (or diminish) the apparent gap between theory and experiment. Yet, even the present situation gives ample reason for speculations. No other experimental result has as many problems to be understood in terms of SM physics. One point should be noted in this context, however. An experiment at that level of accuracy, going one order of magnitude beyond any previous experiment, is a real difficult enterprise and only one such experiment has been performed so far. There is also a certain possibility to overlook some new problem which only shows up at higher precision and escaped the list of explicitly addressed problems by the experiment. It is for instance not 100% clear that what is measured in the experiment is precisely what theoreticians calculate. For example, it is believed that, because radiative corrections in $g-2$ are infrared finite to all orders, real photon radiation can be completely ignored, in spite of the fact that we know that due to the electric interaction via charges a naive S–matrix in QED does not exist. Muons, like any charged particles, produce and absorb continuously photon radiation and therefore are dressed by a photon cloud which is thought not to affect the $g-2$

(Footnote 26 continued)
Presently a possible deficit is on the theory side. What is urgently needed are full $O(\alpha^2)$ QED calculations, for Bhabha luminosity monitoring, μ–pair production as a reference and test process, and π–pair production in sQED as a first step and direct measurements of the final state radiation from hadrons. The CMD-3 and SND measurements take data at the same accelerator (same luminosity/normalization uncertainties) and use identical radiative corrections, such that for that part they are strongly correlated and this should be taken into account appropriately in combining the data. The present state-of-the-art event generator is PHOKHARA [256] for radiative return events and BABAYAGA [257] for the Bhabha channel (see also [258, 259]).

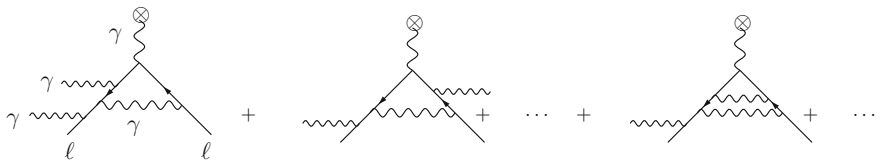

Fig. 7.24 Does soft real radiation affect the muon $g-2$ measurement with highly relativistic muons? Could real radiation yield IR finite correction to the helicity flip amplitude? To LO (with one real photon) a helicity flip is not possible (Steinmann 2002)

measurement. The question has been addressed to leading order by Steinmann [264] (see also [265]). Possible effects at higher orders have not been estimated to my knowledge. Such possible multiple interactions with the external field usually are not accounted for, beyond the classical level. One also should keep in mind that the muon is unstable and the on–shell projection technique (see Sect. 3.5) usually applied in calculating a_μ in principle has its limitation. As $\Gamma_\mu \simeq 3 \times 10^{-16}$ MeV $\ll$ $m_\mu \simeq 105.658$ MeV, it is unlikely that treating the muon to be stable could cause any problem. However, note that the Bargmann-Michel-Telegdi (BMT) equation is obtained by solving the Dirac equation (1st eq. below) as a relativistic one–particle problem with $A_\mu(x) \equiv 0$ only. What is missing, is a derivation of the BMT equation by solving the coupled QED field equations

$$\begin{aligned}
&\left(\mathrm{i}\hbar\gamma^\mu\partial_\mu + Q_\ell\tfrac{e}{c}\gamma^\mu(A_\mu(x) + A^{\mathrm{ext}}_\mu(x)) - m_\ell c\right)\psi_\ell(x) = 0\\
&\left(\Box g^{\mu\nu} - \left(1-\xi^{-1}\right)\partial^\mu\partial^\nu\right)A_\nu(x) = -Q_\ell e\bar{\psi}_\ell(x)\gamma^\mu\psi_\ell(x)\,,
\end{aligned}$$

including the electromagnetic radiation field (see Fig. 7.24). Often it is argued that in case of the $(g_e - 2)$ one has an almost perfect agreement between theory and experiment, so no substantial effect can be missing. However, the measurement of a_e has been performed in a quantum regime where is is possible to essentially control single photon transitions. It is then conceivable that there are no problems with preparing quasi–isolated electron states. In the magic γ type $(g_\mu - 2)$ experiments the setup in not comparable at all and real radiation effects could be significant. In this context the J-PARC experiment [243–245] is a very promising novelty as it will work with ultra–cold muons instead of ultra–hot ones. So if radiation effects would play a role effects obviously would be very different.

Another question one may ask is whether the measurement of the magnetic field strength could not change the magnitude of the field by a tiny but non–negligible amount.[27] On the theory side one should be aware that the important 4–loop contribution has not been crosschecked by a completely independent calculation. Nonetheless, according to the best of our knowledge, the present status of both theory and experiment is as reflected by the systematic errors which have been estimated. Therefore most probably, the difference must be considered as a real indication of a missing piece on the theory side.

[27] Of course such questions have been carefully investigated, and a sophisticated magnetic probe system has been developed by the E821 collaboration.

The anomalous magnetic moment of the muon is a beautiful example of "the closer we look the more we see",[28] however, the efforts to dig even deeper into the structure of matter remains a big adventure also in future.

The $g-2$ measurement is like a peek through the keyhole, you see at the same time an overlay of all things to a certain depth in one projection, but to make sure that what you see is there, you have to open the door and go to check. This will be a matter of accelerator physics, and an ILC would be the preferred and ideal facility to clarify the details. Of course and luckily, the LHC will tell us much sooner the gross direction new physics will go and is able to reach the physics at much higher scales. But, it is not the physics at the highest scales you see first in $g-2$ as we learned in this book.

The Muon Storage Ring experiment on $(g_\mu - 2)$ and similarly the Penning Trap experiment on $(g_e - 2)$ are like microscopes which allow us to look into the subatomic world and the scales which we have reached with a_μ is about 100 GeV, i.e., the scale of the weak gauge bosons W and Z which is the LEP energy scale. As a_μ is effectively by a factor $(m_\mu/m_e)^2 \cdot \delta a_e^{\rm exp}/\delta a_\mu^{\rm exp} \simeq 19$ more sensitive to new heavy physics the mass scale which is tested by a_e is about $100/\sqrt{19} \sim 23$ GeV only, an energy region which we think we know very well as it has been explored by other means. We should keep in mind that the fact that the experiments measuring a_μ and a_e, respectively, hardly can be directly compared from the point of view of the experimental setup and the technical challenges they have to meet. This makes them two rather independent experimental entities. Therefore, the electron $(g_e - 2)$, if not be used to determine α, is the ideal complementary probe of the SM or its failure.

Remember that at LEP-I by electron–positron annihilation predominantly "heavy light" particles Z or at LEP-II predominantly W^+W^-–pairs have been produced, states which were produced in nature mostly in the very early universe.[29] Similarly, the Tevatron acted as a $t\bar{t}$ factory and the LHC reached the Higgs production stage and is hunting for the "new" in the TeV energy range, considerably above the SM spectrum.

Particle accelerators and storage rings are microscopes which allow us to investigates the nature in the subatomic range at distance $< 10^{-15}$ m and at the same time

[28] which is not always true, for example if we read a newspaper or if you read this book.

[29] An energy or an equivalent mass may always be translated into a temperature by means of the Boltzmann constant k which relates $1°\text{K} \equiv 8.6 \times 10^{-5}$eV. Thus $T = E/k$ is the temperature of an event at energy E. As we know the universe expands and thereby cools down, thus looking at higher temperatures means looking further back in the history of the universe. By solving Friedmann's cosmological equations with the appropriate equations of state backwards in time, starting from the present with a cosmic microwave background radiation temperature of 2.728°K and assuming the matter density to be the critical one $\Omega_{\rm tot} = 1$, one may calculate the time at which temperatures realized at LEP with 100 to 200 GeV of center of mass energy where realized. This time is given by $t = 2.4/\sqrt{N(T)}\ (1\ \text{MeV}/kT)^2$ sec, with $N(T) = \sum_{\text{bosons } B} g_B(T) + \frac{7}{8}\sum_{\text{fermions } F} g_F(T)$, the effective number of degrees of freedom excited at temperature T (see Eq. (19.43) in [266]). For LEP energies $m_b \ll kT \simeq M_W$ the numbers $g_{B/F}(T)$ counting spin, color and charge of bosonic/fermionic states in the massless limit include all SM particles except $W^\pm$, Z, H and t one obtains $N(T) = 345/4$. Thus LEP events happened to take place in nature $t \sim 0.3 \times 10^{-10}$ sec after the Big Bang for $T \sim 100$ GeV . With the LHC we reach $t_{\rm LHC} \sim 1.66 \times 10^{-15}$ sec.

have the aim to directly produce new forms of matter, by pair creation, for example. The size of such machines is essentially determined by two parameters: the energy which determines the resolution $\lambda = hc/E_{\text{c.m.}} \simeq 1.2\text{GeV}/E_{\text{c.m.}}(\text{GeV}) \times 10^{-15}\,\text{m}$ and the collision rate $\Delta N/\Delta t = L \times \sigma \simeq 10^{32}\,\sigma(\text{cm}^2)/\text{cm}^2\,\text{sec}$ (luminosity L as it has been reached LEP as an example). Usually projectiles must be stable particles or antiparticles like electrons, positrons and protons and antiprotons. The Muon Storage Ring experiments work with the rather unstable muons which are boosted to highly relativistic quasi–stable muons well selected in energy and polarization before they are injected into the storage ring. The ring in this case more acts as a detector rather than an accelerator as it usually does in the case of typical high energy machines. This allows to study the motion of the muons at incredible precision with very little background.

With the advent of the Large Hadron Collider (LHC) many things already have found a new direction, as we have mentioned several times. Experiments at the LHC take place under extreme conditions. At the LHC one is producing enormous amounts of events, billions per second, of which the overwhelming part of events are too complex to be understood and the interesting "gold platted" events which will tell us about new physics one has to dig out like "searching for a needle in a haystack". Nevertheless, the physics accessible there hopefully will be found, which could tell us what we see in the $(g_\mu - 2)$ discrepancy. At LEP a big machine was able to measure about 20 different observables associated with different final states at the level of 0.1%. The strength of the LHC is that it is able to go far beyond what we have reached so far in terms of the energy scale. But as important, the LHC also is capable of producing milestones in precision physics, like the amazingly precise determination of the Higgs boson mass, the study of the Higgs bosons decay pattern or substantially improving the W and the top quark mass measurements. Other milestones have been achieved in rare processes, like the first observation of $B_s \to \mu^+\mu^-$ events by the LHCb detector. The exclusion limits for many hypothetical new particles already have been moving up to much higher energies, such that several new physics scenarios could be ruled out.

The most remarkable event at the LHC has been the discovery of the Higgs particle. More surprising than its existence was the specific value of its mass found. This has to do with the stability bound of Higgs potential in the SM which has been addressed many times in the past. In 1995 the discovery of the top quark at the Tevatron also reviled its mass and Hambye and Riesselmann (HR) in 1996 [267] (see also references therein) analyzed the stability bound as a function of the yet unknown Higgs boson mass, which is reproduced in Fig. 7.25. The Higgs boson mass at that time has been the only relevant parameter which was not yet known.[30] In a first 2-loop analysis, knowing m_t, HR estimated an upper bound of $M_H < 180$ GeV , below which an extrapolation of the SM Higgs system up to the Planck scale $M_{\text{Planck}} \simeq 1.22 \times 10^{19}$ GeV was possible within a small window. In fact the parameters m^2 and λ in the Higgs potential

[30] A 95% CL lower bound of 77.5 GeV had been estimated by the LEP Collaborations [268] at that time.

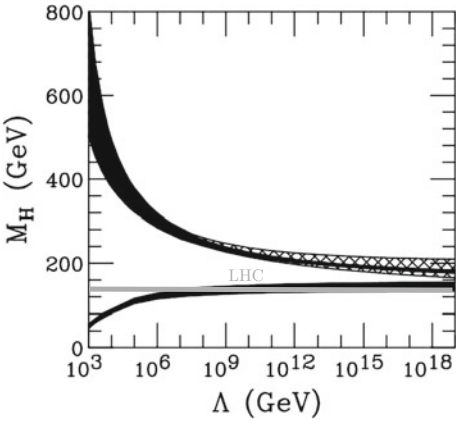

Fig. 7.25 The SM Higgs potential remains perturbative up to the Planck scale $\Lambda = M_{\text{Planck}}$, provided the Higgs boson is light enough (upper bound = avoiding a Landau pole) and the Higgs potential remains stable ($\lambda > 0$) if the Higgs boson is not too light. Parameters used: $m_t = 175[150 - 200]$ GeV ; $\alpha_s = 0.118$. The ATLAS and CMS discovery band has been overlaid. [Reprinted with permission from Ref. [267] http://dx.doi.org/10.1103/PhysRevD.55.7255. Copyright (1996) by the American Physical Society]

$$V(H) = \frac{m^2}{2} H^2 + \frac{\lambda}{24} H^4 , \tag{7.67}$$

decide about the stability of the SM, maybe also about the stability of our universe. The fact that the Higgs mass falls quite precisely into that window is one of the most intriguing findings of recent particle physics.[31]

The Higgs mass just fits into the window of SM parameters which allows for a stable vacuum of the Higgs potential up to the Planck scale. Now all relevant parameters of the SM are known and we can predict how parameters of the SM evolve when we solve the RG up the Planck scale. This also applies to the effective Higgs boson mass, which can be predicted as a function of the renormalization scale μ:

$$m^2_{\text{Higgs,bare}}(\mu) = m^2_{\text{Higgs,ren}} + \delta m^2(\mu)$$
$$\delta m^2(\mu) = \frac{M^2_{\text{Planck}}}{(16\pi^2)} C(\mu) \; ; \quad C(\mu) = \left(\frac{5}{2}\lambda(\mu) + \frac{3}{2} g'^2(\mu) + \frac{9}{2} g^2(\mu) - 12\, y_t^2(\mu) \right).$$

[31] Some analyses [270–272] claim a failure of vacuum stability i.e. $\lambda(\mu)$ has a zero and gets negative at about 10^9 GeV, and find a metastable vacuum instead, just missing stability. This have been questioned in [273] later. A final answer depend on the precise knowledge of the top Yukawa coupling and related problems have been analyzed in [274].

The bare mass here appears as a function of μ as we keep the observed mass as a boundary condition (bottom up approach).[32] Taking into account the running of the SM parameters, at the Planck scale we obtain

$$m_{\text{eff}}^2 \sim \delta m^2 \simeq \frac{M_{\text{Planck}}^2}{32\pi^2}\, C(\mu = M_{\text{Planck}}) \simeq (0.0295\, M_{\text{Planck}})^2 \simeq \left(3.6 \times 10^{17}\ \text{GeV}\right)^2 ,$$

and indeed the effective Higgs potential mass $m(M_{\text{Planck}})$ reaches a huge value which stays clearly below M_{Planck}, however. The non-vanishing quartically enhanced vacuum energy $V(0) = \langle V(H(x))\rangle$ provides a cosmological constant density

$$\begin{aligned} \rho_{\Lambda\,\text{bare}} &= \rho_{\Lambda\,\text{ren}} + \delta\rho(\mu) \\ \delta\rho(\mu) &= \frac{M_{\text{Planck}}^4}{(16\pi^2)^2}\, X(\mu)\ ; \quad X(\mu) = \left(5\,\lambda + 3\,g'^2 + 9\,g^2 - 24\,y_t^2\right). \end{aligned}$$

With SM running parameters at the Planck scale

$$\rho_{\text{eff}} \simeq \delta\rho \sim (1.28\, M_{\text{Planck}})^4 \sim \left(1.57 \times 10^{19}\ \text{GeV}\right)^4 .$$

Surprisingly, because the bosonic couplings and the top quark Yukawa have a different energy dependence both counterterms $\delta m^2(\mu)$ and $\delta\rho(\mu)$ vanish at a scale $\mu = \mu_{\text{CC}}$, which for the specific parameter set happens at

$$\mu_{\text{CC}} \approx 3.1 \times 10^{15}\ \text{GeV} \tag{7.68}$$

clearly below the Planck scale again. There the effective mass changes sign and triggers the Higgs mechanism and the Higgs field acquires a non-vanishing VEV $\langle H(x)\rangle = v(\mu)$, which vanishes identically at higher energies $\mu > \mu_{\text{CC}}$.

Above the Higgs phase transition point μ_{CC} we start to see the bare theory i.e. a SM with its bare short distance effective parameters, so in particular a very heavy Higgs boson, which can be moving at most very slowly, and thus naturally satisfies the slow roll condition that the potential energy dominates the kinetic energy $\frac{1}{2}\dot{H}^2$. Note that the Higgs boson contributes to energy momentum tensor in Einstein's equations a pressure and energy density ($\dot{H}$ the time derivative of H)

$$p = \frac{1}{2}\,\dot{H}^2 - V(H)\ ; \quad \rho = \frac{1}{2}\,\dot{H}^2 + V(H)\,,$$

which then appear in Friedmann's cosmological solutions. As we approach the Planck scale (bare theory) the slow–roll condition $\frac{1}{2}\,\dot{H}^2 \ll V(H)$ comes into play as we

[32] As we have consider the SM to exhibit at cutoff of the size of the Planck mass, we can also calculate the vacuum energy $V(0) \equiv \langle V(H)\rangle$ as a large but finite number. At high energies near the Planck scale the SM is in the symmetric phase i.e. $\langle H\rangle = 0$, while $\langle H^2\rangle$ and $\langle H^4\rangle$ are non-vanishing. This requires a Wick reordering of the potential [60] which is shifting the effective mass such that the coefficient proportional to λ changes from 2 to 5/2.

reach $p \approx -V(H)$, $\rho \approx +V(H)$ and hence $p = -\rho$, which is the equation of state of **DARK ENERGY**. The SM Higgs boson in the early universe provides a huge dark energy, which triggers inflation. That inflation has happened in the early universe is an established fact. The so called hierarchy problem is not a problem it is the solution which promotes the Higgs boson to be the natural candidate for the inflaton. This however only works if no SUSY or GUT is sitting in-between us and the Planck scale, and provided vacuum stability is holds within the SM.

Inflation tunes the total density to $\Omega_{\text{tot}} = 1$ or $\rho_{\text{tot}} = \rho_{\text{crit}} = (0.00216\ \text{eV})^4$. The presently observed dark energy density must be a part of it and actually has the value $\rho_\Lambda = (0.002\ \text{eV})^4$ the known 74% of the total.

Still, dark matter remains a mystery although there are a number of candidates like axions [275], or an extra $SU(4)$ version of QCD forming bound states which could provide bosonic dark matter [276]. So we hope we may soon add more experimentally established terms to the SM Lagrangian and extent our predictions to include the yet unknown. That's how it worked in the past with minimal extensions on theoretical grounds. Why this works so successfully nobody really knows. One observes particles, one associates with them a field, interactions are the simplest non–trivial products of fields (triple and quartic) at a spacetime point, one specifies the interaction strength, puts everything into a renormalizable relativistic QFT and predicts what should happen and it "really" happened essentially without exception. Maybe the muon $g-2$ is the most prominent exception!

This book tried to shed light on the physics encoded in a single real number. Such a single number in principle encodes an infinity of information, as each new significant digit (each improvement should be at least by a factor ten in order to establish the next significant digit) is a new piece of information. It is interesting to ask, what would we know if we would know this number to infinite precision. Of course one cannot encode all we know in that single number. Each observable is a new view to reality with individual sensitivity to the deep structure of matter. All these observables are cornerstones of *one reality* unified self–consistently to our present knowledge by the knowledge of the Lagrangian of a renormalizable quantum field theory. Theory and experiments of the anomalous magnetic moment are one impressive example what it means to understand physics at a fundamental level. The muon $g-2$ reveals the major ingredients of the SM and as we know now maybe even more.

On the theory part the fascinating thing is the technical complexity of higher order SM (or beyond) calculations of in the meantime thousands of diagrams which can only be managed by the most powerful computers in analytical as well as in the numerical part of such calculations. This book only gives little real insight into the technicalities of such calculation. Performing higher order Feynman diagram calculation could look like formal nonsense but at the end results in a number which experimenters indeed measure. Much of theoretical physics today takes place beyond the Galilean rules, namely that sensible predictions must be testable. For anomalous magnetic moment at least we still follow the successful tradition set up by Galileo Galilei, we definitely can check it, including all the speculations about it.

A next major step in this field of research would be establishing experimentally the electric dipole moment. This seems to be within reach thanks to a breakthrough in the

experimental techniques. The electric dipole moments are an extremely fine monitor for CP violation beyond the SM which could play a key role for understanding the origin of the baryon matter–antimatter asymmetry in the universe.

And now we are waiting for the new results on the muon $g-2$ and for new data from the LHC to tell us where we go!

References

1. J. Bailey et al., Nucl. Phys. B **150**, 1 (1979)
2. G.W. Bennett et al., Muon g-2 Collab. Phys. Rev. D **73**, 072003 (2006)
3. T. Kinoshita, M. Nio, Phys. Rev. D **73**, 053007 (2006)
4. T. Aoyama, M. Hayakawa, T. Kinoshita, M. Nio, Phys. Rev. Lett. **109**, 111808 (2012)
5. S. Laporta, arXiv:1704.06996 [hep-ph]
6. M. Knecht, EPJ Web Conf. **118**, 01017 (2016)
7. F. Jegerlehner, R. Szafron, Eur. Phys. J. C **71**, 1632 (2011)
8. F. Jegerlehner, EPJ Web Conf. **118**, 01016 (2016), arXiv:1705.00263 [hep-ph]
9. J. Bijnens, E. Pallante, J. Prades, Phys. Rev. Lett. **75**, 1447 (1995) [Erratum-ibid. **75**, 3781 (1995)]; Nucl. Phys. B **474**, 379 (1996) [Erratum-ibid. **626**, 410 (2002)]
10. M. Hayakawa, T. Kinoshita, Phys. Rev. D **57**, 465 (1998) [Erratum-ibid. D **66**, 019902 (2002)]
11. M. Knecht, A. Nyffeler, Phys. Rev. D **65**, 073034 (2002)
12. K. Melnikov, A. Vainshtein, Phys. Rev. D **70**, 113006 (2004)
13. F. Jegerlehner, A. Nyffeler, Phys. Rep. **477**, 1 (2009)
14. A. Czarnecki, W.J. Marciano, A. Vainshtein, Phys. Rev. D **67**, 073006 (2003) [Erratum-ibid. D **73**, 119901 (2006)]; M. Knecht, S. Peris, M. Perrottet, E. de Rafael, JHEP **0211**, 003 (2002); E. de Rafael, *The muon g-2 revisited*, arXiv:hep-ph/0208251
15. S. Heinemeyer, D. Stöckinger, G. Weiglein, Nucl. Phys. B **699**, 103 (2004)
16. T. Gribouk, A. Czarnecki, Phys. Rev. D **72**, 053016 (2005)
17. C. Gnendiger, D. Stöckinger, H. Stöckinger-Kim, Phys. Rev. D **88**, 053005 (2013)
18. H.N. Brown et al., Muon (g-2) Collab. Phys. Rev. Lett. **86**, 2227 (2001)
19. F. Jegerlehner, Nucl. Phys. Proc. Suppl. **162**, 22 (2006)
20. K.G. Chetyrkin, J.H. Kühn, Phys. Lett. B **342**, 356 (1995); K.G. Chetyrkin, J.H. Kühn, A. Kwiatkowski, Phys. Rept. **277**, 189 (1996); K.G. Chetyrkin, J.H. Kühn, M. Steinhauser, Phys. Lett. B **371**, 93 (1996); Nucl. Phys. B **482**, 213 (1996); **505**, 40 (1997); K.G. Chetyrkin, R. Harlander, J.H. Kühn, M. Steinhauser, Nucl. Phys. B **503**, 339 (1997) K.G. Chetyrkin, R.V. Harlander, J.H. Kühn, Nucl. Phys. B **586**, 56 (2000) [Erratum-ibid. B **634**, 413 (2002)]
21. R.V. Harlander, M. Steinhauser, Comput. Phys. Commun. **153**, 244 (2003)
22. M. Benayoun, P. David, L. DelBuono, F. Jegerlehner, Eur. Phys. J. C **75**, 613 (2015)
23. M. Benayoun, P. David, L. DelBuono, F. Jegerlehner, Eur. Phys. J. C **72**, 1848 (2012) and references therein
24. M. Davier, A. Höcker, B. Malaescu, Z. Zhang, Eur. Phys. J. C **71**, 1515 (2011) [Erratum-ibid. C **72**, 1874 (2012)]
25. K. Hagiwara, R. Liao, A.D. Martin, D. Nomura, T. Teubner, J. Phys. G G **38**, 085003 (2011)
26. M. Davier et al., Eur. Phys. J. C **66**, 127 (2010)
27. M. Davier [BaBar Collab.], Nucl. Part. Phys. Proc. **260**, 102 (2015)
28. Z. Zhang, EPJ Web Conf. **118**, 01036 (2016)
29. K. Hagiwara, A.D. Martin, D. Nomura, T. Teubner, Phys. Lett. B 557, 69; Phys. Rev. D **69**(2004), 093003 (2003)
30. S. Eidelman, F. Jegerlehner, Z. Phys. C **67**, 585 (1995); F. Jegerlehner, in *Radiative Corrections*, ed. by J. Solà (World Scientific, Singapore, 1999) p. 75

31. H. Leutwyler, Electromagnetic form factor of the pion, in *Continuous Advances in QCD 2002*: Proceedings ed. by K.A. Olive, M.A. Shifman, M.B. Voloshin (World Scientific, Singapore 2002) p. 646, arXiv:hep-ph/0212324
32. G. Colangelo, Nucl. Phys. Proc. Suppl. **131**, 185 (2004); ibid. **162**, 256 (2006)
33. B. Ananthanarayan, I. Caprini, D. Das, I.S. Imsong, Phys. Rev. D **93**, 116007 (2016)
34. V. M. Aulchenko et al. [CMD-2 Collab.], JETP Lett. **82**, 743 (2005) [Pisma Zh. Eksp. Teor. Fiz. **82**, 841 (2005)]; R. R. Akhmetshin et al., JETP Lett. **84**, 413 (2006) [Pisma Zh. Eksp. Teor. Fiz. **84**, 491 (2006)]; Phys. Lett. B **648**, 28 (2007)
35. M.N. Achasov et al. [SND Collab.], J. Exp. Theor. Phys. **103**, 380 (2006) [Zh. Eksp. Teor. Fiz. **130**, 437 (2006)]
36. A. Aloisio [KLOE Collab.], Phys. Lett. B 606 (2005) 12; F. Ambrosino et al. et al., KLOE Collab. Phys. Lett. B **670**, 285 (2009)
37. F. Ambrosino et al., KLOE Collab. Phys. Lett. B **700**, 102 (2011)
38. D. Babusci et al., KLOE Collab. Phys. Lett. B **720**, 336 (2013)
39. B. Aubert et al., [BABAR Collab.], Phys. Rev. Lett. 103, 231801 (2009); J.P. Lees et al. Phys. Rev. D **86**, 032013 (2012)
40. M. Ablikim et al., BESIII Collab. Phys. Lett. B **753**, 629 (2016)
41. K. Hagiwara, A.D. Martin, D. Nomura, T. Teubner, Phys. Lett. B **649**, 173 (2007)
42. M. Davier, S. Eidelman, A. Höcker, Z. Zhang, Eur. Phys. J. C **27**, 497 (2003); Eur. Phys. J. C **31**, 503 (2003)
43. S. Eidelman, in Proceedings of the XXXIII International Conference on High Energy Physics, July 27–August 2 2006 (World Scientific, Moscow (Russia) to appear); M. Davier, Nucl. Phys. Proc. Suppl. **169**, 288 (2007)
44. R. Barate et al., [ALEPH Collab.], Z. Phys. C **76**, 15 (1997); Eur. Phys. J. C **4**, 409 (1998); S. Schael et al., [ALEPH Collab.], Phys. Rept. **421**, 191 (2005)
45. M. Davier et al., Eur. Phys. J. C **74**, 2803 (2014)
46. K. Ackerstaff et al., OPAL Collab. Eur. Phys. J. C **7**, 571 (1999)
47. S. Anderson et al., CLEO Collab. Phys. Rev. D **61**, 112002 (2000)
48. M. Fujikawa et al., Belle Collab. Phys. Rev. D **78**, 072006 (2008)
49. M. Davier, arXiv:1612.02743 [hep-ph]
50. R.L. Garwin, D.P. Hutchinson, S. Penman, G. Shapiro, Phys. Rev. **118**, 271 (1960)
51. G. Charpak, F.J.M. Farley, R.L. Garwin, T. Muller, J.C. Sens, V.L. Telegdi, A. Zichichi, Phys. Rev. Lett. **6**, 128 (1961); G. Charpak, F.J.M. Farley, R.L. Garwin, T. Muller, J.C. Sens, A. Zichichi, Nuovo Cimento **22**, 1043 (1961)
52. G. Charpak, F.J.M. Farley, R.L. Garwin, T. Muller, J.C. Sens, A. Zichichi, Phys. Lett. B **1**, 16 (1962); Nuovo Cimento **37**, 1241 (1965)
53. F.J.M. Farley, J. Bailey, R.C.A. Brown, M. Giesch, H. Jöstlein, S. van der Meer, E. Picasso, M. Tannenbaum, Nuovo Cimento **45**, 281 (1966)
54. J. Bailey et al., Phys. Lett. B **28**, 287 (1968); Nuovo Cimento A **9**, 369 (1972)
55. J. Bailey [CERN Muon Storage Ring Collab.], Phys. Lett. B 55, 420 (1975); Phys. Lett. B 67, 225 (1977) [Phys. Lett. B 68, 191 (1977)]; J. Bailey et al., CERN-Mainz-Daresbury Collab. Nucl. Phys. B **150**, 1 (1979)
56. R.M. Carey et al., Muon (g-2) Collab. Phys. Rev. Lett. **82**, 1632 (1999)
57. H.N. Brown et al., Muon (g-2) Collab. Phys. Rev. D **62**, 091101 (2000)
58. G.W. Bennett et al. [Muon (g-2) Collab.], Phys. Rev. Lett. **89**, 101804 (2002) [Erratum-ibid. **89**, 129903 (2002)]
59. G.W. Bennett et al., Muon (g-2) Collab. Phys. Rev. Lett. **92**, 161802 (2004)
60. F. Jegerlehner, Acta Phys. Polon. B **45**(6), 1215 (2014)
61. J.C. Pati, A. Salam, Phys. Rev. Lett. **31**, 661 (1973); Phys. Rev. D **8**, 1240 (1973); H. Georgi, S.L. Glashow, Phys. Rev. Lett. **32**, 438 (1974); H. Fritzsch, P. Minkowski, Ann. Phys. **93**, 193 (1975)
62. A. Galli, Nuovo Cim. A **106**, 1309 (1993)
63. J.R. Ellis, S. Kelley, D.V. Nanopoulos, Phys. Lett. B 249, 441 (1990); ibid 260, 131 (1991); U. Amaldi, W. de Boer, H.Fürstenau, Phys. Lett. B 260, 447 (1991); P. Langacker, M.x. Luo. Phys. Rev. D **44**, 817 (1991)

64. LEP Electroweak Working Group (LEP EWWG), http://lepewwg.web.cern.ch/LEPEWWG/plots/summer2006 [ALEPH, DELPHI, L3, OPAL, SLD Collab.s], *Precision electroweak measurements on the Z resonance*, Phys. Rept. **427**, 257 (2006), arXiv:0509008 [hep-ex/0509008]; http://lepewwg.web.cern.ch/LEPEWWG/Welcome.html
65. J. Erler, P. Langacker, Electroweak model and constraints on new physics in W. M. Yao, et al., Particle Data Group. J. Phys. G **33**, 1 (2006)
66. G. Aad et al., ATLAS and CMS Collab. Phys. Rev. Lett. **114**, 191803 (2015)
67. M. Czakon, J. Gluza, F. Jegerlehner, M. Zrałek, Eur. Phys. J. C **13**, 275 (2000)
68. F. Jegerlehner, Prog. Part. Nucl. Phys. **27**, 1 (1991)
69. Heavy Flavor Averaging Group (HFAG), http://www.slac.stanford.edu/xorg/hfag/, http://www-cdf.fnal.gov/physics/new/bottom/bottom.html
70. G. D'Ambrosio, G.F. Giudice, G. Isidori, A. Strumia, Nucl. Phys. B **645**, 155 (2002)
71. R.S. Chivukula, H. Georgi, Phys. Lett. B **188**, 99 (1987)
72. W. Altmannshofer, A.J. Buras, D. Guadagnoli, JHEP **0711**, 065 (2007)
73. I.B. Khriplovich, S.K. Lamoreaux, *CP Violation Without Strangeness: Electric Dipole Moments of Particles, Atoms and Molecules* (Springer, Berlin, 1997)
74. F.J.M. Farley et al., Phys. Rev. Lett. **93**, 052001 (2004); M. Aoki et al. [J-PARC Letter of Intent]: *Search for a Permanent Muon Electric Dipole Moment at the* $\times 10^{-24}\, e\cdot$ cm *Level*, http://www-ps.kek.jp/jhf-np/LOIlist/pdf/L22.pdf
75. A. Adelmann, K. Kirch, arXiv:hep-ex/0606034
76. M. Aaboud et al., ATLAS collab. Phys. Lett. B **761**, 350 (2016)
77. V. Khachatryan et al., CMS collab. Phys. Rev. D **93**, 072004 (2016)
78. R. Schwienhorst [CDF and D0 Collab.s], arXiv:1612.02311 [hep-ex]
79. B.E. Lautrup, A. Peterman, E. de Rafael, Phys. Rep. **3C**, 193 (1972)
80. J.P. Leveille, Nucl. Phys. B **137**, 63 (1978)
81. A. Freitas, J. Lykken, S. Kell, S. Westhoff, JHEP **1405**, 145 (2014) Erratum: [JHEP **1409**, 155 (2014)]
82. R. Van Royen, V.F. Weisskopf, Nuovo Cim. A **50**, 617 (1967) [Erratum-ibid. A **51**, 583 (1967)]
83. C.T. Hill, E.H. Simmons, Phys. Rep. **381**, 235 (2003) [Erratum-ibid. **390**, 553 (2004)]
84. E. Eichten, K. Lane, Phys. Lett. B **669**, 235 (2008)
85. R. Foadi, M.T. Frandsen, T.A. Ryttov, F. Sannino, Phys. Rev. D 76, 055005 (2007); T.A. Ryttov, F. Sannino. Phys. Rev. D **76**, 105004 (2007)
86. F. Jegerlehner, Helv. Phys. Acta **51**, 783 (1978); F. Jegerlehner, The 'ether-world' and elementary particles, in *Theory of Elementary Particles* ed. by H. Dorn, D. Lüst, G. Weight (WILEY-VCH, Berlin, 1998) p. 386, arXiv:hep-th/9803021
87. A. Czarnecki, W.J. Marciano, Phys. Rev. D **64**, 013014 (2001)
88. H. Okada, K. Yagyu, Phys. Rev. D **89**(5), 053008 (2014)
89. A.M. Baldini et al. [MEG Collab.], Eur. Phys. J. C **76**(8), 434 (2016)
90. R. Barbieri, L.J. Hall, Phys. Lett. B 338, 212 (1994); R. Barbieri, L.J. Hall, A. Strumia, Nucl. Phys. B 445, 219 (1995); J. Hisano, D. Nomura. Phys. Rev. D **59**, 116005 (1999)
91. W.C. Chiu, C.Q. Geng, D. Huang, Phys. Rev. D **91**, 013006 (2015)
92. P. Paradisi, EPJ Web Conf. **118**, 01026 (2016)
93. M. Lindner, M. Platscher, F.S. Queiroz, arXiv:1610.06587 [hep-ph]
94. F. Jegerlehner, Nucl. Phys. B (Proc. Suppl.) **37**, 129 (1994)
95. P. Mery, S.E. Moubarik, M. Perrottet, F.M. Renard, Z. Phys. C **46**, 229 (1990)
96. W.M. Yao et al. [Particle Data Group], J. Phys. G **33**, 1 (2006); K.A. Olive et al., Chin. Phys. C **38**, 090001 (2014); C. Patrignani et al., Chin. Phys. C **40**(10), 100001 (2016)
97. LEP Electroweak Working Group (LEP EWWG), http://lepewwg.web.cern.ch/LEPEWWG/lepww/tgc/
98. D. Chang, W.F. Chang, C.H. Chou, W.Y. Keung, Phys. Rev. D **63**, 091301 (2001)
99. K.M. Cheung, C.H. Chou, O.C.W. Kong, Phys. Rev. D **64**, 111301 (2001)
100. F. Larios, G. Tavares-Velasco, C.P. Yuan, Phys. Rev. D **64**, 055004 (2001)
101. M. Krawczyk, Acta Phys. Polon. B **33**, 2621 (2002); PoS **HEP2005**, 335 (2006), arXiv:0512371 [hep-ph/0512371]

102. K. Cheung, O.C.W. Kong, Phys. Rev. D **68**, 053003 (2003)
103. S.L. Glashow, S. Weinberg, Phys. Rev. D **15**, 1958 (1977)
104. A.G. Akeroyd, A. Arhrib, E.M. Naimi, Phys. Lett. B **490**, 119 (2000)
105. R. Santos, S.M. Oliveira, A. Barroso, arXiv:hep-ph/0112202
106. J.F. Gunion, H.E. Haber, Phys. Rev. D **67**, 075019 (2003)
107. I.F. Ginzburg, M. Krawczyk, Phys. Rev. D **72**, 115013 (2005)
108. F. Jegerlehner, Acta Phys. Polon. B **45**(6), 1167 (2014)
109. V. Ilisie, JHEP **1504**, 077 (2015)
110. C.-Y. Chen, S. Dawson, Phys. Rev. D **87**, 055016 (2013)
111. C.-Y. Chen, S. Dawson, M. Sher, Phys. Rev. D **88**, 015018 (2013)
112. J. Baglio, O. Eberhardt, U. Nierste, M. Wiebusch, Phys. Rev. D **90**, 015008 (2014)
113. O. Eberhardt, U. Nierste, M. Wiebusch, JHEP **1307**, 118 (2013)
114. X.D. Cheng, Y.D. Yang, X.B. Yuan, Eur. Phys. J. C **74**, 3081 (2014)
115. A. Barroso, P.M. Ferreira, R. Santos, M. Sher, J.P. Silva, arXiv:1304.5225 [hep-ph]
116. S. Chang, S.K. Kang, J.P. Lee, K.Y. Lee, S.C. Park, J. Song, JHEP **1305**, 075 (2013)
117. G. Belanger, B. Dumont, U. Ellwanger, J. Gunion, S. Kraml, Phys. Rev. D **88**, 075008 (2013)
118. V. Barger, L.L. Everett, H.E. Logan, G. Shaughnessy, Phys. Rev. D **88**, 115003 (2013)
119. S. Chang, S.K. Kang, J.P. Lee, K.Y. Lee, S.C. Park, J. Song, JHEP **1409**, 101 (2014)
120. K. Cheung, J.S. Lee, P.-Y. Tseng, JHEP **1401**, 085 (2014)
121. A. Celis, V. Ilisie, A. Pich, JHEP **1312**, 095 (2013)
122. P.M. Ferreira, R. Guedes, J.F. Gunion, H.E. Haber, M.O.P. Sampaio, R. Santos, arXiv:1407.4396 [hep-ph]
123. O.C.W. Kong, arXiv:hep-ph/0402010
124. A. Cherchiglia, P. Kneschke, D. Stöckinger, H. Stöckinger-Kim, JHEP **1701**, 007 (2017)
125. A. Broggio, E.J. Chun, M. Passera, K.M. Patel, S.K. Vempati, JHEP **1411**, 058 (2014)
126. S.M. Barr, A. Zee, Phys. Rev. Lett. **65**, 21 (1990) [Erratum-ibid. **65**, 2920 (1990)]
127. M. Krawczyk, J. Zochowski, Phys. Rev. D **55**, 6968 (1997)
128. A. Wahab El Kaffas, P. Osland, O. Magne, Ogreid. Phys. Rev. D **76**, 095001 (2007)
129. G.C. Branco, P.M. Ferreira, L. Lavoura, M.N. Rebelo, M. Sher, J.P. Silva, Phys. Rept. **516**, 1 (2012)
130. L. Basso, A. Lipniacka, F. Mahmoudi, S. Moretti, P. Osland, G.M. Pruna, M. Purmohammadi, JHEP **1211**, 011 (2012)
131. A. Pich, P. Tuzon, Phys. Rev. D **80**, 091702 (2009)
132. M. Aoki, S. Kanemura, K. Tsumura, K. Yagyu, Phys. Rev. D **80**, 015017 (2009)
133. E. Ma, Verifiable radiative seesaw mechanism of neutrino mass and dark matter. Phys. Rev. D **73**, 077301 (2006)
134. R. Barbieri, L.J. Hall, V.S. Rychkov, Phys. Rev. D **74**, 015007 (2006)
135. A. Crivellin, A. Kokulu, C. Greub, Phys. Rev. D **87**, 094031 (2013)
136. M. Misiak, M. Steinhauser, arXiv:1702.04571 [hep-ph]
137. A. Dedes, H.E. Haber, JHEP **0105**, 006 (2001)
138. J.F. Gunion, JHEP **0908**, 032 (2009)
139. A. Arhrib, S. Baek, Phys. Rev. D **65**, 075002 (2002)
140. S. Heinemeyer, D. Stöckinger, G. Weiglein, Nucl. Phys. B **690**, 62 (2004); ibid **699**, 103 (2004)
141. K. Cheung, O.C.W. Kong, J.S. Lee, JHEP **0906**, 020 (2009)
142. J. Ellis, T. Hahn, S. Heinemeyer, K.A. Olive, G. Weiglein, JHEP **0710**, 092 (2007)
143. A. Crivellin, M. Ghezzi, M. Procura, JHEP **1609**, 160 (2016)
144. F. Jegerlehner, Frascati Phys. Ser. **54**, 42 (2012). [arXiv:1203.0806 [hep-ph]]
145. P. Bechtle, H.E. Haber, S. Heinemeyer, O. Stål, T. Stefaniak, G. Weiglein, L. Zeune, Eur. Phys. J. C **77**, 67 (2017)
146. S. Heinemeyer, arXiv:1612.08249 [hep-ph]
147. J. Wess, B. Zumino, Nucl. Phys. B 70, 39 (1974); R. Haag, J. T. Lopuszanski, M. Sohnius. Nucl. Phys. B **88**, 257 (1975)

148. D.Z. Freedman, P. van Nieuwenhuizen, S. Ferrara, Phys. Rev. D 13, 3214 (1976); S. Deser, B. Zumino. Phys. Lett. B **62**, 335 (1976)
149. H. P. Nilles, Phys. Rep. **110**, 1 (1984); H.E. Haber, G.L. Kane, Phys. Rep. **117**, 75 (1985); L. Ibáñez, Beyond the Standard Model, in CERN Yellow Report, CERN 92-06, 131–237 (1992)
150. E. Dudas, Y. Mambrini, A. Mustafayev, K.A. Olive, Eur. Phys. J. C **72**, 2138 (2012) Erratum: [Eur. Phys. J. C **73**, 2340 (2013)]
151. F. Jegerlehner, arXiv:1305.6652 [hep-ph]; arXiv:1503.00809 [hep-ph]
152. J.R. Ellis, J.S. Hagelin, D.V. Nanopoulos, K.A. Olive, M. Srednicki, Nucl. Phys. B **238**, 453 (1984)
153. C.L. Bennett et al., [WMAP Collab.], Astrophys. J. Suppl. **148**, 1 (2003); D.N. Spergel et al., [WMAP Collab.], Astrophys. J. Suppl. **148**, 175 (2003)
154. P.A.R. Ade et al., Planck collab. Astron. Astrophys. **594**, A13 (2016)
155. J.R. Ellis, K.A. Olive, Y. Santoso, V.C. Spanos, Phys. Lett. B **565**, 176 (2003); Phys. Rev. D **71**, 095007 (2005)
156. H. Baer, A. Belyaev, T. Krupovnickas, A. Mustafayev, JHEP **0406**, 044 (2004); J. Ellis, S. Heinemeyer, K.A. Olive, G. Weiglein, *Indications of the CMSSM mass scale from precision electroweak data*, arXiv:hep-ph/0604180
157. J. Ellis, K.A. Olive, Eur. Phys. J. C **72**, 2005 (2012). doi:10.1140/epjc/s10052-012-2005-2
158. G. Aad et al., [ATLAS Collab.], JHEP **1510**, 134 (2015)
159. V. Khachatryan et al., [CMS Collab.], JHEP **1610**, 129 (2016)
160. H.E. Haber, R. Hempfling, Phys. Rev. Lett. 66, 1815 (1991); Y. Okada, M. Yamaguchi, T. Yanagida. Prog. Theor. Phys. **85**, 1 (1991)
161. P. Athron, J.h. Park, T. Steudtner, D. Stöckinger, A. Voigt, JHEP **1701**, 079 (2017)
162. R. Hempfling, A.H. Hoang, Phys. Lett. B **331**, 99 (1994); H.E. Haber, R. Hempfling, A.H. Hoang, Z. Phys. C **75**, 539 (1997); S. Heinemeyer, W. Hollik, G. Weiglein, Phys. Lett. B **455**, 179 (1999); Phys. Rept. **425**, 265 (2006)
163. P. Bechtle, O. Brein, S. Heinemeyer, O. Stål, T. Stefaniak, G. Weiglein, K.E. Williams, Eur. Phys. J. C **74**, 2693 (2014)
164. P. Diessner, J. Kalinowski, W. Kotlarski, D. Stöckinger, Adv. High Energy Phys. **2015**, 760729 (2015)
165. S. Ferrara, E. Remiddi, Phys. Lett. B **53**, 347 (1974)
166. J.L. Lopez, D.V. Nanopoulos, X. Wang, Phys. Rev. D 49, 366 (1994); U. Chattopadhyay, P. Nath. Phys. Rev. D **53**, 1648 (1996)
167. T. Moroi, Phys. Rev. D **53**, 6565 (1996) Erratum: [Phys. Rev. D **56**, 4424 (1997)]
168. S.P. Martin, J.D. Wells, Phys. Rev. D **64**, 035003 (2001)
169. D. Stöckinger, J. Phys. G: Nucl. Part. Phys. **34**, 45 (2007)
170. G. Degrassi, G.F. Giudice, Phys. Rev. D **58**, 053007 (1998)
171. M.A. Ajaib, B. Dutta, T. Ghosh, I. Gogoladze, Q. Shafi, Phys. Rev. D **92**, 075033 (2015)
172. S. Marchetti, S. Mertens, U. Nierste, D. Stöckinger, Phys. Rev. D **79**, 013010 (2009)
173. M. Bach, J.h. Park, D. Stöckinger, H. Stöckinger-Kim, JHEP **1510**, 026 (2015)
174. H. Fargnoli, C. Gnendiger, S. Paßehr, D. Stöckinger, H. Stöckinger-Kim, JHEP **1402**, 070 (2014)
175. T.F. Feng, X.Q. Li, L. Lin, J. Maalampi, H.S. Song, Phys. Rev. D **73**, 116001 (2006)
176. M.J. Ramsey-Musolf, S. Su, *Low Energy Precision Test of Supersymmetry*, arXiv:hep-ph/0612057
177. C.H. Chen, C.Q. Geng, Phys. Lett. B **511**, 77 (2001)
178. S. Heinemeyer, W. Hollik, G. Weiglein, L. Zeune, JHEP **1312**, 084 (2013)
179. M. Baak et al., Gfitter group. Eur. Phys. J. C **74**, 3046 (2014)
180. M. Aaboud et al., [ATLAS Collab.], arXiv:1701.07240 [hep-ex]
181. O. Buchmueller et al., Phys. Lett. B **657**, 87 (2007)
182. S. Heinemeyer, W. Hollik, A.M. Weber, G. Weiglein, JHEP **0804**, 039 (2008)
183. O. Buchmueller et al., Phys. Rev. D **81**, 035009 (2010)

184. ALEPH, CDF, D0, DELPHI, L3, OPAL, SLD Collab.s, the LEP Electroweak Working Group, the Tevatron Electroweak Working Group and the SLD electroweak and heavy flavour groups, arXiv:1012.2367 [hep-ex],
185. M. Awramik, M. Czakon, A. Freitas, G. Weiglein, Phys. Rev. D **69**, 053006 (2004)
186. S. Heinemeyer, W. Hollik, D. Stöckinger, A.M. Weber, G. Weiglein, JHEP **0608**, 052 (2006)
187. S. Bertolini, F. Borzumati, A. Masiero, G. Ridolfi, Nucl. Phys. B **353**, 591 (1991)
188. M. Misiak et al., Phys. Rev. Lett. **98**, 022002 (2007)
189. M. Misiak et al., Phys. Rev. Lett. 98, 022002 (2007). M. Ciuchini, G. Degrassi, P. Gambino, G.F. Giudice, Nucl. Phys. B 534, 3 (1998); G. Degrassi, P. Gambino, G.F. Giudice, JHEP 0012, 009 (2000); M.S. Carena, D. Garcia, U. Nierste, C.E.M. Wagner, Phys. Lett. B **499**, 141 (2001)
190. D. Asner et al., The Heavy Flavor Averaging Group, arXiv:1010.1589 [hep-ex]
191. R. Aaij et al., LHCb collab. Phys. Rev. Lett. **111**, 101805 (2013)
192. R. Barbieri, G.F. Giudice, Phys. Lett. B 309, 86 (1993); M. Carena, D. Garcia, U. Nierste, C.E.M. Wagner. Phys. Lett. B **499**, 141 (2001)
193. L.F. Abbott, P. Sikivie, M.B. Wise, Phys. Rev. D 21, 1393 (1980); M. Ciuchini, G. Degrassi, P. Gambino, G.F. Giudice. Nucl. Phys. B **527**, 21 (1998)
194. G. Isidori, P. Paradisi, Phys. Lett. B 639, 499 (2006); G. Isidori, F. Mescia, P. Paradisi, D. Temes. Phys. Rev. D **75**, 115019 (2007)
195. S.P. Martin, J.D. Wells, Phys. Rev. D **67**, 015002 (2003)
196. K.J. de Vries, *Global fits of supersymmetric models after LHC Run 1,*, Thesis; K.J. de Vries [MasterCode Collab.], Nucl. Part. Phys. Proc. **273–275**, 528 (2016)
197. H. Baer, V. Barger, A. Mustafayev, Phys. Rev. D **85**, 075010 (2012)
198. P. Bechtle et al., Nucl. Part. Phys. Proc. **273–275**, 589 (2016)
199. J. Ellis, arXiv:1504.03654 [hep-ph]
200. M. Endo, K. Hamaguchi, S. Iwamoto, T. Yoshinaga, JHEP **1401**, 123 (2014)
201. M. Endo, K. Hamaguchi, S. Iwamoto, N. Yokozaki, Phys. Rev. D 85, 095012 (2012); M. Endo, K. Hamaguchi, S. Iwamoto, K. Nakayama, N. Yokozaki. Phys. Rev. D **85**, 095006 (2012)
202. G. Bhattacharyya, B. Bhattacherjee, T.T. Yanagida, N. Yokozaki, Phys. Lett. B **730**, 231 (2014)
203. A. Djouadi et al., [MSSM Working Group], arXiv:hep-ph/9901246
204. T. Nihei, L. Roszkowski, R. Ruiz de Austri, JHEP **0207**, 024 (2002)
205. B. Dutta et al., Phys. Rev. D **91**, 055025 (2015)
206. P. Fayet, Phys. Rev. D **75**, 115017 (2007)
207. M. Pospelov, Phys. Rev. D **80**, 095002 (2009)
208. D. Tucker-Smith, I. Yavin, Phys. Rev. D **83**, 101702 (R) (2011)
209. H. Davoudiasl, H.S. Lee, W.J. Marciano, Phys. Rev. D **85**, 115019 (2012)
210. J.D. Bjorken et al., Phys. Rev. D **80**, 075018 (2009)
211. D. Babusci et al., KLOE-2 collab. Phys. Lett. B **720**, 111 (2013)
212. S. Abrahamyan et al., APEX collab. Phys. Rev. Lett. **107**, 191804 (2011)
213. P. Adlarson et al., WASA-at-COSY collab. Phys. Lett. B **726**, 187 (2013)
214. G. Agakishiev et al., HADES collab. Phys. Lett. B **731**, 265 (2014)
215. H. Merkel et al., A1 collab. Phys. Rev. Lett. **112**, 221802 (2014)
216. D. Babusci et al., KLOE-2 collab. Phys. Lett. B **736**, 459 (2014)
217. J.P. Lees et al., BaBar collab. Phys. Rev. Lett. **113**, 201801 (2014)
218. J.P. Lees et al., [BaBar Collab.], arXiv:1702.03327 [hep-ex]
219. J.R. Batley et al., NA48/2 collab. Phys. Lett. B **746**, 178 (2015)
220. D. Banerjee et al., NA64 collab. Phys. Rev. Lett. **118**, 011802 (2017)
221. A. Anastasi et al., KLOE collab. Phys. Lett. B **750**, 633 (2015)
222. A. Anastasi et al., KLOE-2 collab. Phys. Lett. B **757**, 356 (2016). doi:10.1016/j.physletb.2016.04.019
223. R.D. Peccei, H.R. Quinn, Phys. Rev. Lett. **38**, 1440 (1977)
224. S. Weinberg, Phys. Rev. Lett. **40**, 223 (1978)

225. F. Wilczek, Phys. Rev. Lett. **40**, 279 (1978)
226. W.J. Marciano, A. Masiero, P. Paradisi, M. Passera, Phys. Rev. D **94**, 115033 (2016)
227. C.Y. Chen, H. Davoudiasl, W.J. Marciano, C. Zhang, Phys. Rev. D **93**, 035006 (2016)
228. L. Wang, X.F. Han, Phys. Lett. B **739**, 416 (2014); X.F. Han, L. Wang, arXiv:1701.02678 [hep-ph]
229. D. Zhuridov, Phys. Rev. D **93**, 035025 (2016)
230. M. Knecht, A. Nyffeler, M. Perrottet, E. De Rafael, Phys. Rev. Lett. **88**, 071802 (2002)
231. N.N. Achasov, A.V. Kiselev, JETP Lett. **75**, 527 (2002) [Pisma Zh. Eksp. Teor. Fiz. **75**, 643 (2002)]. doi:10.1134/1.1500713
232. J.I. Collar et al., New light, weakly-coupled particles, in *Fundamental Physics at the Intensity Frontier*, J.L. Hewett et al. (ed.). doi:10.2172/1042577, arXiv:1205.2671 [hep-ex]
233. S.J. Brodsky, S.D. Drell, Phys. Rev. D **22**, 2236 (1980)
234. H. Chavez, J.A. Martins, Simoes. Nucl. Phys. B **783**, 76 (2007)
235. X. Calmet, H. Fritzsch, D. Holtmannspotter, Phys. Rev. D **64**, 037701 (2001)
236. S.C. Park, J.h. Song, Phys. Rev. D **69**, 115010 (2004)
237. T. Appelquist, B.A. Dobrescu, Phys. Lett. B **516**, 85 (2001)
238. G. Cacciapaglia, M. Cirelli, G. Cristadoro, Nucl. Phys. B **634**, 230 (2002)
239. B.L. Roberts Nucl. Phys. B (Proc. Suppl.) **131**, 157 (2004); R.M. Carey et al., Proposal of the BNL Experiment E969, 2004; J-PARC Letter of Intent L17
240. J. Grange et al., [Muon g-2 Collab.], arXiv:1501.06858 [physics.ins-det]
241. D.W. Hertzog, EPJ Web Conf. **118**, 01015 (2016)
242. G. Venanzoni, [Fermilab E989 Collab.], Nucl. Part. Phys. Proc. **273–275**, 584 (2016). doi:10.1016/j.nuclphysbps.2015.09.087; PoS EPS **-HEP2015**, 568 (2015)
243. N. Saito, J-PARC g-2/EDM collab. AIP Conf. Proc. **1467**, 45 (2012). doi:10.1063/1.4742078
244. H. Iinuma, J-PARC muon g-2/EDM collab. J. Phys. Conf. Ser. **295**, 012032 (2011). doi:10.1088/1742-6596/295/1/012032
245. T. Mibe, [J-PARC g-2 Collab.], Nucl. Phys. Proc. Suppl. **218**, 242 (2011). doi:10.1016/j.nuclphysbps.2011.06.039
246. W. Gerlach, O. Stern, Zeits. Physik **8**, 110 (1924)
247. G.E. Uhlenbeck, S. Goudsmit, Naturwissenschaften 13, 953 (1925). Nature **117**, 264 (1926)
248. G. Colangelo, M. Hoferichter, B. Kubis, M. Procura, P. Stoffer, Phys. Lett. B **738**, 6 (2014)
249. V. Pauk, M. Vanderhaeghen, Phys. Rev. D **90**, 113012 (2014)
250. G. Colangelo, M. Hoferichter, M. Procura, P. Stoffer, JHEP **1409**, 091 (2014)
251. G. Colangelo, M. Hoferichter, M. Procura, P. Stoffer, JHEP **1509**, 074 (2015)
252. T. Blum, S. Chowdhury, M. Hayakawa, T. Izubuchi, Phys. Rev. Lett. **114**, 012001 (2015)
253. J. Green, O. Gryniuk, G. von Hippel, H.B. Meyer, V. Pascalutsa, Phys. Rev. Lett. **115**, 222003 (2015)
254. T. Blum, N. Christ, M. Hayakawa, T. Izubuchi, L. Jin, C. Lehner, Phys. Rev. D **93**, 014503 (2016)
255. J. Green, N. Asmussen, O. Gryniuk, G. von Hippel, H.B. Meyer, A. Nyffeler, V. Pascalutsa, PoS LATTICE **2015**, 109 (2016), arXiv:1510.08384
256. H. Czyż, J.H. Kühn, Eur. Phys. J. C **18**, 497 (2001); H. Czyż, A. Grzelińska, J.H.Kühn, G. Rodrigo, Eur. Phys. J. C **39**, 411 (2005); H. Czyż, Int. J. Mod. Phys. Conf. Ser. **35**, 1460402 (2014). doi:10.1142/S2010194514604025
257. C.M. Carloni Calame, C. Lunardini, G. Montagna, O. Nicrosini, F. Piccinini, Nucl. Phys. B **584**, 459 (2000); C.M. Carloni Calame, G. Montagna, O. Nicrosini, F. Piccinini, Nucl. Phys. Proc. Suppl. **131**, 48 (2004); C.M. Carloni Calame et al., Nucl. Phys. Proc. Suppl. **225–227**, 293 (2012)
258. S. Actis et al., Working group on radiative corrections and Monte Carlo generators for low energies. Eur. Phys. J. C **66**, 585 (2010)
259. F. Jegerlehner, K. Kołodziej, arXiv:1701.01837 [hep-ph]
260. F.A. Harris, Nucl. Phys. Proc. Suppl. **162**, 345 (2006)
261. S. Eidelman, Nucl. Phys. Proc. Suppl. **162**, 323 (2006)
262. G. Abbiendi et al., Eur. Phys. J. C **77**, 139 (2017)

263. C.M. Carloni Calame, M. Passera, L. Trentadue, G. Venanzoni, Phys. Lett. B **746**, 325 (2015)
264. O. Steinmann, Commun. Math. Phys. **237**, 181 (2003)
265. A.B. Arbuzov, T.V. Kopylova, Phys. Part. Nucl. Lett. **11**, 339 (2014); EPJ Web Conf. **125**, 04005 (2016)
266. K.A. Olive, J.A. Peacock, Big-Bang cosmology, in S. Eidelman, et al., Particle Data Group. Phys. Lett. B **592**, 191–201 (2004)
267. T. Hambye, K. Riesselmann, Phys. Rev. D **55**, 7255 (1997). doi:10.1103/PhysRevD.55.7255
268. P. Bock et al., [ALEPH, DELPHI, L3 and OPAL Collab.s], CERN-EP-98-046, CERN-EP-98-46
269. M. Baak et al., Gfitter group collab. Eur. Phys. J. C **74**, 3046 (2014)
270. F. Bezrukov, MYu. Kalmykov, B.A. Kniehl, M. Shaposhnikov, JHEP **1210**, 140 (2012)
271. S. Alekhin, A. Djouadi, S. Moch, Phys. Lett. B **716**, 214 (2012)
272. D. Buttazzo et al., JHEP **1312**, 089 (2013)
273. A.V. Bednyakov, B.A. Kniehl, A.F. Pikelner, O.L. Veretin, Phys. Rev. Lett. **115**, 201802 (2015)
274. F. Jegerlehner, M.Yu. Kalmykov, B.A. Kniehl, Phys.Lett. B 722, 123 (2013); J. Phys. Conf. Ser. **608**, 012074 (2015)
275. R.D. Peccei, J. Korean Phys. Soc. **29**, S199 (1996), arXiv:hep-ph/9606475
276. T. Appelquist et al., Lattice strong dynamics (LSD) collab. Phys. Rev. D **89**, 094508 (2014)